OPERATIONAL PROBLEMS IN A UASB SYSTEM TREATING DISTILLERY WASTEWATERS

by

A.C.J. Laubscher

Thesis submitted in full thesis fulfilment of the requirements for the degree of Master of Science in Applied Science at the University of Cape Town.

Department of Civil Engineering
University of Cape Town

October 2000

DECLARATION BY CANDIDATE

I, **ANTON CHRISTO JOHANN LAUBSCHER**, hereby declare that this thesis is my own work and it has not been submitted for a degree at another University.

A Laubscher

October 2000

SYNOPSIS

BACKGROUND AND MOTIVATION

The upflow anaerobic sludge bed (UASB) reactor was developed in the Netherlands in the early 70's and has found wide application for treatment of industrial wastes, in particularly distillery wastewaters. In 1993, as a result of more stringent regulations for discharge of industrial wastewaters, Stellenbosch Farmers' Winery (SFW) installed an Upflow Anaerobic Sludge Bed (UASB) reactor at the SFW Wellington Distillery as a way of pre-treating all distillery wastewaters, before discharge via the municipal sewer to the local municipal wastewater treatment works. This was the first full-scale BIOPAQ® UASB system (450 m^3) in South Africa treating distillery wastewater, and it was commissioned during the 1995/1996-wine season.

The SFW Wellington Distillery produces wastewaters that can be categorised into two basic groups – (i) grain wastewater produced in distillation of grain "wort" and (ii) wine wastewater produced in distillation of grapewine. Both types of wastewater were to be treated in the UASB system.

During commissioning of the UASB system at the SFW Wellington Distillery, several minor and major operational problems were encountered. Some of these problems could be effectively resolved at the treatment plant. However, two major problems could not be effectively resolved and impacted severely on operation of the UASB system – (i) formation of a sludge layer when treating grain wastewater, and (ii) precipitation of struvite when treating wine wastewater.

With the treatment of grain wastewater, a major problem experienced in operation of the UASB system, was the accumulation of a sludge layer on the liquid surface at the top of the UASB reactors. This sludge layer was first observed in November 1995 when the small UASB reactor was fed grain wastewater only and was observed subsequently whenever grain wastewater served as influent to the UASB system. This operational problem stimulated an investigation into this phenomenon, and is the first objective in this research project.

With the treatment of wine wastewater, the precipitation of struvite ($MgNH_4PO_4$) was another major operational problem experienced. Struvite deposits were observed on the effluent overflow launders and extensive quantities of struvite deposited on the walls of the pipework collecting the effluent and discharging it, particularly close to and at bends in the pipes. At these points the deposits narrowed the 90 mm pipe diameter to less than 20 mm within two weeks. This restricted flows, eventually leading to operational failure and system shutdown. This stimulated an investigation into the causes for struvite precipitation, to identify possible methods to reduce or even eliminate struvite precipitation; this is the second objective of this research project.

OBJECTIVES

From the background set out above, the following objectives were set out for this research investigation:

- Investigate formation of the sludge layer on treatment of grain wastewater, to identify (i) whether this phenomenon is due to grain wastewater only, (ii) possible causes for the phenomenon and (iii) possible solutions to remedy this operational problem.

- Investigate struvite precipitation with wine wastewater, to (i) assess the struvite saturation state and precipitation potential in the UASB supernatant/effluent, (ii) delineate struvite solubility products in pure water and UASB supernatant at 37°C, (iii) delineate struvite precipitation kinetics in UASB supernatant at 37°C, the above to (iv) identify possible solutions to remedy the problem.

EXPERIMENTAL METHODS

Sludge layer accumulation

In a preliminary investigation, a laboratory-scale UASB system was operated with grain wastewater as influent, with or without prior filtration through a rotary drum filter.

This preliminary investigation clearly demonstrated that the sludge layer observed at full-scale could be reproduced in the laboratory-scale system. This prompted a more detailed investigation into this operational problem. Two laboratory-scale UASB systems were operated in parallel. One system served as a control and received wine wastewater as influent. The other system served as the experimental system, and was switched from wine wastewater to grain wastewater as influent, either as a blend with the wine wastewater or on its own with and without prior settling.

Struvite precipitation with wine wastewater

To investigate struvite precipitation with wine wastewater as influent to the UASB system, the following were undertaken:

(1) Determination of the struvite solubility product in distilled water at 20°C and 37°C, to validate the value at 20°C obtained from the literature and the experimental protocol, and develop a value for 37°C.

(2) Aeration batch tests at 37°C on supernatant drawn directly from the UASB system, and kinetic modelling of these batch test results to develop a deeper understanding of the processes operating in the precipitation.

RESULTS AND CONCLUSIONS

Sludge layer accumulation with grain wastewater

- In the preliminary and main investigations, when treating grain wastewater, a sludge layer was formed on the liquid surface of the laboratory-scale UASB system, appearing as a thick gelatinous mass. This confirmed that the problem identified at full-scale could be reproduced at laboratory scale, validating the experimental protocol.

- The sludge layer above was present with the grain wastewater in any form, i.e. blended with wine wastewater, or settled, unsettled or drum filtered grain wastewater only. The sludge layer accumulation was most severe with unsettled grain wastewater, and reduced in the blend and settled grain wastewater – blending

the grain wastewater with wine wastewater, settling the grain wastewater or filtering it reduced, but did not eliminate sludge layer accumulation.

- With wine wastewater, sludge layer accumulation was never observed.

- The observations above indicate that sludge layer accumulation is a property of the grain wastewater, and not distillery wastewaters in general. Further, the sludge layer accumulation appears to be linked to the solids content of the grain wastewater. Reducing the solids content by drum filtration, settling or blending can reduce but not eliminate the sludge layer accumulation.

- During periods of successful operation, % COD removal of >90 % could be achieved with both the centrifuged and filtered grain wastewater. However, the system was prone to upsets with relatively long recovery periods, of about 11 days.

- The bed profiles measured for the UASB system treating wine wastewater conform to those measured previously with apple juice wastewater (Sam-Soon *et al.*, 1987), glucose (Sam-Soon *et al.*, 1990), protein (Moosbrugger *et al.*, 1990), brewery wastewater (Moosbrugger *et al.*, 1993a) and wine distillery wastewater (Moosbrugger *et al.*, 1993b). In these profiles the typical three distinct zones of behaviour can be identified, namely lower active, upper active and upper inactive zones. The action of microorganisms in these zones conforms to the proposals of Sam-Soon and co-workers (Wentzel *et al.*, 1994).

- For the UASB system treating grain wastewater, the bed profile differs markedly from that above. The three zones of behaviour do not develop to any marked extent. A possible explanation proposed for this behaviour is that the grain wastewater contains considerable suspended solids. The rate of acidogenesis with suspended solids as substrate, would be limited by the rate of hydrolysis. Typically, hydrolysis rates would be much slower than acidogenesis rates with a soluble substrate. The net effect is to lower the overall rate of acidogenesis. With the lower acidogenic rates, the short chain fatty acids would be consumed in subsequent reactions as they are produced.

- With grain wastewater, the absence of a differentiation into the three zones of behaviour raises the question of the long term viability of a UASB system treating this type of wastewater. In developing their hypothesis for pelletization in UASB systems, Sam-Soon *et al.* (1987) proposed that partial phase separation of the anaerobic processes and development of a zone with a high hydrogen partial pressure were essential for pellet formation (Wentzel *et al.*, 1994). In the UASB system treating grain wastewater here, observations (no HAc and little HPr) indicate that these prerequisites for pellet formation are not achieved. If this is true, according to the hypothesis of Sam-Soon *et al.* pellet growth will not occur, or will be greatly reduced. This indicates that, in the long term in switching from wine wastewater (where pellet growth has occurred) to grain wastewater there will be a gradual loss of the pelletized sludge bed, until the pelletized bed declines to such low values that the system will fail. This aspect requires further investigation.

- The investigation here does indicate that when switching from wine wastewater, where a well-defined pelletized sludge bed has been developed, to grain wastewater, the grain wastewater can be effectively treated in the short term. However, most likely the sludge bed will diminish with time. To re-establish the pelletized bed, the system will have to be switched back to wine wastewater for a period.

Struvite precipitation with wine wastewater

Precipitation of minerals from the UASB system at the SFW Distillery at Wellington has been investigated. The following conclusions were drawn:

<u>Struvite solubility product in distilled water</u>

From 9 tests at 20°C and 13 at 37°C:

- The average struvite solubility products (pK_{sp}) in distilled water at 20°C and 37°C were 12.66 (sample standard deviation 0.08) and 12.46 (sample deviation 0.194) respectively.

- The pK_{sp} value at 20°C falls within the range of values recorded in the literature (pK_{sp}=12.6 to 13.26), indicating the experimental protocol and data are acceptable.

- The pK_{sp} value at 37°C is lower than the value at 20°C, and this difference is statistically significant at the 95 % confidence interval.

Thus, it would appear that the effect of an increase in temperature is to decrease the pK_{sp} value for struvite. However, this effect is relatively small, with the 17°C increase in temperature causing the pK_{sp} to decrease by only 0.2 units.

Aeration batch tests and modelling

From this investigation, the following conclusions can be drawn:

- The dominant mineral that precipitates is struvite ($MgNH_4PO_4 \cdot 6H_2O$), with some amorphous calcium phosphate (ACP, $Ca_3(PO_4)_2$) and magnesite ($MgCO_3$), and negligible newberyite ($MgHPO_4 \cdot 3H_2O$) and calcite ($CaCO_3$).

- For the two batch tests conducted, from modelling respectively
  - 562 and 415 mg/ℓ struvite,
  - 63 and 78 mg/ℓ ACP,
  - 36 and 92 mg/ℓ magnesite

  precipitated. With the large volumes of flow passing through the UASB system these represent substantial precipitation potentials,.

- The precipitation of struvite is stimulated by the increase in pH when CO_2 is lost from the UASB supernatant. Within the UASB digester, the partial pressure of CO_2 is high due to anaerobic processes acting in the digester. When the supernatant leaves the digester it comes into contact with atmospheric conditions where the partial pressure of CO_2 is much lower than inside the digester. This causes CO_2 loss from the supernatant to the air, until equilibrium between the CO2 concentration in the supernatant and the air is reached. Loss of CO_2, represents an increase in acidity which means that the pH of the supernatant will increase. This increase in pH causes struvite to become supersaturated, and hence it precipitates.

- When the supernatant leaves the digester, it is initially undersaturated with respect to struvite. Depending on the initial conditions in the supernatant, significant struvite starts precipitating when the pH increases above pH=7.3 to 7.5.

- With aeration, the critical pH for struvite precipitation is reached after 2 to 3½ minutes aeration. However, this time will depend on a number of factors, including aeration rate, initial pH, buffer capacity, initial P and Mg concentrations, etc.

- The increase in pH with aeration also stimulates precipitation of ACP. However, as noted above, the mass of ACP precipitating is relatively small compared with struvite. Similarly to struvite, ACP is initially undersaturated but starts precipitating after 2 to 3½ minutes aeration, when the critical pH for ACP precipitation of 7.3 to 7.5 is reached.

- The increase in pH with aeration also stimulates precipitation of magnesite. However, magnesite is significantly undersaturated at the start of the test and only starts precipitating after 10 to 13 minutes, when the critical pH for magnesite precipitation of 8.1 to 8.2 is reached.

- For struvite and ACP, the precipitations are essentially complete after 20 to 30 minutes aeration, and further aeration results in minor precipitation of these two minerals. For magnesite, this continues precipitating throughout both batch tests. It should be noted that the time to complete precipitation will depend on the aeration conditions applied – the greater the aeration, the faster the CO_2 stripping rate, the faster the increase in pH, and hence the shorter the time to reach complete precipitation.

- In the kinetic model, the pK_{sp} value for struvite was pK_{sp}=13.16. This value is the same as that of Musvoto *et al.* (2000) from similar batch tests and falls within the range of values reported in the literature (12.6 to 13.26). The value is larger than the value measured at 37°C in distilled water (12.46). This increase in value probably is due to the presence of organics and other compounds in the UASB supernatant. A similar increase was noted by Loewenthal and Morrison (1998) for

activated sludge effluent (12.92) compared to distilled water (12.83) at 20°C. Furthermore, the effect of ion pair formation on struvite precipitation is taken into account in the kinetic model, but was not considered when calculating the pK_{sp} value in distilled water.

- In the simulations with the kinetic model, the specific rate constant for struvite precipitation was 3000 $g/m^3.d$. This is the same value as that of Musvoto *et al.* (2000).

Future research

From this investigation two areas have been identified for further research:

(1) In the treatment of grain distillery wastewaters, this investigation has raised the question of the long term viability of a UASB system treating this type of wastewater. From the hypothesis for pelletization in UASB systems of Sam-Soon *et al.* (1987), it appears that with this wastewater the conditions may not be conducive for pellet formation. This aspect requires further investigation.

(2) The investigation here confirms that the precipitation problem experienced at the full-scale UASB system at SFW Wellington Distillery is predominantly due to struvite, and to a smaller extent ACP. The precipitation is stimulated by CO_2 loss which causes the pH to increase, which results in struvite and ACP supersaturation and hence precipitation. To limit struvite and ACP precipitation within the full-scale UASB system, the investigation has clearly demonstrated that stimulating struvite precipitation by aeration in a controlled environment is feasible. If introduced at the full-scale UASB system as a side-stream process, this controlled struvite precipitation possibly will reduce the Mg and P concentration sufficiently so that precipitation within the UASB effluent collection pipework will be reduced significantly. This proposal requires evaluation at pilot-scale on the full-scale UASB reactor at the SFW Wellington Distillery.

ACKNOWLEDGEMENTS

I wish to express my sincere gratitude and appreciation to:

Assoc. Prof. M.C. Wentzel, Department of Civil Engineering, University of Cape Town, for his advice and guidance throughout this study. His critical review of this thesis is much appreciated.

Prof. G. A. Ekama and Prof. R. E. Loewenthal, Department of Civil Engineering, University of Cape Town for their advice during this study.

Dr. E. V. Musvoto, Department of Civil Engineering, University of Cape Town, for her advice and willingness to help at all times.

Mr. Taliep Lakay, Chief Technical Officer and Mr. Percival Wilsnach, Department assistant, for their invaluable help in running the experimental units and the laboratory.

Mr. Gunnar Sigge, Department of Food Science, University of Stellenbosch, for his help in analysing some of the results reported here.

To Stellenbosch Farmers' Winery for their financial support, and special thanks to Mr. J. M. W. le Roux, General Manager, SFW Distilleries together with Mr. A. Watts, Manager of SFW Wellington Distillery for initiating this research and granting me this opportunity.

My wife, for her love and encouragement throughout this study.

My parents, for their love and support.

All my friends and colleagues, for their support during the course of this study.

THE ALMIGTHY – the honour is His alone.

TABLE OF CONTENTS

LIST OF FIGURES

LIST OF TABLES

LIST OF SYMBOLS

SYMBOL	DESCRIPTION
AcCoA	Acetyl Coenzyme A
A^-	Dissociated weak acid/base
Alk HAc	Acetate subsystem alkalinity (mg/ℓ as $CaCO_3$)
Alk H_2CO_3*	Carbonate subsystem alkalinity (mg/ℓ as $CaCO_3$)
Alk H_3PO_4	Phosphate subsystem alkalinity (mg/ℓ as $CaCO_3$)
Alk H_2O	Water subsystem alkalinity (mg/ℓ as $CaCO_3$)
Alk NH_4^+	Ammonia subsystem alkalinity (mg/ℓ as $CaCO_3$)
A_T	Total acetate species concentration (mg/ℓ as $CaCO_3$)
Buteryl CoA	Buteryl Coenzyme A
Ca^+	Calcium ion
$CaCO_3$	Calcium carbonate (Calcite)
Cl^-	Chloride ion
$CaHCO_3^+$	The $CaHCO_3^+$ ion pair
$CaHPO_4$(aq)	The $CaHPO_4$ ion pair
$CaH_2PO_4^+$	The $CaH_2PO_4^+$ ion pair
$CaOH^+$	The $CaOH^+$ ion pair
$CaPO_4^-$	The $CaPO_4^-$ ion pair
$Ca_3(PO_4)_2 \cdot xH_2O$	Amorphous Calcium Phosphate
CoA	Coenzyme A
CO_2	Carbon dioxide
CO_2^{3-}	Carbonate ion
CH_4	Methane
C_T	Total inorganic carbonate species concentration (mg/ℓ as $CaCO_3$)
f_m	Monovalent activity coefficient
f_d	Divalent activity coefficient
f_t	Trivalent activity coefficient
H^+	Hydrogen ion
HAc	Undissociated acetic acid
HCl	Hydrochloric acid

HCO_3^-	Bicarbonate ion
H_2CO_3	Undissociated carbonic acid
$H_2CO_3^*$	Sum of molecularly dissolved carbon dioxide and undissociated carbonic acid
HPO_4^{2-}	Hydrogen orthophosphate ion
$H_2PO_4^-$	Dihydrogen orthophosphate ion
H_3PO_4	Orthophosphoric acid
HPr	Undissociated propionic acid
K^+	Potassium ion
K_a, K'_a	Thermodynamic and apparent dissociation equilibrium constants for the acetate weak acid/base
K_{c1}, K'_{c1}	First thermodynamic and apparent dissociation equilibrium constants for the carbonate weak acid/base
K_{c2}, K'_{c2}	Second thermodynamic and apparent dissociation equilibrium constants for the carbonate weak acid/base
K_{p1}, K'_{p1}	First thermodynamic and apparent dissociation equilibrium constants for the phosphate weak acid/base
K_{p2}, K'_{p2}	Second thermodynamic and apparent dissociation equilibrium constants for the phosphate weak acid/base
K_{p3}, K'_{p3}	Third thermodynamic and apparent dissociation equilibrium constants for the phosphate weak acid/base
K_H	Henry's law constant
K'_{spm}	Thermodynamic solubility product for struvite adjusted for Debye-Hückel effects
K_{sp}	Solubility product for struvite
K_{ST}	Ion pair stability product
K_W, K'_W	Thermodynamic and apparent ion product constants respectively for the water weak acid/base
K_2HPO_4	Potassium Hydrogen Phosphate
m^3	Cubic meters
Mg^{2+}	Magnesium ion
$MgCl_2 \cdot H_2O$	Magnesium Chloride
$MgCO_3(aq)$	The $MgCO_3$ ion pair

$MgCO_3(s)$	Magnesite
$MgHCO_3^+$	The $MgHCO_3^+$ ion pair
$MgHPO_4(aq)$	The $MgHPO_4$ ion pair
$MgHPO_4(s)$	Newberyite
$MgNH_4PO_4 \cdot 6H_2O$	Magnesium Ammonium Phosphate (Struvite)
$MgOH^+$	The $MgOH^+$ ion pair
$MgPO_4^-$	The $MgPO_4^-$ ion pair
N	Normality
$NaHCO_3$	Sodium Hydrogen Bicarbonate
NH_3	Ammonia
NH_4^+	Ammonium ion
NH_3-N	Free and Saline Ammonia
NH_4Cl	Ammonium Chloride
N_T	Total inorganic nitrogen species concentration (mg/ℓ as $CaCO_3$)
P	Phosphorus
pH	Negative log (activity of hydrogen ions)
pCO_2	Partial pressure of carbon dioxide (atm)
pH_2	Hydrogen partial pressure (atm)
pK, pK'	Negative log (thermodynamic and apparent dissociation constant)
pK_a, pK'_a	Negative log (K_a, K'_a)
pK_{c1}, pK'_{c1}	Negative log (K_{c1}, K'_{c1})
pK_{c2}, pK'_{c2}	Negative log (K_{c2}, K'_{c2})
pK_{p1}, pK'_{p1}	Negative log (K_{p1}, K'_{p1})
pK_{p2}, pK'_{p2}	Negative log (K_{p2}, K'_{p2})
pK_{p3}, pK'_{p3}	Negative log (K_{p3}, K'_{p3})
pK_{sp}	Negative log K_{sp}
pK_{ST}	Negative log K_{ST}
PO_4^{3-}	orthophosphate
P_T	Total inorganic phosphate species concentration (mg/ℓ as $CaCO_3$)
C_i	Concentration of species i
μ	Ionic strength (mol/ℓ)
Z_i	Ionic charge of species i (mol/ℓ)
Σ	Total sum

GLOSSARY AND ABBREVIATIONS

GLOSSARY

Aldehydes	Aromatic substances produced during the distillation of alcohol.
Fusel oils	The general term for high alcohols present in the distilled spirit.
"Heads"	The first part of a distillate, which comes over when distilling with a pot still, and is usually volatile substances.
"Heart"	This is the middle and greater part of a distillate during distillation with a pot still, containing pleasant aromas and the required alcohols.
"Tails"	This usually contains the higher alcohols, which are not so desirable, and is usually the last part of the distillate with a pot still.

ABBREVIATIONS

ACP	Amorphous Calcium Phosphate
ADL	Anaerobic Digester Liquor
ADP	Adenosine diphosphate
ATP	Adenosine triphosphate
COD	Chemical Oxygen Demand (mg/ℓ)
EMP	Embden Meyerhof pathway
FSA	Free and Saline Ammonia (mg/ℓ)
M.Strain AZ	Methanobacterium strain AZ
NAD^+	Nicotinamide adenine dinucleotide (oxidised form)
NADH	Nicotinamide adenine dinucleotide (reduced form)
PYR	Pyruvic acid
SCFA	Short chain fatty acids (mg/ℓ)
SFW	Stellenbosch Farmers' Winery
TKN	Total Kjeldahl Nitrogen
TSS	Total suspended solids
UASB	Upflow anaerobic sludge bed

CHAPTER 1

INTRODUCTION

1. ANEROBIC DIGESTION AND UASB PROCESS

Anaerobic digestion processes offer considerable potential for the treatment of mainly soluble non-complex wastewaters (Lettinga and Hulshoff Pol, 1991). Anaerobic reactors for the treatment of these wastewaters, have found wide application particularly since the development of the Upflow Anaerobic Sludge Bed (UASB) by Lettinga *et al.* (1980) in the 70's. The UASB technology has been successfully applied to treat wastewaters from sugar, potato processing, brewery, winery, slaughterhouse, meat packing, paper mill, soft drink food and yeast industries (Lin & Yang, 1991). Also, anaerobic treatment with the UASB process has shown to be a feasible method for treatment of alcohol distillery effluents (Driessen *et al.*, 1994). COD removal efficiencies in the range of 65-95 % can be achieved, largely depending on the kind of feedstock used and on the process conditions in the distillery (Driessen *et al.*, 1994). Furthermore, anaerobic treatment is an attractive method to treat wine distillery wastewaters which are normally acidic, high in organic content, containing residual organic acids and their salts, soluble proteins and carbohydrates.

Up to 1988, 82 full-scale UASB reactors were constructed around the world (Britz *et al.*, 1999). In Europe and Canada, the UASB system is generally known as the commercial BIOPAQ® system and by October 1991, 106 full-scale BIOPAQ® UASB plants were in operation throughout the world (Britz *et al.*, 1999). Today more than 450 UASB plants are in operation, with 225 being manufactured by PAQUES, the leader in anaerobic digestion in Holland (Britz *et al.*, 1999).

In South Africa anaerobic digestion has a long history of application in the treatment of industrial effluents (Ross, 1989). Anaerobic digestion has been used as pre-treatment process for wine distillery wastewaters at the Paarl and Stellenbosch sewage works (Steffen Robertson and Kirsten, 1993). The first full-scale BIOPAQ® UASB

system (450 m^3) in South Africa treating distillery wastewater was commissioned during the 1995/1996-wine season at the SFW Distillery at Wellington, Western Cape, South Africa. This UASB system consists of two parallel reactors of 150 m^3 and 300 m^3 respectively and can be operated using only the 150 m^3 or 300 m^3 reactors or both reactors simultaneously. A peak loading of 15 $kgCOD/m^3/d$ is specified. The UASB system treats a variety of distillery wastewaters generated at the SFW Wellington Distillery.

2. DISTILLERY WASTEWATERS

Distillery wastewaters generated as a residue from ethyl alcohol distillation differ considerably as a result of the different raw materials used in the distillation and/or the distillation process implemented. Two main types of wastewater streams are produced at the SFW Wellington Distillery, wine wastewater and grain wastewater. These two types of wastewaters are generated in column and pot distillation processes on different raw materials to produce a variety of end products. Column distillation is employed in both grain whisky spirit and absolute alcohol (±96.4 % ethyl alcohol/volume) production. The latter uses distilling wine as raw material (see Chapter 2) and the wastewater generated is referred to as *wine wastewater*. The raw material used for grain whisky spirit production is originally maize meal (high starch source) which, after the addition of water, gets converted via enzymatic processing and heating into a grain mash slurry. The mash slurry contains fermentable sugars and is fermented by yeast addition. The fermented mash (±9 % A/V), now referred to as wort, is then distilled in a column still. The wastewater generated from this distillation is referred to as *grain wastewater*. Brandy spirit is also produced at the SFW Wellington Distillery. Compared to absolute alcohol distillation from distilling wine, brandy spirit distillation differs in the following two distinct ways: Firstly, although the raw material used is also originally from a fermented grape juice base, the specific quality for brandy spirit distillation is superior and is referred to as rebate wine (see Chapter 2). Secondly, the distillation process implemented is a double batch process where a pot still is used (see Chapter 2). The wastewater generated from brandy spirit distillation is also referred to as *wine wastewater*.

All the wastewaters mentioned above generally contain high concentrations of organic matter (COD), suspended solids (SS) and protein, particularly the grain wastewater. High SS content has been found to be detrimental to the operation of the UASB system (Fourie, 1974; Steffen Robertson and Kirsten, 1993). Accordingly, usually pre-treatment stages are implemented for distillery wastewaters for removal of the SS content prior to biological treatment (Fourie, 1974; Steffen Robertson and Kirsten, 1993). SS removal has been implemented at the SFW Wellington Distillery: In the case of grain wastewater, the stream undergoes decanting followed by centrifuging while the wine wastewater undergoes centrifuging (see Chapter 2).

3. OPERATIONAL PROBLEMS

During commissioning of the UASB system at the SFW Wellington Distillery, several minor and major operational problems were encountered. Some of these problems could be effectively resolved at the treatment plant. However, two major problems could not be effectively resolved and impacted severely on operation of the UASB system – formation of a sludge layer when treating grain wastewater, and precipitation of struvite when treating wine wastewater. These are set out in more detail below.

With the treatment of grain wastewater, a major problem experienced in operation of the UASB system, was the accumulation of a sludge layer on the liquid surface at the top of the UASB reactors. This sludge layer was first observed in November 1995 when the small UASB reactor was fed grain wastewater only. The sludge layer manifested as a thick gelatinous layer that accumulated on top of the liquid surface of the UASB reactors. This layer was highly viscous and interfered with effluent overflow at the overflow launders; the sludge layer completely inhibited overflow along some sections of the launders causing correspondingly increased flow and higher overflow rates at the other sections. On occasion, the development of the sludge layer was so severe, it forced operational shutdown of the UASB system for physical removal of the layer. The layer formation proved persistent, as it manifested whenever grain wastewater was treated after the 1996 wine season. This operational problem stimulated an investigation into this phenomenon, and is the first objective in this research project.

With the treatment of wine wastewater, the precipitation of struvite ($MgNH_4PO_4$) was another major operational problem experienced. Struvite deposits were observed on the effluent overflow launders and extensive quantities of struvite deposited on the walls of the pipework collecting the effluent and discharging it, particularly close to and at bends in the pipes. At these points the deposits narrowed the 90 mm pipe diameter to less than 20 mm within two weeks. This restricted flows, eventually leading to operational failure and system shutdown (see Chapter 2). Physical removal of the precipitant with high-pressure jet sprays and scraping equipment were unsuccessful. Furthermore, the structural design and layout of the effluent discharge pipe network limited access for cleaning. Laboratory tests on dissolving struvite with various strong acids and bases were conducted at SFW Laboratories at Stellenbosch. These indicated that a 30-40 % solution of concentrated caustic soda dissolved the crystal to form a slurry that could be easily removed with high pressure water. On implementing this scheme at the full-scale UASB system, it was found successful provided the caustic soda was continually circulated through the pipework by pumping, to promote contact with the struvite deposits. A caustic soda pumping system was installed and is currently in use. However, this strategy requires shutdown of the plant and the caustic soda and disposal of the resultant struvite/caustic soda slurry are expensive. This stimulated an investigation into the causes for struvite precipitation, to identify possible methods to reduce or even eliminate struvite precipitation; this is the second objective of this research project.

4. OBJECTIVES

From the background set out above, the following objectives were set out for this research investigation:

- Investigate formation of the sludge layer on treatment of grain wastewater, to identify (i) whether this phenomenon is due to grain wastewater only, (ii) possible causes for the phenomenon and (iii) possible solutions to remedy this operational problem.

- Investigate struvite precipitation with wine wastewater, to (i) assess the struvite saturation state and precipitation potential in the UASB supernatant/effluent, (ii) delineate struvite solubility products in pure water and UASB supernatant at 37°C, (iii) delineate struvite precipitation kinetics in UASB supernatant at 37°C, the above to (iv) identify possible solutions to remedy the problem.

5. REPORT LAYOUT

To address the objectives above, this research report details:

- Chapter 2 – General description of the distillation processes, end products produced and wastewater generation and treatment at the SFW Wellington Distillery. The operational problems experienced related with UASB operation are also discussed.

- Chapter 3 – Literature review of anaerobic processes in general, and the UASB system in particular.

- Chapter 4 – Preliminary investigation into the reproducibility of the sludge layer formation on laboratory-scale. The successful reproducibility of the sludge layer at laboratory-scale in turn led to a detailed investigation into the reasons for this phenomenon.

- Chapter 5 – Detailed investigation into the sludge layer formation at laboratory-scale by operating two identical UASB reactors in parallel (one serving as a control and the other as an experimental unit) and comparing system performance of the two systems on various combinations of the two main wastewaters generated at the SFW Wellington Distillery, wine and grain wastewater.

- Chapter 6 – Investigation into struvite precipitation with wine wastewater. Assessment of the struvite solubility product at 20°C and 37°C in distilled water, to validate the value at 20°C in distilled water obtained from the literature and develop a value for 37°C. Evaluate the deviation of the 37°C distilled water value

from the 20°C distilled water value. Determine the struvite solubility product at 37°C in UASB digester supernatant. Determine from aeration batch tests on the full-scale UASB digester supernatant and modelling the test results, the types of minerals that precipitate, the concentrations of the different minerals that form, the specific mineral precipitation rates and the time taken for complete precipitation.

CHAPTER 2

THE SFW WELLINGTON DISTILLERY: DISTILLATION PROCESS AND WASTEWATER TREATMENT

1. . INTRODUCTION

The Wellington Distillery of Stellenbosch Farmers' Winery is located at Wellington, Western Cape Province, South Africa. This distillery generates wastewaters during two different distillation processes, pot still and column still distillation, which are implemented in the production of five main end-products; neutral spirit, brandy spirit, grain whisky spirit, vodka and gin spirit. The wastewaters generated in all processes for all end products are high in organic content with a low pH.

The wastewaters are not discharged directly to the local municipal wastewater treatment works, but are treated on site before discharge. The on-site treatment facility consists of a pre-treatment stage and a main treatment stage. Predominantly, the wastewater pre-treatment stage consist of stainless steel holding tanks, a cooling tower, heat exchangers, a centrifuge and a decanter. The main treatment stage consists of a 450 m^3 Upflow Anaerobic Sludge Bed (UASB) reactor, a buffer tank, a 150 m^3 sludge storage reactor and gas holding tank.

This chapter describes briefly the SFW Wellington Distillery and the distillation processes, the wastewaters generated and their on-site treatment. Additionally operational problems experienced with the treatment of the wastewaters will be discussed, together with conditions that contribute to these problems.

2. SFW WELLINGTON DISTILLERY

2.1 Introduction

Distillation is the process whereby alcohols are concentrated: Fermented liquids are heated to selectively volatise the ethyl alcohol, which is then condensed and collected

for use. The collected product has a much higher alcohol content than can be produced by direct fermentation. Virtually any alcoholic liquid can be distilled and each yields a characteristic distilled beverage.

SFW Wellington Distillery stills a number of different alcohols from three main raw materials, namely grain "wort" (fermented grain "mash"), distilling wine (fermented grape juice), and rebate wine that is fermented from selective grape varieties. Only grain wash is produced on-site, while distilling and rebate wines are purchased from wine cellars in the region. The required quality for the raw materials depends on the end products. This section describes briefly the main distillation processes and the end products produced, including the wastewaters generated as by-products.

2.2 Processes

There are two kinds of distillation processes at the SFW Wellington Distillery; namely pot still distillation and column still distillation.

2.2.1 Pot still distillation

The pot still (Figure 2.1) is the simplest and oldest form of distillation and consists of:

The pot: - where the wine (rebate wine for brandy distillation) is heated
The head: - conducting the vapours to
The condenser: - where the vapours are condensed
The receiver: - where the alcohol is collected.

The pot (manufactured from copper) is heated by means of steam, normally passed into a coil inside the pot or a jacket around the pot. This form of distillation is operated as a batch process, and is used in the production of brandy spirit, see below.

2.2.2 Column still distillation

Here a five to six in-series column still is used. Each column consists of perforated plates dividing the column into various sections, each column with its own condenser(s). The result is that throughout the series of columns the separation of the

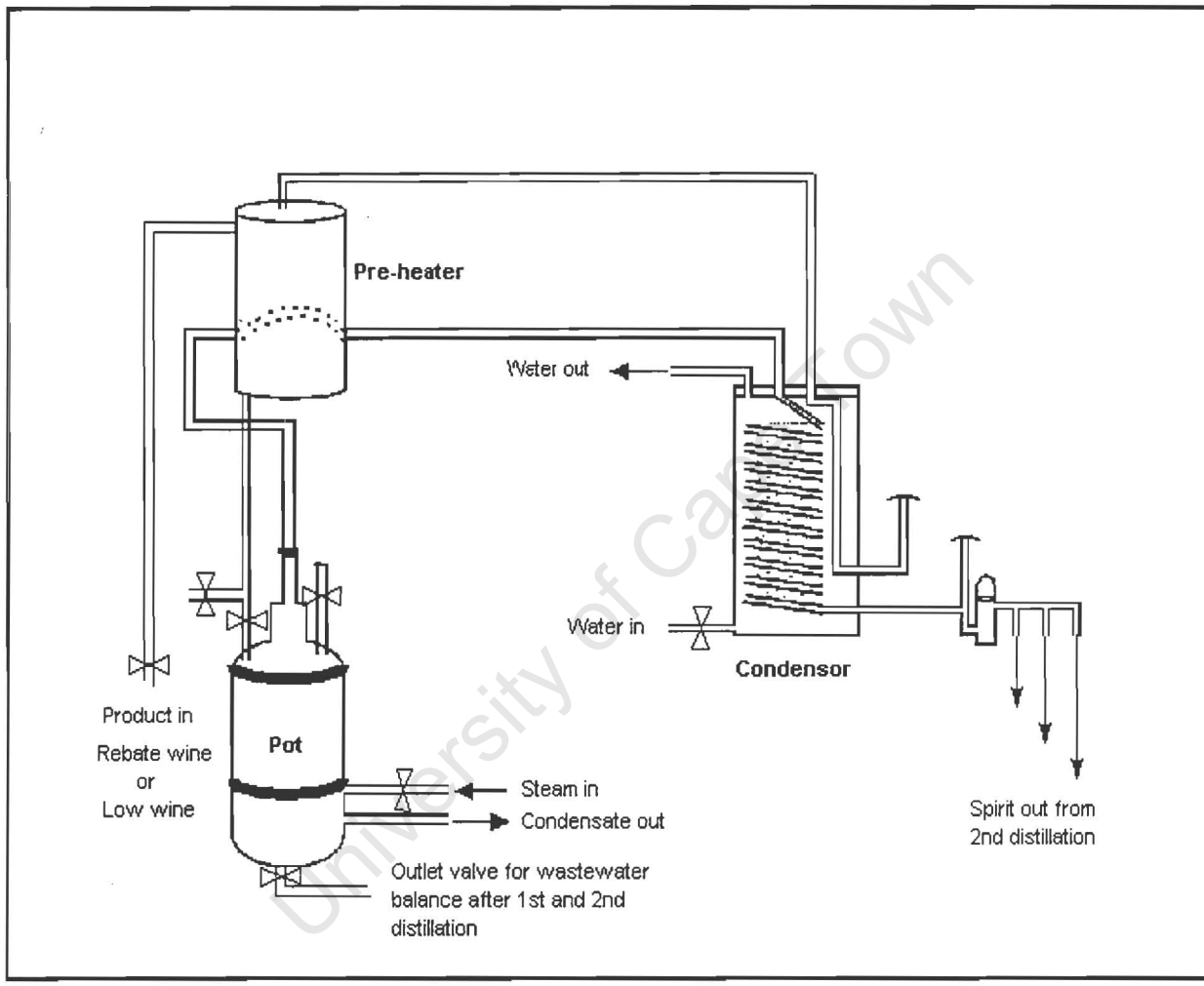

Fig 2.1 Schematic diagram of a pot still.

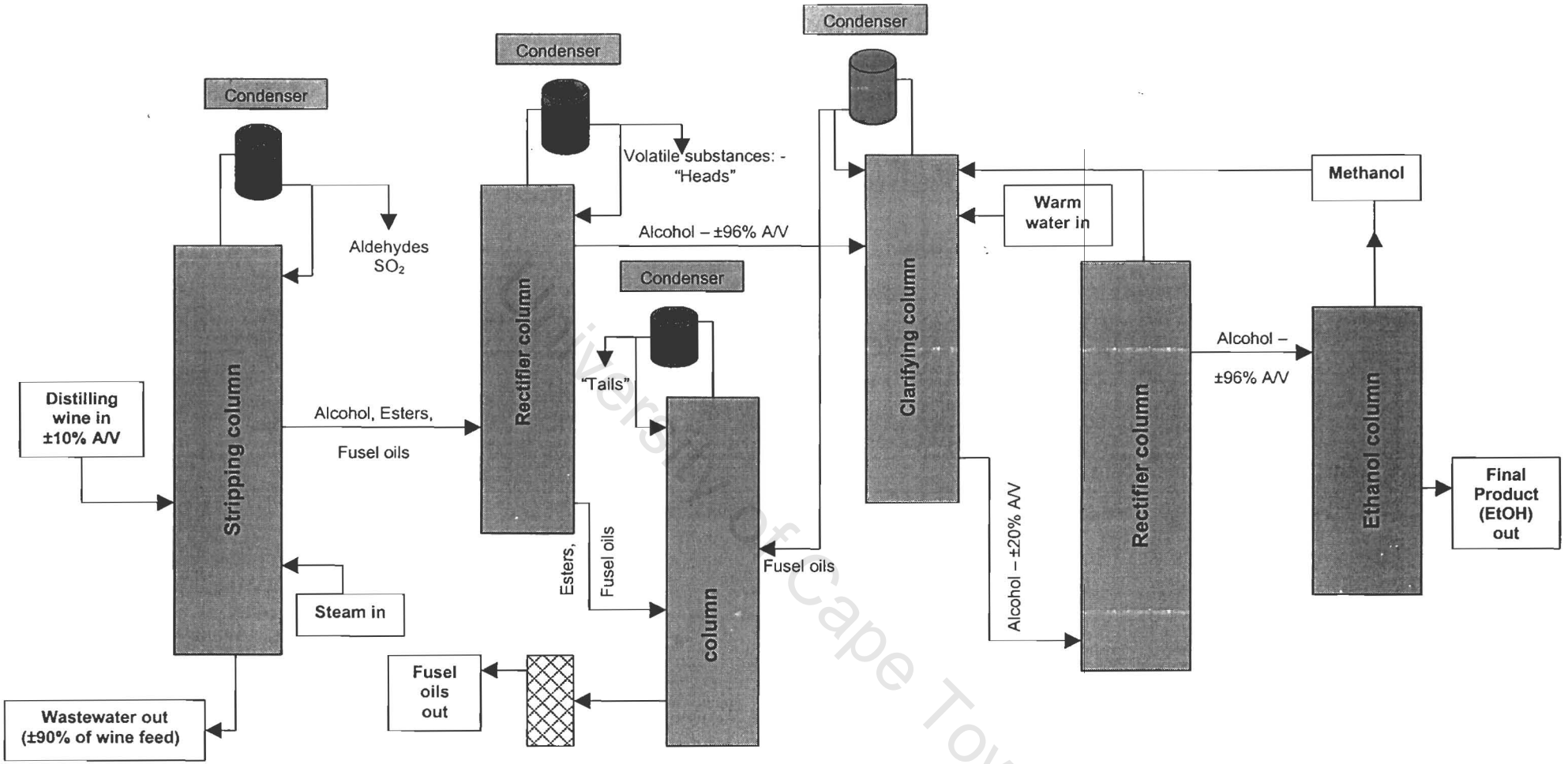

Fig 2.2 Simple configuration showing six stage column distillation.

Ethyl alcohol from the other constituents in the wine takes place. The resulting alcohol is 96.4 % A/V. Fig.2.2 shows a simple configuration of a six-stage column still.

2.3 Products

The SFW Wellington Distillery is equipped to produce the following spirit products:

- Neutral spirit
- Brandy spirit for maturation
- Grain Whisky spirit for maturation
- Vodka and Gin spirit

- **Neutral spirit**

In producing this spirit, the distiller is only interested in recovering the alcohol and not any flavour. Distilling wine from any grape variety in any condition can be used as raw material. The column still above (Fig 2.2) is used for neutral spirit distillation. The result is the separation of the alcohol from the other constituents, giving a clear, odourless and flavourless alcohol with strength of ±96.4 % A/V, which is usually not matured. This alcohol is used in the fortification of port and sherries and in the blending of brandies.

- **Brandy spirit**

Only specially produced rebate wine approved by the Government Brandy Board may be used for the making of South African Brandy. The main grape varieties fermented are Chenin Blanc and Colombard resulting in a wine with specified limits for SO_4, Sugar, Acetic acid and Tannin content. The resultant wine is distilled in the copper pot still above (Fig 2.1), as prescribed by law, and undergoes two separate distillations. The first distillation produces what is known as low wine, with an alcohol content of ±30 % A/V. This distillate contains unwanted flavours and undergoes a second distillation where the distiller separates three fractions in the distillation according to the time collected, i.e. from first to last, *the heads, the hearts and the tail.* The heart fraction contains the most favourable substances and this is collected for maturation. Only rebate brandy spirit that has been matured for a

minimum period of three years as prescribed by law may be used in the blending of brandies. Brandy produced in South Africa must have at least a 30 % 3 year matured pot still rebate brandy content, and when bottled the alcoholic strength must be at least 43 % A/V.

- **Grain whisky spirit**

Two types of whisky are produced in the world i.e.:

1. Malt whisky: - malted barley is used as raw material.
2. Grain whisky: - milled maize is used as raw material.

The processes by which these two kinds of whiskies are made are also different; malt whiskies are made by the pot still process and grain whisky by the column still process. The whisky produced at the SFW Wellington Distillery is grain whisky, and like brandy spirit is also matured in oak barrels for a minimum of 3 years. Fig 2.3 shows a flow diagram of the steps for producing grain wort. From Fig 2.3, the meal of maize (fixed mass weighed out) is mashed with heated tap water (fixed volume at 55°C). This mixture (mash slurry) is heated further to 90°C to allow the starch particles to burst, releasing the starch. An enzyme (α-amylase) is added before the heating process to maintain liquefaction of the mash for one hour at 90°C. Thereafter the mash is cooled down to a lower temperature (60°C for another hour), and a second enzyme (Gluco-amylase) is added to convert the soluble starch particles into shorter fermentable sugars, a process called saccharification. The product is referred to as grain mash and yeast is added to it for fermentation at ±35°C for ±48 hours. The grain wort (±9 % A/V) produced from fermentation is then distilled to grain whisky spirit for maturation. The balance of the grain wort flows out as grain wastewater.

- **Vodka and Gin spirit**

Vodka is distilled from the most economically available raw material or spirit, for example, cane sugar spirit. It is column distilled, as described above for neutral spirit and is normally neutral in flavour. However, flavours can be added, for example fruit, herbs etc., or distillation can be controlled to leave natural flavours in the spirit.

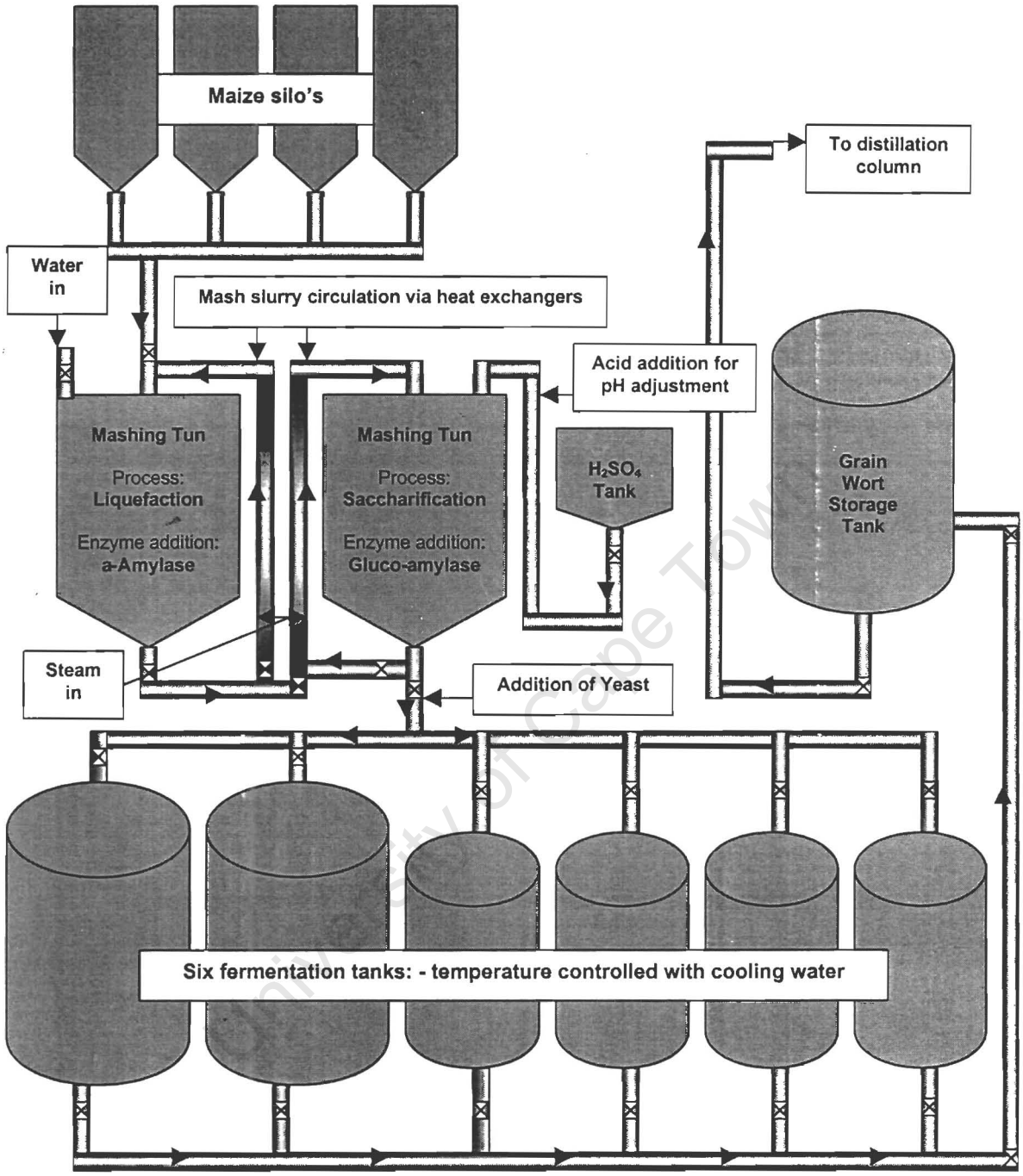

Fig 2.3 Schematic diagram of the mashing process, producing grain wort.

Gin is a neutral spirit of fermented grain, sugar cane or grape wine, which is distilled or re-distilled with Juniper berries and other botanicals. There are three ways of producing gin:

1. The traditional and premium way involves the distillation of alcohol with neutral herbs and spices – known as botanicals.

2. The slightly cheaper process involves adding the distillate of botanicals in concentrated form (called gin concentrate) to neutral alcohol, grape, cane or grain spirit. The distilleries buy the distilled gin concentrate.

3. Finally the third process is addition of "gin flavourings", normally from spice or herb origin to neutral spirit, or grape, cane or grain spirit; this is the cheapest method.

2.4 Wastewater production

From the description above, distillation at the SFW Wellington Distillery is on three main raw products, namely distilling wine, rebate wine and grain wort. Distillation to produce vodka and gin is relatively small in the total and contributes negligible to the wastewater production. None of the wastewasters generated in distilling these raw products are stored on-site, to regulate substrate feed to the wastewater treatment system, but are treated when generated.

The grain wort can be produced throughout the year. Accordingly, spirit production on grain wort is not seasonally bound and wastewater from this process (called grain wastewater) also can be produced through out the year. However, grain whisky distillation on grain wort will depend on the production schedule and grain spirit target. Typically, grain whisky distillation occurs throughout the year. In contrast, brandy and neutral spirit distillation on rebate and distilling wine respectively are seasonally bound since grapes are harvested only in the first quarter of the year; accordingly wastewater production from these processes (called wine wastewater) is restricted to this period. During this period, wine wastewater generated will be influenced by production schedules.

There are however situations when wine wastewater generated from neutral spirit distillation on distilling wine is available for an extended period or later in the year due to, for example, later harvesting or purchasing of distilling wine from overseas wine regions that harvest later due to the different seasons.

When generated, typical volumes of the different wastewaters produced are as follows:

Grain wastewater: ±30-50 m^3/d

Wine wastewater:

From Neutral spirit distillation: ±60-70 m^3/d

From Brandy spirit distillation: ±12-48 m^3 per batch/d

From Gin / vodka distillation: (intermediate)

3. WASTEWATER TREATMENT

3.1 Introduction

Wastewaters produced in the distillation processes consists of very high strength organic material (COD) and are generally acidic. At the SFW Wellington Distillery wastewater streams are treated on site, before discharge via the sewer to the local municipal works for further treatment. The treatment consists of two stages, a physical pre-treatment stage followed by a biological stage incorporating anaerobic treatment in a UASB system.

3.2 Wastewater characteristics

The wastewaters are collected into two streams, in the following way:

- Neutral, brandy, gin and vodka distillation wastewaters flow into a single line and are referred to as wine wastewater.

- Grain whisky distillation wastewater is kept separate from wine wastewater and is referred to as grain wastewater.

The two wastewater streams are hot and normally leave the distilling house with temperatures ranging between 80 to 90°C. Typical wine and grain wastewater characteristics are given in Table 2.1 and 2.2 respectively, representing analysis after pre-treatment. The wastewater streams consist of variable concentrations of organic material (COD) and suspended solids, with relatively low nutrient (N and P) concentrations. The effluents are generally acidic with a low buffer capacity.

Table 2.1: Average wine wastewater characteristics (after pre-treatment).

Parameter	Units	Value
COD total	mg/ℓ	24,000 – 45,000
COD filtered	mg/ℓ	23,000 – 44,000
pH		3.5 - 4
TSS	mg/ℓ	100 - 400
Ammonia (as N)	mg/ℓ	80
Ortho Phosphate (as P)	mg/ℓ	25

Table 2.2: Average grain wastewater characteristics (after pre-treatment).

Parameter	Units	Value
COD total	mg/ℓ	25,000 – 30,000
COD filtered	mg/ℓ	20,000 – 25,000
pH		3.5 - 4
TSS	mg/ℓ	>500
Ammonia (as N)	mg/ℓ	185
Total Phosphate (as P)	mg/ℓ	270

The two wastewater streams undergo pre-treatment before treatment in the UASB system, either separately, or as a blend depending on the distillation process in operation.

3.3 Pre-treatment

A schematic layout of the pre-treatment stages for wastewater treatment is given in Figure 2.4. Grain and wine wastewater streams discharge separately into two ±30 000 ℓ stainless steel holding tanks respectively. The contents of the tanks are constantly mixed by means of a side entry agitator. Small temperature drops do occur as the effluent undergoes the sequence of pre-treatment.

The grain effluent is pumped from its holding tank through a decanter (Pieralisi model, ±3 500 rpm) which removes the coarse grain solids. The decanter filtrate is then pumped into the wine effluent holding tank from where it follows the same route as the wine wastewater. Thus, when grain and grape wine spirits are distilled simultaneously, the watstewaters are effectively blended. From the wine holding tank, the wine, grain or blended wastewater is pumped to a heat exchanger where it is cooled to 30-45°C, and then to a centrifuge (Westfalia model, 7 270 rpm) which removes suspended solids. The wastewater then flows to an inline alkalinity dosing process where alkalinity may be added for pH control using caustic soda (see Fig 2.4), and then to the buffer tank of the UASB system.

In operation of the UASB system difficulties were experienced in treating the grain wastewater separately or as a blend with wine effluent. Consequently, treatment of grain wastewater by itself or as a blend in the UASB system was stopped. Currently, only pH adjustment with concentrated caustic soda is performed on grain wastewater after the decanting stage. The decanter filtrate with a pH between 5-8 is then pumped directly to the municipality treatment works without further treatment.

During the pre-treatment of grain wastewater the spent grains from the decanting unit process have a moisture content of ±70 % and are collected in bins for removal from the site by cattle farmers.

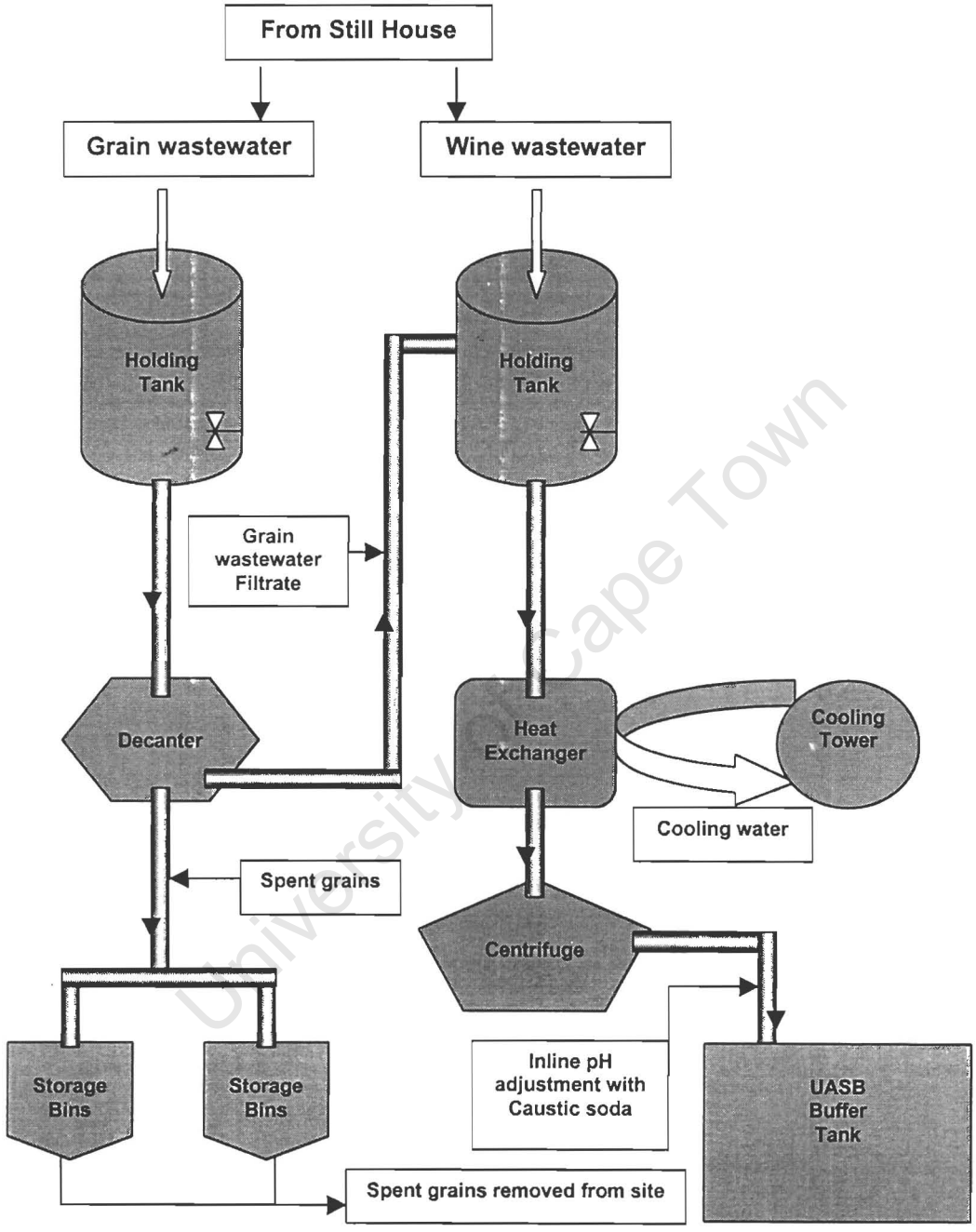

Fig 2.4 Schematic diagram illustrating the pre-treatment stages.

3.4 UASB

3.4.1 General description

Figure 2.5 shows the layout of the main treatment facility and schematic diagram of the UASB system. Wastewater from the pre-treatment above is pumped into the UASB buffer tank. From design specifications, the flow rate into the buffer tank should not exceed 180 m^3/day, with a maximum TSS not exceeding 500 mg/ℓ. The pre-treated wastewater entering the buffer tank is mixed with treated effluent recycled from the UASB reactor(s); treated effluent is drawn from the UASB where it overflows the reactor weirs and are re-circulated to the buffer tank. The buffer tank is mixed by means of a side entry agitator. The buffer tank contents are pumped into the UASB reactor(s) via evenly spaced distribution pipelines at the bottom of the reactor(s); four for the large reactor and two for the small reactor. The influent escapes through small holes (diameter ±3 mm) in the pipe, flowing upwards through the UASB.

The UASB system consists of two parallel reactors of 150 m^3 and 300 m^3 respectively and can be operated using only the 150 m^3 or 300 m^3 reactors or both reactors simultaneously. From design specifications it is recommended that with a flow rate of up to 75 m^3/day pre-treated wastewater into the buffer tank, only the 150 m^3 reactor be used; with a flow rate from 75 to 155 m^3/day only the 300 m^3 reactor be used and with a flow rate in excess of 150 m^3/day (i.e. up to the anticipated peak of 180 m^3/day) both reactors should be used.

It must be ensured that the influent wastewater entering the UASB reactor(s) is at a temperature of approximately 35°C, and pH between 6 and 7. The pH of the influent into the buffer tank is increased with automatic in-line caustic (45 % NaOH) dosing when required.

The treated effluent overflowing the v-notch weirs is collected in a header. From this header effluent can be re-circulated back to the buffer tank. The remaining effluent flows into a ±8 000 ℓ effluent storage tank from where it is pumped to the local municipal sewer. It is important to note that the re-circulated ratio can be varied from zero with respect to influent to >4. High recycles are desirable for alkalinity reuse (see

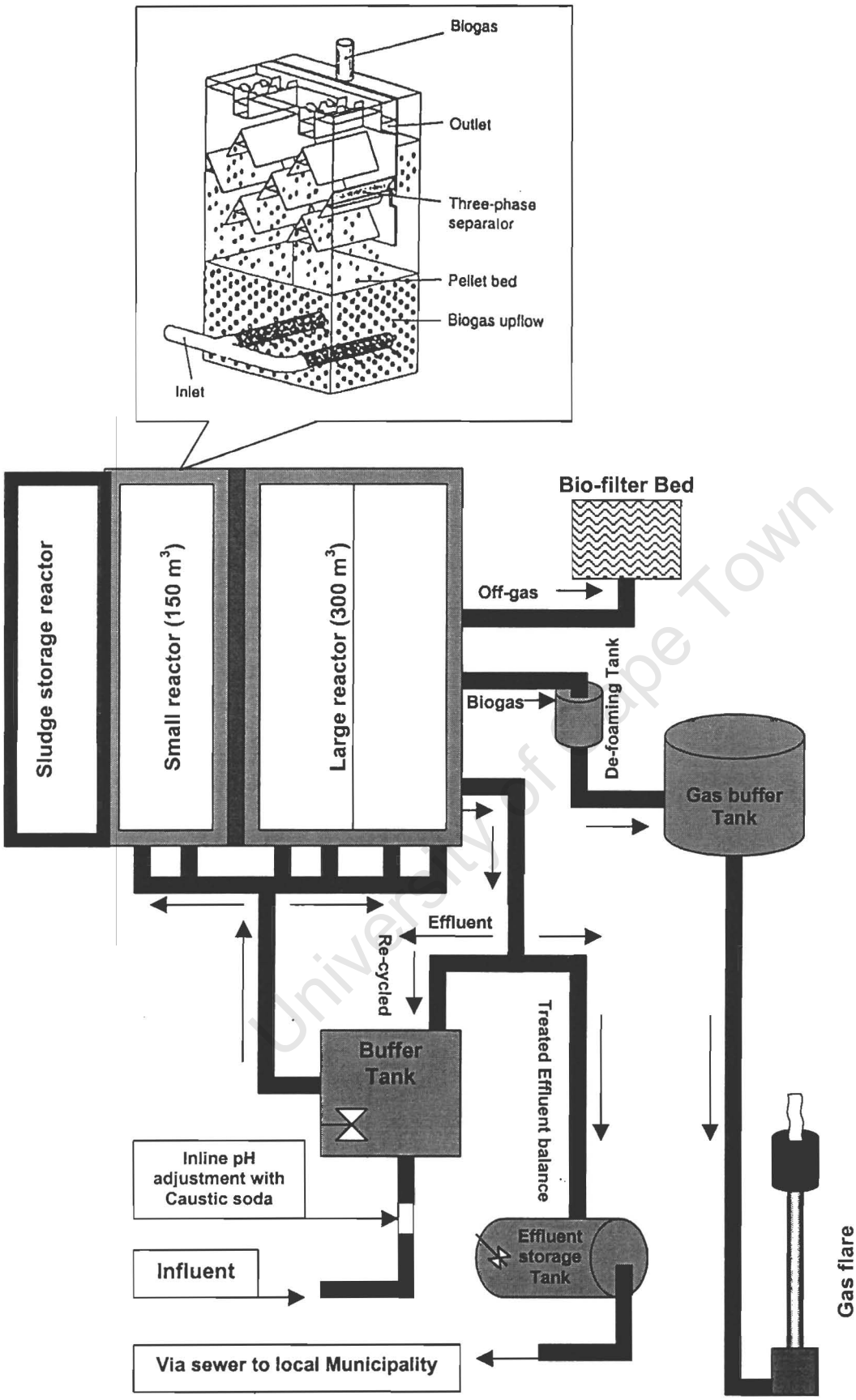

Fig 2.5 Schematic layout of the main treatment facility.

Section 3.6.2 below). During the treatment process, biogas (mixture of CH_4 and CO_2) is produced which is collected via inverted cones inside the reactor(s) into a gas header. From this header the gas flows via a de-foaming tank to a 10 m^3 gas buffer tank. The biogas may contain some foam and therefore passes through a de-foaming tank, which is fitted with a water spray nozzle. Continuous water spraying creates a constant water level in the tank. Gas flows by means of positive pressure from the gas header through the water and escapes from the water out through a pipeline on top and into the gas buffer tank. From the gas buffer tank the gas flows via a gas meter for monitoring, to the gas flare where the gas is burnt off. This gas flare can operate automatically by responding to the high and low level limit switches fitted on the gas buffer tank indicating gas production.

Odour control is by means of an "off-gas" system, consisting of a bio-filter fan, which blows the "off-gas" through a bio-filter bed to eliminate odours. The bio-filter bed is fitted with water sprays and it is suggested that the bio-filter bed be sprayed frequently to avoid drying out of the bed. The compost in the bed must be thoroughly turned over once bad odours are detected from the bio-filter.

The reactors are fitted with a total of 63 covers to minimise gas loss (CO_2 and CH_4) to the atmosphere, but also to provide access. Sample ports are also provided for monitoring the systems performance. A single sample tap is fitted at the influent; reactor feed and treated effluent line respectively. Six sample ports, for both reactors respectively are fitted on the one side of the reactor(s) wall; sample ports start at 0.4 m from the base and are spaced 0.4 m apart. These are designed for monitoring sludge at different levels in the bed.

3.5 System start-up

3.5.1 Introduction

This section describes the start-up of the UASB system, and the feeding regimes imposed.

3.5.2 System start-up and feeding regime

The commissioning of the full-scale wastewater treatment system was planned for the

1995 wine season. The UASB reactors were seeded at the end of 1994 with granular sludge obtained from a UASB system treating brewery wastewater. The first effective commissioning date was 3 May 1995 when start up commenced with wine wastewater as feed to both reactors. This was ± two months later than the planned commissioning date due to delays in material supplies and mechanical problems with the centrifuge and heat exchanger. On 18 May 1995, approximately 30 m^3 of additional "fresh" sludge was purchased and placed into the small reactor. From 12 June 1995, wine wastewater was fed to the small reactor only (the large UASB reactor received no feed and remained idle). During May and June 1995 the feed to the reactor(s) was terminated on several occasions due to excessive volatile fatty acids in the treated effluent which indicated poor performance of the UASB system. When the feed to the reactors was terminated the plant was operated on full re-circulation, but this resulted in the cooling down of the reactors as no fresh warm influent was fed. A temporary heating system to warm the contents of the buffer tank and consequently the reactors also was installed on 11 July 1995.

On the 31 of July 1995, commissioning commenced and, wine wastewater was fed to the small reactor only. From 25 October 1995 the feed was changed to a blend of wine wastewater and untreated wine wastewater collected from evaporation dams near the local municipal treatment works. The 5 evaporation dams stored untreated wine wastewater from earlier in the 1995 wine season that was pumped via the municipal sewer directly into the dams when UASB treatment of wine wastewater was not possible because the UASB reactor had not been commissioned. The reason for using this stored wastewater was to achieve flow volumes and COD loads to the reactors that could not be reached with only the wine wastewater produced at the SFW Wellington Distillery at that time.

This resulted in the dams being emptied, alleviating the problem of bad odours from the dams. The above feed was exhausted in the middle of November 1995 and grain wastewater was fed to the small UASB reactor, with the COD load being progressively increased. The reactor reached a COD loading of 11 kgCOD/m^3 reactor volume/d before the feed had to be stopped due to severe operational problems, namely accumulation of a sludge layer at the overflow weirs (see Section 3.6.4 below). The reactor feed was switched back to only wine wastewater operating only

on the large reactor. An average COD loading of ±2 kgCOD/m^3 reactor volume/d was obtained. Production at the distillery was stopped after middle December and the UASB system shutdown.

In early January 1996, the production of wine wastewater at the distillery recommenced and the large reactor was started up on this wine wastewater. Since the 1996 wine season effectively only starts from the middle of February, the available raw material only allowed for the large reactor to be operated at a low loading rate of ≈5 kgCOD/m^3 reactor volume/d. Grain wastewater was not considered, due to the operational problems experienced earlier with this wastewater.

In middle February 1996 when the new wine season commenced, both UASB reactors were operated on the wastewater. From design specifications treated effluent of both reactors flows into one line before it is recycled back to the buffer tank or partially discharged to the treated effluent storage tank. The latter operation resulted in one of the operating problems discussed below (see Section 3.6.3).

From May 1996, after the wine season ended, the small reactor was fed only grain wastewater and the sludge layer manifested again. This confirmed that the sludge layer formation could be reproduced and was persistent whenever grain wastewater was used as substrate feed. A decision was made not to feed grain wastewater to the UASB system until the reasons for the formation of the sludge layer could be investigated. The UASB system was shutdown after the small reactor was flushed with clean water in order to remove grain particles.

From the 1997 wine season both reactors were subsequently operated only on wine wastewater. During the wine season another major operational problem manifested as discussed below, namely precipitation of struvite (see Section 3.6.5). This operational problem stimulated an investigation into struvite precipitation as no specific information regarding the control and kinetics of struvite precipitation in UASB systems was available.

3.6 Operational problems

In operation of the UASB system a number of problems were experienced that on occasion were so severe that they forced the shutdown of the UASB plant. This section describes a number of these problems and the solutions implemented for those problems that could be resolved, to identify the problems that required further investigation.

3.6.1 Slow start-up

In bioreactors of the UASB design, Britz *et al.* (1999) concluded that the biomass is promoted by bacterial self-aggregation into dense granules. This granulation enhances the performance since the good settling properties of granules minimises biomass washout and the close cell packing in the granules optimises the interspecies exchange of metabolites. However, one of the main problems still remaining in the application of the UASB process is the extensively long start-up periods needed for the development of granules. This may be in part related to the extended generation time of the acetogenic and methanogenic bacteria within the granules. It can take several months before a highly effective granular bed can be cultivated. Since the operational efficiency and performance of these systems are mainly dictated by the formation, amount and specific activity of the granules, the rather extended start-up times may limit the potential application of the system.

The UASB system at the SFW Wellington Distillery also experienced slow start-up because the granular sludge in the reactors was originally from a UASB reactor treating brewery wastewater. The acclimatising of the sludge to the distillery wastewaters took longer than expected and other contributing factors such as availability of wine wastewater and low re-cycle ratios extended this period. However, once the granular sludge bed had been developed on wine wastewater, the system could be stopped for extended periods (±2 months) and be restarted on the same wastewater relatively easily.

3.6.2 High external caustic dosage

Initially the UASB system was started with a recycle from effluent to influent of 1:1 with respect to influent flow. Since during the treatment process a distillery

wastewater generates considerable alkalinity (see Chapter 3), it was envisaged that the recycle would return part of the generated alkalinity that flows out of the system with the effluent, to the influent. This would reduce the quantity of caustic soda that needed to be dosed externally to maintain the pH near neutral. In operation it was found that the recycle of 1:1 still required considerable caustic soda dosing. From the literature (see Chapter 3), it was determined that by increasing the recycle ratio, a greater quantity of the alkalinity could be recycled to the influent, further reducing the required caustic addition. Accordingly, during the treatment of wine wastewater from the 1996 season, the recycle ratio was increased. It was found that with recycle ratios >4:1 with respect to influent flow, caustic soda dosing could be decreased to almost zero.

3.6.3 Foaming

With the start of the 1996 wine season, the UASB system was again started up with wine wastewater. The large reactor was started up first and the small reactor later when the wine season was in full production. A better control of recycle ratios and volumetric loading was maintained. Initially reactor performance was good, with COD removals >90 %. However after ±1 month of operation extensive foaming on top of both the UASB reactor weirs, as well as in the buffer tank was experienced. It was thought that the foaming could be ascribed to differences between wine wastewater from the previous (1995) and current (1996) wine seasons. To control the foaming, anti-foam agent was dosed into the buffer tank. However, subsequent experience indicated that the cause for foaming appeared to be due to grain particles (high in protein) remaining enmeshed in the sludge bed of the small reactor from grain wastewater treatment the previous year (November 1995). It was noted that the yellowish particulates present in the grain wastewater became entrapped in the UASB sludge bed and did not biodegrade readily. This caused an accumulation of these grain particles in the UASB sludge bed of the small reactor (this reactor was fed the grain wastewater). During the shutdown, biodegradation of these grain particles continued and when the small reactor was restarted with wine wastewater, these partly biodegraded particles washed out of the small reactor and were re-circulated to the buffer tank and hence to the large reactor also. It appears that these particulates cause foaming. The foaming is undesirable because it causes solids carryover to the effluent and therefore deterioration in the effluent quality.

To resolve the foaming problem, feed to the UASB system was terminated and the reactors were fed with clean water pumped into the buffer tank. No recycle was operated to allow for complete flushing of the system. After flushing, wine wastewater was fed again until the end of the wine season (May 1996). Severe foaming was not encountered again, indicating successful resolution of the problem. The UASB feed was then switched to grain wastewater, which caused another operating problem discussed below (see Section 3.6.4).

3.6.4 Sludge layer formation

A major problem experienced in operation of the UASB system, was the accumulation of a sludge layer on the liquid surface at the top of the UASB reactors. This sludge layer was initially experienced in November 1995 when the small UASB reactor was fed grain wastewater only (see Section 3.5.2 above) and was so severe that it forced shutdown of the UASB system. Subsequently the system was fed a grain and wine wastewater blend for 2 days to attempt to overcome this problem; however, the sludge layer also accumulated with the blend.

The sludge layer manifested as a thick gelatinous layer that accumulated on top of the liquid surface of the UASB reactors. This layer was highly viscous and interfered with effluent overflow at the overflow launders; the sludge layer completely inhibited overflow along some sections of the launders causing correspondingly increased flow and higher overflow rates at the other sections. The increased overflow rates in turn caused UASB sludge granules to carry over to the effluent, and accordingly a corresponding deterioration in effluent quality, an undesirable event. Also, some sludge layer overflowed the launders to the effluent. The UASB sludge granules and the sludge layer carry over were partly recycled to the inlet to the UASB reactors. The gelatinous nature of the sludge layer recycled into the UASB reactor caused the UASB sludge granules within the sludge bed to tend to stick together, and these aggregates were lifted to the top of the UASB reactor by gas bubbles produced by the granules that could not escape the aggregates. This caused granule loss from the UASB sludge bed. To prevent further loss of the UASB sludge bed, the sludge layer on top of the UASB reactors was removed. To remove the sludge layer, influent feed was stopped, and a mobile piston pump used to physically extract the layer while it was simultaneously diluted with tap water by spraying.

The difficulties experienced with accumulation of the sludge layer during treatment of the grain wastewater, and the corresponding deterioration in effluent quality caused that this wastewater could not be treated in the full-scale UASB reactor, by itself or as a blend. Consequently, after decanting the pH of the grain wastewater was adjusted to 5-8 with concentrated caustic soda, and then discharged to the municipal sewer for further treatment at the municipal wastewater treatment works. Clearly this was an undesirable situation, and stimulated research into identifying possible causes for the sludge layer accumulation, see Chapter 4 and 5. Preliminary investigation on treatment of the grain wastewater in laboratory-scale UASB systems indicated that the accumulation of the sludge layer may be related to the TSS content of this wastewater (see Chapter 4).

From design specifications it is recommended that the total suspended solids (TSS) concentration in the influent feed to the UASB should not exceed 500 mg/ℓ. Wastewaters were subjected to pre-treatment where one of the main objectives was to remove the suspended solids, to at least less than 500 mg/ℓ before UASB treatment. This was to be achieved with centrifugation. However it was found that the TSS concentration of the grain wastewater after centrifugation was much greater than 500 mg/ℓ. This could be ascribed to the following reasons:

- Suspended solids were of such a nature that they could not be removed by centrifugation.

- There was a fine oily layer noticeable in the wastewater before and after the decanting stage attributed to the natural oil from the maize.

Pilot scale investigations into this problem confirmed that due to the above two reasons, effective removal of the solids in the grain wastewater with the current centrifuge is not possible. The centrifuge is one of the more expensive unit processes in the pre-treatment facility; accordingly alternative methods for removing solids were investigated, for example membrane technology. Currently no new method has been implemented and the grain effluent is discharged as described in Section 3.3.

3.6.5 Struvite precipitation

With the treatment of wine wastewater, the precipitation of struvite ($MgNH_4PO_4$), was a major operational problem experienced. Extensive quantities of struvite deposited on the walls of the pipework collecting the effluent and discharging it, particularly close to and at bends in the pipes. At these places the deposits narrowed the 90 mm pipe diameter to less than 20 mm within two weeks. Additionally, struvite deposits were observed on the effluent overflow launders. These areas of struvite precipitation have conditions in agreement with those identified by Loewenthal *et al.* (1994) as conducive to causing struvite precipitation: On the overflow launders the effluent comes into contact with the air causing CO_2 loss, and in the pipe bends pressure drops also cause CO_2 loss. This loss of CO_2 causes an increase in pH which results in the supersaturation of struvite and hence precipitation (see Chapter 6 for a more detailed review).

The struvite deposits in the pipework caused severe operational problems due to throttling of flows through the pipes, and eventually resulted in the plant shutdown.

Physical removal of the precipitant with high-pressure jet sprays and scraping equipment were unsuccessful. Furthermore, the structural design and layout of the effluent discharge pipe network limited access for cleaning. Laboratory tests on dissolving struvite with various strong acids and bases were conducted at SFW Laboratories at Stellenbosch. These indicated that a 30-40 % solution of concentrated caustic soda dissolved the crystal to form a slurry that could be easily removed with high pressure water.

The above practise was implemented at the full-scale plant but proved unsuccessful unless the caustic soda is constantly pumped through the pipework, promoting mixing with the struvite deposits. A pumping system was eventually designed and is currently in use at the plant. Unfortunately, this practise necessitates plant shutdown and the caustic treatment and disposal of the resultant slurry are expensive. Thus, a more permanent solution for controlled struvite precipitation is needed. Chapter 6 investigates the struvite precipitation problem in more detail.

4. CLOSURE

In operation of the full-scale UASB system at the SFW Wellington Distillery a number of operational problems were encountered. Of these, the two main operating problems causing operational failure of the UASB system that remain unresolved are (i) sludge layer formation on treatment of grain wastewater and (ii) struvite precipitation on treatment of wine wastewater. It was propose to investigate both problems on a laboratory scale to identify possible causes and solutions. Chapters 4 and 5 will discuss the sludge layer formation and Chapter 6 the struvite precipitation.

CHAPTER 3

LITERATURE REVIEV

1. INTRODUCTION

Since its first development in The Netherlands in the 1970s (Lettinga *et al.*, 1980), the Upflow Anaerobic Sludge Bed (UASB) system has found wide application in the treatment of various types of wastes, both soluble and partially soluble (Lin and Yang, 1991): By September 1990, 205 full-scale UASB reactors were constructed around the world (Lettinga and Hulshoff, 1991). Wastes produced by different alcohol producing industries have also been successfully treated by the UASB process, despite expected toxicity problems arising from high concentrations of COD, sulfide and salts (Driessen *et al.*, 1994), and difficulties experienced with high concentrations of suspended solids (SS) and protein found in the distillery wastewater from barley-, rice-, or sweet potato-*shochu* distillation (Kida *et al.*, 1994).

Following the successful implementation of the UASB system to treat wastewaters generated in alcohol producing industries, a full-scale UASB system was constructed and commissioned at the SFW Distillery at Wellington, Western Cape, South Africa, see Chapter 2. This research project investigates problems experienced in operation of this system, in (i) particular formation of a sludge layer on the liquid surface of the UASB reactor when treating grain wastewater, and (ii) struvite precipitation when treating wine wastewater.

To provide greater insight into the UASB system, in this Chapter processes operative in general in anaerobic systems (including the UASB) are reviewed. Also reviewed are the UASB system and experiences with this system in treating distillery wastewaters, to ascertain whether the operational problems with the UASB system at SFW Wellington Distillery have been experienced elsewhere.

2. ANAEROBIC DIGESTION

The various types of anaerobic systems known at present (as shown in Fig 3.1), including including the commercial BIOPAQ® UASB system (as shown in Fig 3.2) are all based on the conventional concept for anaerobic digestion; the fermentation of a carbohydrate, lipid or protein substrate to methane gas in four stages and involving three groups of organisms. The four stages and groups of organisms are: solubilization and acidogenesis (by acidogenic organisms), acetogenesis (by acetogenic organisms) and methanogenesis (by methanogenic organisms) (Sam-Soon *et al.*, 1989). Product formation pathways for various substrates are set out in Fig 3.3 and for glucose, a carbohydrate, in greater detail in Fig 3.4 (a, b and c) (Sam-Soon *et al.*, 1990).

Stage 1: Solubilization

In this stage complex long chain macromolecules such as carbohydrates, lipids and proteins are solubilized extracellularly by acidogenic organisms to short-chain compounds, sugars, fatty acids and amino acids respectively.

Stage 2: Acidogenesis

Substrate molecules from Stage 1 (i.e. fatty acids, amino acids and sugars) are ingested by the acidogenic organisms and fermented intracellularly to short chain fatty acids (SCFA) (e.g. acetic, propionic and butyric acids), carbon dioxide and hydrogen gas. The biochemical pathways by which the substrate is fermented and the nature of the end product (i.e. the type of SCFA produced) will depend primarily on the type of substrate and the hydrogen partial pressure (pH_2). For example, fatty acids usually are fermented via β-oxidation either to acetic acid and hydrogen under low pH_2 or, to butyric and propionic acids under high pH_2, see Fig 3.3. Sugars usually are fermented via the Embden-Meyerhof pathway to SCFA (such as acetate, butyrate and propionate), hydrogen and carbon dioxide. Cohen *et al.* (1979) for example, showed that, during fermentation of glucose, the fermentation products consisted of acetate, propionate, butyrate, hydrogen and CO_2, and that these represented 96 per cent of the soluble products. The relative fractions of the various SCFA, however, are dependent upon the pH_2 in the medium, see below. At low pH_2, glucose is fermented to acetic acid, butyric acid, hydrogen and carbon dioxide and at high pH_2, glucose is fermented to acetic acid, propionic acid, butyric acid, hydrogen and carbon dioxide.

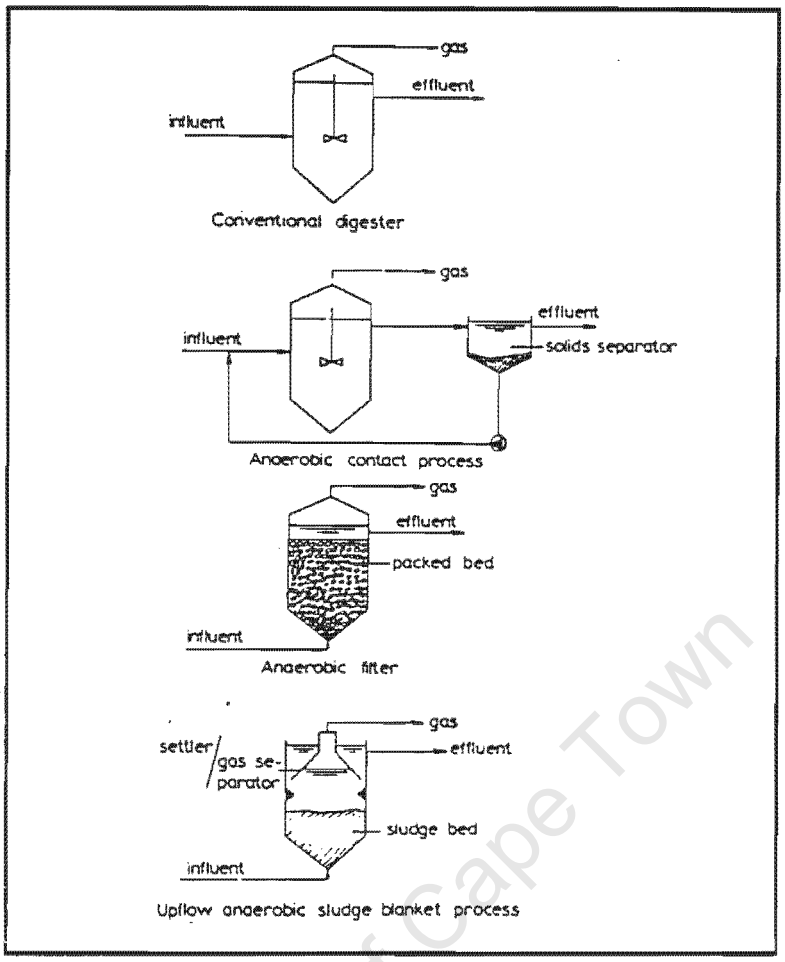

Fig 3.1 Schematic diagram of various anaerobic treatment processes (Lettinga *et al.*, 1979).

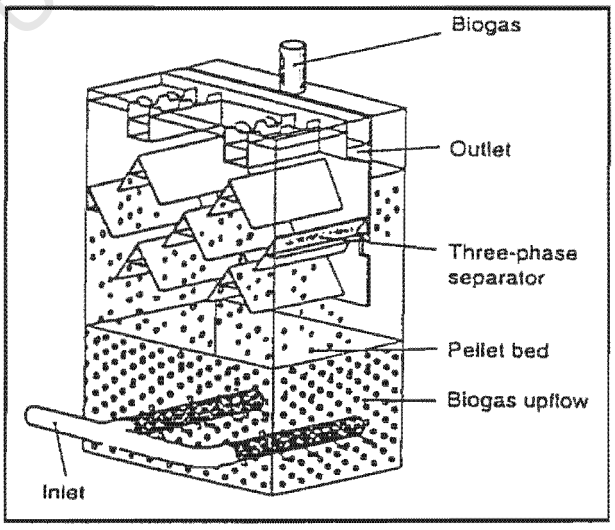

Fig 3.2 Schematic diagram of the BIOPAQ UASB system (Wolmarans *et al.*, 1996).

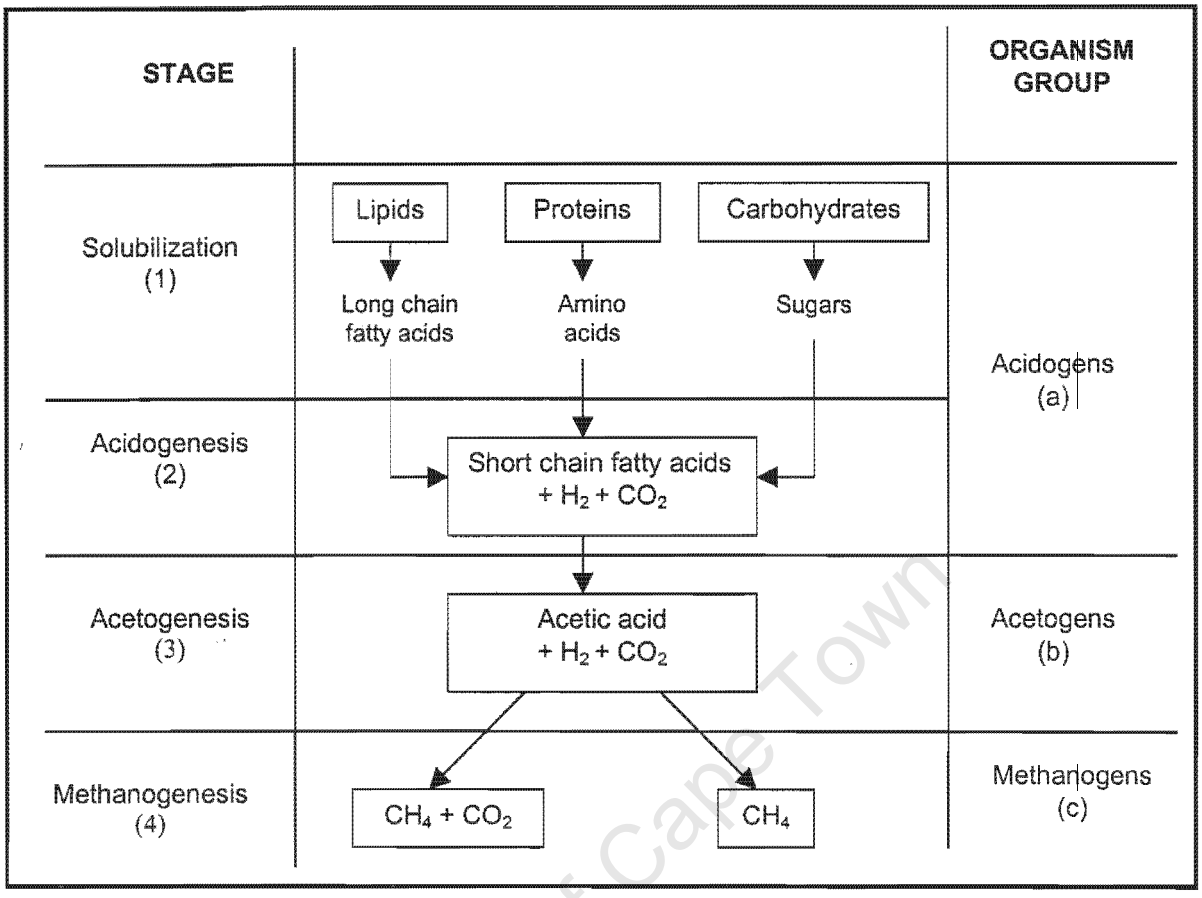

Fig 3.3 The four stages of the anaerobic methane fermentation process are effected by three groups of organisms (Sam-Soon *et al.*, 1989).

The detailed fermentation pathways for glucose under low and high pH_2, are shown in Fig 3.4 (a, b and c). Under both low and high pH_2 glucose is fermented first to pyruvic acid and intracellular generated electrons (attached to the electron accepting co-enzyme NAD^+, forming NADH) via the Embden-Meyerhof Pathway (EMP), see Fig 3.4; thereafter the pathways differ depending on the electron sink utilised to dehydrogenate the NADH: under low pH_2, only intracellular protons (H^+) act as the terminal electron acceptor (i.e. H^+ is the electron sink), under high pH_2, pyruvic, acetyl-CoA and protons act as electron acceptors. The sequences whereby the electron transfer takes place in the respective acidogenic stages are described below:

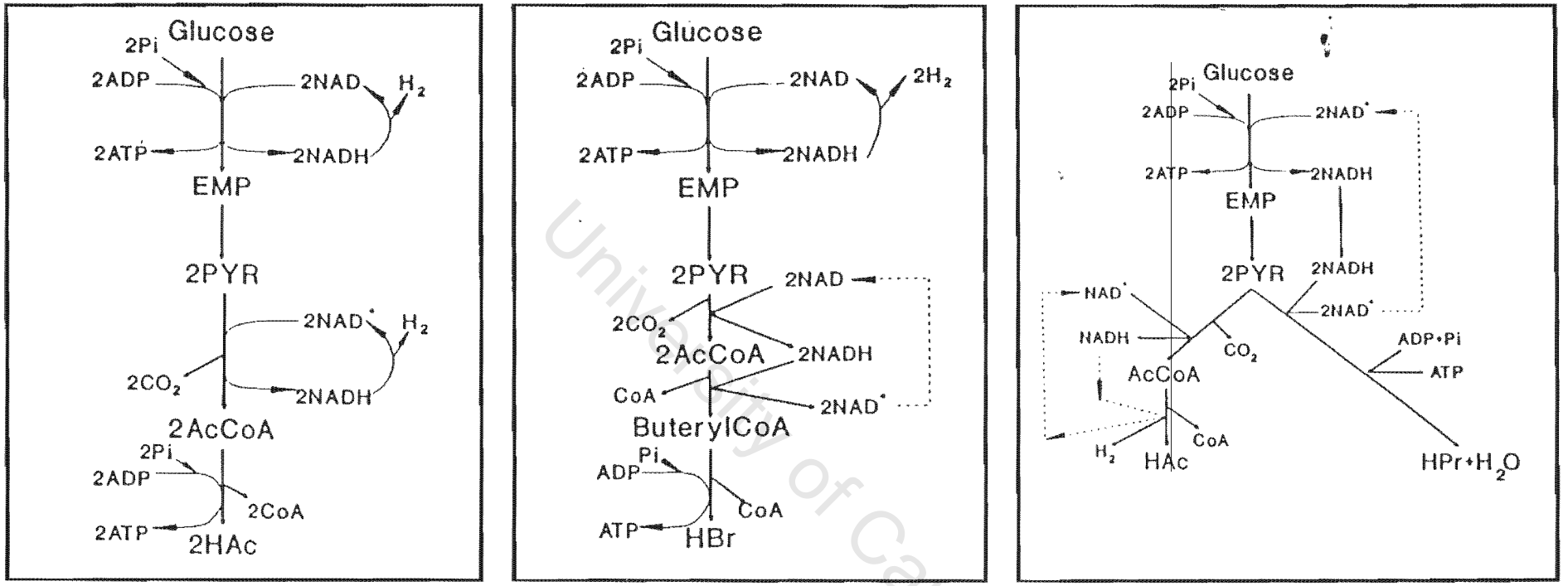

(c) Acetic acid generation ($pH_2 < 10^{-3,7}$ atm)

(b) Butyric acid generation ($pH_2 < 10^{-3,7}$ atm and $> 10^{-3,7}$)

(a) Acetic + propionic acid generation ($pH_2 > 10^{-3,7}$ atm

Fig 3.4 Acidogenic phase of glucose fermentation under low and high H_2 partial pressures to form acetic acid, butyric acid and propionic acid (Sam Soon *et al.*, 1990).

Sequence 1: (Embden-Meyerhof pathway, both high and low pH_2)

Glucose is fermented to pyruvic acid and hydrogen via the Embden-Meyerhof pathway (EMP). The hydrogen is attached to the electron-carrying co-enzyme, NAD^+, and 2 moles ATP per mole glucose are conserved by the organisms, i.e.

$$C_6H_{12}O_6 \text{ (glucose)} + 2\ NAD^+ + 2\ ADP + 2\ P \rightarrow 2\ CH_3COCOOH \text{ (pyruvic acid)} + 2\ NADH + 2\ ATP \quad (3.1)$$

That is, one mole of glucose generates 2 moles of pyruvic acid. Sequence 1 is common to both low and high pH_2; Fig 3.4 (a, b and c).

Sequence 2: (Dehydrogenation)

The NADH formed in sequence 1 needs to be dehydrogenated to maintain a high level of NAD^+ in order that the Embden-Meyerhof pathway remains operative (NAD^+ acts as the electron acceptor in this pathway). Dehydrogenation can take place in one of three ways depending on pH_2:

Low pH_2:

Under low pH_2 (pH_2 of less than 10^{-4} atm, calculated from data of Lehninger, 1972) (see Fig 3.4a) oxidation of NADH is a downhill reaction, i.e. NADH is oxidised spontaneously to NAD^+ and hydrogen gas, i.e.

$$2\ NADH \rightarrow 2\ NAD^+ + 2\ H_2 \quad (3.2)$$

The NAD^+ thus regenerated acts as electron acceptor for further oxidation of glucose to pyruvic acid via the EMP (sequence 1, Eq 3.1). The two moles pyruvic acid generated in sequence 1, Eq (3.1) are oxidised further to acetyl CoA and carbon dioxide (Fig 3.4a):

$$2\ CH_3COCOOH + 2\ NAD^+ \rightarrow 2\ CH_3CoA + 2\ CO_2 + 2\ NADH \quad (3.3)$$

The 2 moles NADH formed from this step again are dehydrogenated spontaneously to form hydrogen gas, as in Eq (3.2); the two moles of acetyl-CoA are converted to 2 moles acetic acid with concomitant generation of 2 moles ATP, i.e.

$$2\ CH_3CoA + 2\ ADP + 2\ P \rightarrow 2\ CH_3COOH + 2\ ATP \quad (3.4)$$

Hence, under low pH_2 the overall fermentation of 1 mole glucose is:

$$C_6H_{12}O_6 + 2\ H_2O + 4\ ADP + 4\ P \rightarrow CH_3COCOOH + 2\ CO_2 + 4\ H_2 + 4\ ATP \quad (3.5)$$

The overall reaction depicted by Eq (3.5) is only slightly downhill; a small change in pH_2, for example, will cause the reaction to become thermodynamically unfavourable. Noting from Eq (3.5) that H_2 is released, the rate of H_2 removal must be at least as fast as H_2 generation in order to maintain the low pH_2 condition required for acetate generation only. In the production of H_2, if the pH_2 increases only slightly, the reaction could become thermodynamically unfeasible until the H_2 is removed, i.e. pH_2 declines again. It would seem that in the intermediate state the acidogens utilise an alternative pathway (Fig 3.4b) in which butyric acid is produced. Experimental investigations have shown that during acidogenic fermentation of glucose under low pH_2 conditions, acetate was not the only SCFA generated, butyrate also is generated (Thauer *et al.*, 1977; Jones and Woods, 1986):

In the fermentation of 1 mole glucose to acetate as the only SCFA, hydrogen and carbon dioxide, 4 moles ATP are generated; this implies an 85 per cent energy conversion approximately (Thauer *et al.*, 1977). This high percentage energy conversion implies that the reaction (glucose to acetate) is only slightly downhill ($\approx$ -2 Kcal/mole glucose oxidised). The conversion of glucose to butyric acid is energetically strongly downhill at the expense that only 3 moles ATP are produced per mole of glucose oxidised (cf 4 moles ATP in acetic acid production) and only 2 moles H_2 are produced (cf 4 moles H_2 in acetic acid production). The possible overall pathway for butyric acid production is shown in Fig 3.4b. The overall reaction of butyric acid formation is as follows:

$$C_6H_{12}O_6 + 3\ ADP + 3P \rightarrow CH_3CH_2CH_2COOH + 2\ CO_2 + 2\ H_2 + 3\ ATP \quad (3.6)$$

In summary, the classification of butyric acid formation in a low pH_2 system arises from the experimental difficulty of effecting glucose oxidation to acetate only (with generation of H_2 and CO_2) in pure culture systems in the absence of H_2 utilising bacteria to maintain a low pH_2.

High pH_2:

Under high pH_2 (see Fig 3.4c), the forward reaction in Eq (3.2) is no longer thermodynamically feasible. Consequently an alternative method for oxidising the NADH generated in the EMP is needed. This is effected in two ways, which may take place simultaneously or alternatively (by the same or different groups of acidogens):

Alternative 1 – The two moles of acetyl-CoA are reduced to butyric acid, see Fig 3.4b, (Wolin 1974, Thauer *et al.*, 1977).

$$2\ \text{Ac-CoA} + 2\ \text{NADH} + \text{ADP} + \text{P} \rightarrow \text{CH}_3\text{CH}_2\text{CH}_2\text{COOH} + 2\ \text{NAD}^+ + 2\ \text{H}_2 + \text{ATP} \quad (3.7)$$

This reaction is thermodynamically favourable, but at the cost of producing a less oxidised SCFA and only one ATP (cf. 2 ATP produced when the 2 moles acetyl-CoA are converted to acetic acid under low pH_2, Eq (3.4)).

Alternative 2 – One of the 2 moles of pyruvic acid, Eq (3.1), is reduced to propionic acid so as to oxidise the NADH produced from the EMP (Wood, 1982), see Fig 3.4c:

$$\text{CH}_3\text{COCOOH} + 2\ \text{NADH} + \text{ADP} + \text{P} \rightarrow \text{CH}_3\text{CH}_2\text{COOH} + 2\ \text{NAD}^+ + \text{ATP} + \text{H}_2\text{O} \quad (3.8)$$

The remaining mole of pyruvic acid is oxidised to acetyl-CoA as in Eq (3.3), i.e.

$$\text{CH}_3\text{COCOOH} + \text{NAD}^+ \rightarrow \text{CH}_3\text{CoA} + \text{CO}_2 + \text{NADH} \quad (3.9)$$

The NADH cannot be spontaneously oxidised to NAD^+ as the reaction is not thermodynamically favourable at high pH_2. However, the organism can achieve dehydrogenation of the NADH by coupling this reaction with the thermodynamically favourable reaction in which acetyl-CoA is converted to acetic acid, but at the cost that no ATP is generated [cf the low pH_2 reaction where 2 moles ATP are generated, Eq (3.4)]. The coupled reaction is as follows:

$$\text{CH}_3\text{-CoA} + \text{NADH} \rightarrow \text{CH}_3\text{COOH} + \text{H}_2\ \text{NAD}^+ \quad (3.10)$$

Hence, for alternative 2 under high pH_2, the overall fermentation of glucose becomes:

$$C_6H_{12}O_6+2\ H_2O+3ADP+3P \rightarrow CH_3CH_2COOH+CH_3COOH+CO_2+H_2+3ATP \quad (3.11)$$

in which only 3 ATP are produced.

Stage 3: Acetogenesis from short chain fatty acids

Acetogenic organisms have an important intermediate role between acidogenesis and methanogenesis. Methanogenic organisms use substrate source, formic acid, acetic acid (by cleavage), hydrogen, methanol and methylamines to form methane; however short chain fatty acids with more than 2 carbon atoms (i.e. $>C_2$) (such a propionic and butyric acids) cannot be fermented directly to methane (McInerney *et al.*, 1979). However, *hydrogen-producing acetogenic* bacteria are capable of converting short chain fatty acids longer than C_2, to acetic acid, carbon dioxide and hydrogen gas, *provided the hydrogen partial pressure is low*, below $10^{-2,7}$ atm and $10^{-4,1}$ atm for the degradation of butyric and propionic acids respectively (McInerney *et al.*, 1979).

Propionic acid is oxidised as follows (for $pH_2 < 10^{-4,1}$ atm):

$$CH_3CH_2COOH + 2\ H_2O \rightarrow CH_3COOH + CO_2 + 3\ H_2 \quad (3.12)$$

and butyric acid is oxidised as follows for $pH_2 < 10^{-2,7}$ atm:

$$CH_3CH_2COOH + 2\ H_2O \rightarrow 2\ CH_3COOH + 2\ H_2 \quad (3.13)$$

Under high pH_2 (i.e. $>10^{-2,7}$ atm) the forward reactions of both Eqs (3.12) and (3.13) are thermodynamically unfavourable so that propionic and butyric acids remain unaltered.

Stage 4: Methanogenesis

For a carbohydrate type substrate the two main sources for methane production are: (1) Hydrogen oxidation and (2) Acetate cleavage. Methane can also be formed from formic acid, methanol and methylamines by specific groups of methanogens. However, their production tends to be relatively insignificant in the fermentation of carbohydrates and hence will not form part of the discussion.

The methanogens can be classified into three groups according to their energy source:

Hydrogenotrophs (H_2-utilising methanogens): These methanogens can utilise hydrogen only as their energy source. Examples of mesophilic hydrogenotrophs are *Methanbrevibacter* spp. and *Methanobacterium* spp.

Acetoclastic methanogens: These methanogens can utilise acetate only as their energy source, an example of mesophilic acetoclastic methanogen is *Methanothrix* spp.

Hydrogen/acetate utilising methanogens: These methanogens can utilise both acetate and hydrogen as energy source; for example *Methanosarcina* spp.

Methane formation takes place according to the following reactions:

For acetate,

$$CH_3COO^- + H_2O \rightarrow CH_4 + HCO^-_3 \qquad (3.14)$$

For hydrogen,

$$4\ H_2 + HCO^-_3 \rightarrow CH_4 + 3\ H_2O \qquad (3.15)$$

Variations in pH_2 do not appear to affect either the hydrogenotrophs or the acetoclastic methanogens. However, for the H_2/acetate utilising methanogens, in particular *Methanosarcina* spp., there are reports that high pH_2 results in the catabolic repression of acetate cleavage. For example Smith and Mah (1978) observed that *Methanosarcina* strain 227 utilises hydrogen (with CO_2 as carbon source) preferentially over acetate in mixtures of these substrates resulting in the inhibition of acetate cleavage; when hydrogen concentration was reduced to a low level by utilisation, acetate cleavage took place. In other *Methanosarcina* spp., such as *Methanosarcina barkeri*, rapid inhibition of acetate cleavage also occurred in the presence of H_2/CO_2 (Baresi *et al.*, 1978 and Ferguson and Mah, 1983).

The above pathways are applicable to UASB systems in general, including the UASB system.

3. THE UASB SYSTEM

3.1 System layout

The UASB process was first developed in The Netherlands in the 1970s (Lettinga *et al.*, 1980). The UASB design concept is based on the upward movement of soluble organic feeds through a blanket of bio-solids consisting primarily of microoganisms (Britz *et al.*, 1999). Lin and Yang (1991) describes the UASB reactor as consisting of four major components: (1) sludge bed; (2) sludge blanket; (3) gas-solids separator (GSS), and (4) settlement compartment (see Fig 3.1). The sludge bed in the UASB is a layer of biomass settled at the bottom of the bioreactor. The sludge blanket lies above the sludge bed and is a suspension of sludge particles mixed with gases produced in the process. The sludge bed is responsible for 80-90 % of degradation of the wastewater and occupies 30 % of the reactor volume, and the sludge blanket, the remaining 70 % (Britz *et al.*, 1999). Wastewater enters the bottom of the reactor and is degraded in both the sludge bed and sludge blanket (Britz *et al.*, 1999), via the anaerobic processes described above.

3.2 Advantages of the UASB system

In the UASB system, all the benefits of anaerobic systems over aerobic systems are retained, e.g. energy production, low excess sludge production, low volume requirements, etc. In addition, the UASB system offers many advantages over conventional systems (Wentzel *et al.*, 1994):

- loading rates up to several times greater than those for completely mixed anaerobic systems; this implies that smaller reactor volumes are required;

- high nitrogen removal; in fact the UASB system is the only anaerobic system that can remove significant concentrations of nitrogen;

- no artificial mixing of the mixed liquor is required; this can be an expensive and difficult operation in completely mixed anaerobic systems;

- no separate gravity sedimentation tanks are required;

- reactor "footprint" is small;

- no added compounds or carrier materials are required for biomass attachment, nor biomass support systems in the reactor (Britz *et al.*, 1999).

3.3 Principle requirement for UASB system

In the UASB system, the waste flows upwards through the bed of biosolids which mediates the anaerobic process.

Thus, successful application of UASB technology hinges on the generation of sludge aggregating into bio-conglomerates with high settling velocities, to facilitate retention of the sludge in the reactor. In the literature a number of different types of bio-conglomerates have been identified. Dolfing *et al.* (1985), for example, identifies:

- flocs: Conglomerates with a loose structure;
- pellets: Conglomerates with a well-defined structure (similar to lead shot) that settle rapidly;
- granules: Pellets having a granular appearance.

In the UASB system, pellets and granules are desirable biomass conglomerates, as these have high settling velocities.

3.4 UASB system behaviour

In laboratory-scale UASB systems treating apple juice concentrate, Sam-Soon *et al.* (1987, 1989) identified the three zones of behaviour along the axis flow through the system:

- A lower active zone in which concentrations of the SCFAs, propionate and acetate, increased to maxima, soluble COD reduced to about half its influent value, NH_3-H

reduced to a minimum, organic nitrogen (orgN) increased to a maximum and alkalinity and pH declined to minima.

- An upper active zone in which the propionate and acetate concentrations decreased to minima, COD decreased to a near minimum, NH_3-N remained near constant, orgN decreased to a minimum, alkalinity increased to near its value in the influent and pH increased to a stable value.

- An upper inactive zone in which no observable biokinetic activity was observed.

This behaviour was confirmed in investigations on glucose (Sam-Soon *et al.*, 1990), protein (Moosbrugger *et al.*, 1990), brewery wastewater (Moosbrugger *et al.*, 1993a) and wine distillery wastewater (Moosbrugger *et al.*, 1993b).

From the biochemistry of digestion processes (McInerney *et al.*, 1979), the action of anaerobic microorganisms (see Section 2 above) in the zones could be identified:

- In the lower active zone – acidogens generate SCFA, principally acetic (HAc) and propionic (HPr), carbon dioxide (CO_2) and hydrogen (H_2) from the influent substrate. The hydrogen is generated at such a rate that a high hydrogen partial pressure (high pH_2) is created; this is indicated by the observed increase in HPr which is produced only under high pH_2 ($>10^{-3.7}$ atm). Hydrogenotrophic methanogens generate methane (CH_4) from H_2 and CO_2; Acetoclastic methanogens convert some HAc to CH_4 and CO_2; Acetogens are inactive due to the high pH_2.

- In the upper active zone – the pH_2 has been reduced to, and maintained at, such low values due to action of hydrogenotrophs that; acetogens can convert HPr to HAc, H_2 and CO_2; acetoclastic methanogens convert all the HAc to CH_4 and CO_2.

- In the upper inactive zone – no observable biological activity takes place.

From the above, it is apparent that the differentiation of the sludge bed into lower and upper active zones is based on whether HPr generation takes place (lower active, high pH_2) and whether HPr oxidation to HAc occurs (upper active, low pH_2) or not (lower

active, high pH_2); HPr is generated by acidogens only under high pH_2 and oxidized to HAc by acetogens only under low pH_2.

3.5 Hypothesis for pelletization

From the observations on laboratory-scale UASB systems, Sam-Soon *et al.* (1987, 1989) developed an hypothesis for the formation of the conglomerates consisting of biopellets. They concluded that an extracellular polymer consisting predominantly of peptides enmeshed the organism mass into pellets. Since generation of the peptide polymer took place principally in the lower active (high pH_2) zone (see above), they concluded that the polymer must be generated by the action of acidogens or hydrogenotrophic methanogens. From a literature survey of these groups, the characteristics of one species (Zehnder and Wuhrmann, 1977) appeared to be directly relevant: a hydrogenotrophic methanogen, Methanobacterium strain AZ (M. Strain AZ), now classified as *Methanobrevibacter arboriphilicus*. Essentially the species utilizes hydrogen (H_2) as sole energy source and can produce its amino acid requirements with the exception of the sulphur containing amino acid, cysteine; an external cysteine source is necessary for growth. In an H_2 rich environment, with an adequate supply of nitrogen and a limitation of cysteine, the species in pure culture secretes high concentrations of amino acids (orgN) to the surrounding medium. Having identified M. Strain AZ as the organism most likely mediating pelletization, its characteristics provide a basis for formulating an hypothesis on pellet formation (Sam-Soon *et al.*, 1987).

When the M.Strain AZ is surrounded by excess H_2 substrate, i.e. high pH_2, the ATP/ADP ratio will be high. The high ATP level will stimulate amino acid production and cell growth. However, because M. Strain AZ cannot manufacture the essential amino acid cysteine, cell synthesis will be limited by the rate of cysteine supply. If free and saline ammonia is present in excess there will be an over-production of the other amino acids; the organism reacts to this situation by releasing some of these excess amino acids to the surrounding medium, to restore the amino acid balance in polypeptide chains, which are secreted extracellularly by extrusion from active sites. These polypeptide chains bind the species and other organisms into clusters forming a separate microbiological environment – the so-called biopellets.

From the hypothesis, Wentzel *et al.* (1994) identified conditions necessary for pellet formation as follows:

- An environment with a high pH_2.
- A nitrogen source, in the free and saline ammonia form, well in excess of the metabolic requirement of the organisms.
- A limited source of cysteine either from the feed or the action (e.g. death) of other organisms.

In terms of these criteria, Wentzel *et al.* (1994) could identify wastewater types that could be successfully treated in the UASB system. These types corresponded to observations in the literature.

3.6 Application of the UASB system

In 1978, a full-scale UASB reactor with a working volume of 800 m^3 was constructed for the treatment of sugar beet wastewater and achieved COD removals of 88 % under a organic loading rate of 16.25 $kg/m^3/day$ (Lettinga *et al.*, 1980). Since then, many full-scale UASB reactors have been installed around the world, successfully treating various types of wastewaters e.g. from sugar, potato processing, brewery, winery, alcohol distillery etc. (Lin and Yang, 1991). The increasing popularity of this system is due to the ability of the UASB to handle high organic loading rates and to reduce the COD of wastewaters efficiently and economically in a short time (Britz *et al.*, 1999).

3.7 Treatment of distillery effluent in the UASB system

Goodwin *et al.* (1994) investigated the anaerobic treatment of pot-ale, a liquid waste product from malt whisky distillation at laboratory-scale using UASB reactors. COD removal efficiencies of around 90 % were achieved after dilution, pH adjustment and settlement of the pot-ale. The maximum space-loading rate was around 15 kg $COD/m^3/d$ at a retention time of 2.1 days during stable operation. Thermophilic anaerobic digestion using sugar-cane vinasse was demonstrated by Souza *et al.* (1992)

in a pilot-scale UASB reactor. COD removal efficiencies of 72 % and gas production of 10 Nm^3 gas/m^3/d was achieved at organic loading rates of 25-30 kgCOD/m^3/d. Harada *et al.* (1996), also investigated the feasibility of thermophilic (55°C) anaerobic treatment of an alcohol distillery wastewater (cane molasses vinasse) using a 140 litre UASB reactor. Organic loading rates were applied up to 28 kgCOD/m^3/d by reduction of the hydraulic retention time at a fixed influent COD concentration. COD removals were relatively low (37-39 %), while BOD removals were more satisfactory, more than 80 %. The poor performance of the reactor for COD elimination was attributed to the degradability of the waste itself. High concentrations of suspended solids (SS) and protein found in the distillery wastewater from barley-, rice-, or sweet potato-*shochu* distillation, are difficult to treat with the UASB process (Kida *et al.*, 1994).

Driessen *et al.* (1994) concluded that anaerobic treatment with the UASB process has been shown to be a very feasible method of treating alcohol distillery effluents. Several types of vinasse including evaporator condensate have been treated successfully by the Biopaq-UASB system. COD removal efficiencies in the range of 65-95 % can be achieved, largely depending on the kind of feedstock used and depending on the process conditions in the distillery. Cane juice vinasse can be treated anaerobically applying volumetric loading rates up to 22 kg/m^3/d with COD removal efficiencies up to 88 %. Cane molasses based vinasse can be successfully treated anaerobically applying volumetric loading rates up to 10-15 kg/m^3/d with COD removal efficiencies of 65-70 %. Wine vinasse is readily anaerobically biodegradable. When applying loading rates up to 20 kg/m^3/d removal efficiencies of 90-95 % can be achieved. Condensate from a beet molasses based distillery is easily biodegradable. COD removal efficiencies of 85 % have been achieved at volumetric loading rates up to 18 kg/m^3/d.

Sam-Soon *et al.* (1989) and Moosbrugger *et al.* (1990) showed that for effective pelletization, the pH in the lower active zone should not decrease below a minimum of 6.7. Moosbrugger *et al.* (1993a) found that launter tun (brewery) waste developed a pelletized sludge bed in a laboratory UASB reactor. In assessing of H_2CO_3* alkalinity requirements when treating launter tun (brewery) at laboratory-scale using a UASB system, Moosbrugger *et al.* (1993a) found that this waste generates very little H_2CO_3* alkalinity internally and virtually all H_2CO_3* alkalinity has to be supplied externally. Moosbrugger *et al.* (1993b) also found that grape wine distillery waste developed a

pellitized sludge bed in a UASB system. COD removal was greater than 94 per cent for COD loading rates up to the maximum of 19 kg/(m^3 sludge bed·d), the maximum COD loading rate was determined by gas lifting pellets into the settling section, not by process failure.

Although the investigations in the literature do indicate that a wide variety of distillery wastewaters are amenable to successful treatment in UASB systems, there is no information on treatment of grain distillery wastewaters, and the associated operational problem observed at the SFW Wellington Distillery UASB system, namely formation of a sludge layer. Accordingly, this emphasizes the need for research in this area (see Chapters 4 and 5).

4. STRUVITE PRECIPITATION IN UASB SYSTEMS

The uncontrolled precipitation of the mineral struvite is a major problem in many wastewater conveyance and treating systems, for example in anaerobic treatment of wine distillery and piggery wastewaters and sludge waste derived from biological excess phosphorus removal activated sludge systems (Loewenthal *et al.*, 1994; Mamais *et al.*, 1994; Pitman 1995). The pipe networks transporting the treated effluents in these and similar anaerobic digesters, are particularly prone to scaling and clogging as a result of struvite precipitation, since in these wastes ammonia, magnesium and phosphates are present at relatively high concentrations. This problem has been observed at the full-scale UASB system at the SFW Wellington Distillery with wine wastewater as influent, where struvite precipitation has caused periodic plant shutdown for removal (see Chapter 2). The conditions causing struvite precipitation are reviewed in detail in Chapter 6. However, from the review in Chapter 6, it is evident that there is no information in the literature on struvite precipitation in UASB systems treating wine distillery wastewater. This prompted research into this area.

5. DISCUSSION

In this Chapter, to provide greater insight into the UASB system behaviour, processes

operative in anaerobic systems in general have been reviewed. Also reviewed are, the UASB system behaviour and experiences with this system in treating distillery wastewaters, and struvite precipitation, to ascertain whether the operational problems experienced with the UASB system at the SFW Wellington Distillery have been experienced elsewhere. Specifically, these problems are (i) formation of a sludge layer on the UASB system liquid surface when treating grain wastewater, and (ii) struvite precipitation when treating wine wastewater (see Chapter 2).

From the literature review, it is evident that there is no information of relevance for treatment of grain distillery wastewaters, emphasizing the need for research in this area (see Chapters 4 and 5). Information does exist on struvite precipitation (for more detailed review, see Chapter 6), but this is not specific for UASB systems treating wine distillery wastewaters, also emphasizing the need for research in this area (see Chapter 6).

CHAPTER 4

PRELIMINARY INVESTIGATION INTO TREATMENT OF GRAIN WASTEWATER IN A UASB SYSTEM

1. INTRODUCTION

From Chapter 2, one operational problem experienced at the full-scale UASB system at the SFW Wellington Distillery, was the formation of a thick viscous sludge/foam layer on top of the UASB reactor. This layer formed during the treatment of grain wastewater, either by itself or as a blend with wine wastewater, and caused severe operational problems, i.e. biomass washout and termination of feed. Accordingly, in this Chapter the formation of this layer is investigated further.

The principle aims of this part of the investigation were: (i) to reproduce at laboratory-scale the phenomenon describe in Chapter 2, namely where the anaerobic digestion of grain wastewater forms a sludge scum layer on top of the weirs of the full-scale UASB bio-reactor at the SFW Wellington Distillery, and (ii) to identify possible causes for the formation of the sludge layer.

To investigate the sludge layer phenomenon, in August 1997 a UASB system was set up at laboratory scale, seeded with granular sludge from the full-scale UASB system. The laboratory-scale UASB system was operated under conditions very similar to those at full-scale. To identify possible causes for formation of the sludge layer, it was noted that this layer did not form on the full-scale plant when wine wastewater served as influent. From a preliminary comparison of the two wastewasters, it was evident that the solids content (as TSS) of the grain wastewater was significantly higher than that of the wine wastewater. Accordingly, it was proposed that these solids may cause the formation of the sludge layer and the role of the grain wastewater solids content on the sludge layer formation was investigated.

2. EXPERIMENTAL SET-UP

The laboratory-scale UASB used in this investigation was identical to the reactor used by Sam-Soon *et al.* (1989), for investigating pelletization in the upflow anaerobic sludge bed (UASB) reactor.

Sam-Soon *et al.* (1989) describes the laboratory-scale UASB reactor as a transparent perspex cylinder (Fig 4.1). The inside diameter of the reactor is 100 mm and the height 1 200 mm, giving a total effective reactor volume of 9.0 litres. The bottom of the reactor is flat with four inlet ports evenly spaced around the circumference discharging in a horizontal direction. At the top of the reactor is the gas/liquid/solid separator. Gas collection is by means of a hollow inverted cone; rising gas bubbles are defected into the cone by a collar around the inside wall of the reactor below the cone. The gas passes from the cone, along a gas line, through a conical flask which served as a liquid trap to prevent carry over of liquid in the gas line.

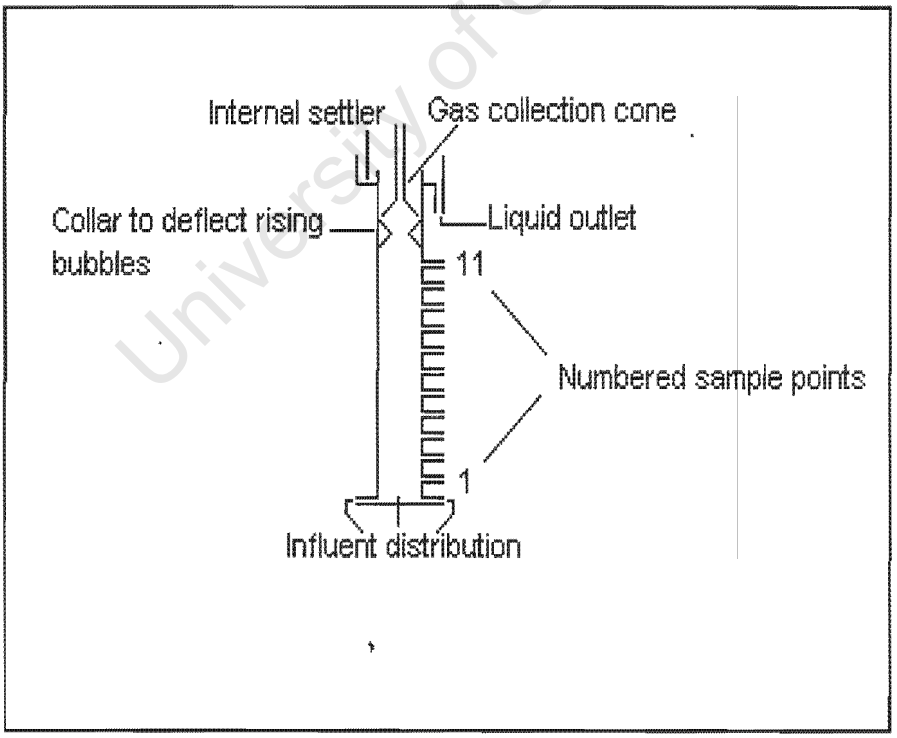

Fig 4.1 Schematic diagram of the laboratory-scale UASB reactor showing the numbered sampling ports.

The volume of the gas produced is measured by a wet gas meter (model No. DM3A, Alexander Wright, London). Effluent discharge is via an annular space between the gas collection cone and the reactor wall to enter a small solid/liquid separator (volume approximately 500 mℓ). Clarified effluent flows over a launder (v-shaped weirs) to the collection vessel while solids, which settle out, are returned into the reactor by gravity. Eleven sampling ports are evenly spaced along the length of the reactor. Temperature in the reactor was maintained at 35°C (±1°C) by a thermostat controlled electrical heating tape wrapped around the reactor.

The UASB system was operated in a flow through mode with no recycle for alkalinity reuse (Wentzel *et al.*, 1994) since the objective was not to investigate pH control and the flow through system is simple to operate.

To prevent channelling in the sludge bed and to ensure free movement of gas out of the sludge bed, the reactor contents were stirred by means of a slow internal stirrer (2 rpm) driven by a magnetic stirrer motor.

3. WASTEWATER CHARACTERISTICS

The influent feed stock was of two types:

1. Grain wastewater with a high TSS concentration (>1 000 mgTSS/ℓ)
2. Grain wastewater with a lower TSS concentration (<500 mgTSS/ℓ)

The feed stock in 1 above was the influent feed to the full-scale UASB system, i.e. after the grain wastewater had passed through the decanter and centrifuge (see Chapter 2). The nature of the finer solids following decanting, but prior to centrifugation, was such that total removal of these solids in the centrifuge was not possible. Analysis done by the Wellington laboratory showed that there was only a small reduction in solids concentration due to centrifugation. The decanted centrifuged feedstock (1 above) served as feed to the laboratory-scale UASB system

to ensure that the sludge slayer observed at full-scale could be duplicated at laboratory-scale.

To assess the role of the grain wastewater solids in the sludge layer formation, the solids were removed by drum filtration:

The feed stock in 2 above was also decanted first, followed by batch filtration through a drum filter using filter aid (diatomaceous earth). This method is commonly used in the wine industry when wines are clarified. A batch of this wastewater was collected when drum filtration was implemented on the site as part of an experiment to see if the fine grain solids could be removed at full-scale. Unfortunately, this operation proved not practical on large scale, because of the batch method of operation; continuous feed flow is needed for operation of the full-scale UASB reactor. Furthermore, sufficient storage and effective specific temperature control of the filtered grain wastewater were not possible. The common characteristics of the two waste types are listed in Table 4.1.

Table 4.1: Characteristics of the grain wastewaters.

	COD (mg/ℓ)	**pH**	**TSS (mg/ℓ)**
1. Grain wastewater after decanting and centrifuging	20,000-30,000	3.5-4.0	>1 000
2. Grain wastewater after decanting and filtering	15,000-20,000	3.5-4.0	<500

The feed to the laboratory-scale reactor was made up each day by diluting to a COD concentration of 3 000–5 000 mg/ℓ using tap water. This influent COD concentration was selected according to Sam-Soon *et al.* (1990); for flow through systems, dilution of the influent COD into the range 2 000 to 5 000 mgCOD/ℓ provides more stable operation and simulates effluent recycle for alkalinity reuse. Furthermore, for influent COD concentrations in this range in flow-through systems, for the same increment of

loading rate increase, the maximum loading appears to be independent of the influent COD concentration (Wentzel *et al.*, 1994). The pH in the grain wastewater was low, pH=3.5 to 4.

The flow through mode of the UASB operation selected, and the production of short-chain fatty acids in the lower part of the UASB reactor will cause the pH to remain low (Sam Soon *et al.*, 1989). This low pH will inhibit methanogenesis. Accordingly, alkalinity was added in the form of 100–200 mg $NaHCO_3$ per 20 litres diluted feed to prevent the pH from falling below the levels that inhibits methanogenesis (pH<6.8, Wentzel *et al.*, 1994). This caused the pH in the UASB reactor sludge bed to stabilise in the region of 7. Furthermore, no trace metal solution was added to the feed, as these would be present in adequate quantity in the feed.

4. ANALYTICAL METHODS

The following parameters were measured to assess the reactor performance:

1. COD (filtered and unfiltered influent and effluent)
2. pH in settler
3. Gas production
4. TSS in feed
5. Influent feed flow rate

COD and TSS were measured in accordance with Standard Methods (1985). The pH in the settler was measured with a portable Hanna pH meter (Hanna HI 9025) fitted with an epoxy combined pH electrode (Hanna HI 1230). Gas monitoring was by means of a wet gas meter (model No. DM3A, Alexander Wright, London). Considerable mechanical problems were experienced with the gas flow meter so that only intermittent readings could be obtained. Where readings were lacking, rising bubbles in the collection cone gave a qualitative indication of gas production.

5. START-UP

The laboratory-scale reactor was inoculated with ±3-4 ℓ of granular sludge taken from the full-scale UASB reactor at the SFW Wellington Distillery. The sludge was rinsed with tap water to remove all possible particles other than UASB sludge granules. To further wash the sludge, the sludge was placed in the UASB reactor and fed with tap water. The reactor was also heated and the temperature controlled at ±35°C. This washing phase was implemented to ensure that any formation of a sludge layer in the laboratory-scale unit was not simply because of a carryover with the sludge from the full-scale system. This washing phase lasted for two days and further washout of fine particles was observed. Substrate feeding was then started using the diluted unfiltered grain wastewater (feedstock 1) as influent, at an influent COD concentration of ±1 600 mg/ℓ.

The influent feed before dilution appeared as a yellowish homogeneous liquid, with fine suspended grain solids. By diluting the influent feedstock, the visual appearance of the feed was less turbid and contained less suspended solids per litre influent. TSS analysis on the influent feed indicated values less than 500 mg/ℓ.

Within a week it was accepted that the sludge was fully acclimatised to the waste as the COD removal efficiencies reached an average value of 90 percent for filtered effluent COD analysis.

6. SYSTEM OPERATION AND FEEDING REGIME

As noted above, the reactor was operated in a flow-through fashion with no recycle employed. Details of the feeding regimes are given in Table 4.2.

The influent flow rate at the start of the study was 8 ℓ/d and was kept constant for the entire investigation. The start-up influent COD concentration was ±1 600 mg/ℓ giving a loading rate of 3.2 kgCOD/m^3 sludge volume/d. This low loading rate was selected to acclimatise the sludge bed to the grain wastewater. Thereafter, the loading rate was

Table 4.2: Details of the feeding regime.

feeding periods day no.'s	average values for feeding periods			substrate feeding	comments
	COD in (unfiltered) (mg/ℓ)	Flow rate (ℓ/d)	loading rate kgCOD/m^{3}s-vol*/d		
1-2	0	0	0	WATER	Feed water for 2 days
3-6	no values	no values	no values	US	Feedstock type 1. Sludge volume 4 ℓ
7-14	2120	8	4.2	US	Feedstock type 1. Sludge volume 4 ℓ
15-33	1623	8	3.2	S	Feedstock type 2. Sludge volume 4 ℓ
34-76	3157	8	6.4	US	Feedstock type 1. Sludge volume 4 ℓ
77-102	3935	8	7.8	S	Feedstock type 2. Sludge volume 4 ℓ

*s-vol = sludge bed volume

US = grain wastewater with a high TSS concentration (>1 000 mgTSS/ℓ)

S = grain wastewater with a low TSS concentration (<500 mgTSS/ℓ)

increased by keeping the feed rate constant at 8 ℓ/d and increasing the feed concentration, eventually to a maximum of ±4 000 mg/ℓ by the end of the investigation, giving a loading rate of 3.5 kgCOD/m^3 reactor volume/d =7.8 kgCOD/m^3 sludge bed vol./d. Subsequent to each change of loading, the COD removal efficiency and gas production were monitored. When COD removal decreased the feed concentration was also decreased and visa versa. Figure 4.2 shows a record of the COD loading versus time for unfiltered COD analysis over the period of the study.

To investigate the effect of influent wastewater solids content on the formation of the sludge layer, at regular intervals the feed was switched between centrifuged grain wastewater with high TSS and drum filtered grain wastewater with low TSS, and the sludge layer on top of the UASB reactor inspected visually. Further, the following were assessed to investigate the formation of the sludge layer, and its impact on the system:

- What is the system's performance with respect to COD removal?
- Is the TSS concentration in the substrate the cause for scum layer formation?
- Does the sludge bed eventually washout and system performance deteriorate when continuing with this substrate feed over an extensive period?
- What other constituents in the substrate feed other than the fine particles contribute to the scum layer formation?

7. RESULTS

7.1 Sludge bed changes

Granular sludge was taken from the full-scale UASB reactor at the SFW Wellington Distillery and inoculated in the laboratory-scale reactor. At the time the full-scale

UASB reactor was not in operation. As a precautionary measure, the sludge was rinsed with tap water beforehand to remove all fine grain particles and debris particles.

The level of the sludge could be monitored through the transparent reactor wall, and it stayed stable throughout the entire investigation, at approximately ½ the reactor volume. From time to time dead pellet debris washout was observed, but this is common to UASB anaerobic fermentation. This pellet debris became entrapped in the sludge layer that formed on the liquid surface of the UASB reactor (see below). Sludge granule size remained approximately constant, at diameter 1-2 mm.

The fine grain particles suspended in the feed flocculated as distinct yellowish flocs when the pH was increased with $NaHCO_3$ to near neutral, particularly in the unfiltered feed. These particles tended to be captured in the sludge bed and did not seem to biodegrade readily. Eventually the sludge bed became saturated with fine grain particles giving the sludge bed a yellowish appearance. These yellowish particles were also washed out of the sludge bed, and became entrapped in the sludge layer which formed on top of the reactor, see below. Further, there was always a thin layer (±5 mm) of fine gelatinous sludge visible on top of the sludge bed, which continuously formed and was washed out to the effluent.

7.2 Sludge layer formation

The formation of the sludge layer on top of the laboratory-scale UASB reactor was determined visually. The sludge layer was present throughout the investigation, appearing on the liquid surface at the top of the UASB reactor. This confirmed that the problem observed at full-scale could be reproduced at laboratory-scale, validating the experimental protocol.

The sludge layer appeared as a thick gelatinous layer which contained debris particles, dead granular sludge and fine particles, which tended to be extremely sticky and oily, covered by a thin crust. Microscopic examination (Britz, personal communication) indicated in the crust layer the presence of a long rod shaped motile organism with

point flagella using a "spin-turn" action for movement, and in the oily layer a number of filamentous type bacteria.

The depth of the layer was found to depend on the substrate feed composition, and was not a consequence of biomass changes or reactor performance. Although it was established that the layer formed when treating both the centrifuged and drum filtered grain wastewaters (Table 4.1), there was a distinct physical difference in appearance of the layers which formed with the two wastewaters:

- Centrifuged grain wastewater: A thicker and more viscous layer consisting of the composition described above.

- Drum filtered grain wastewater: A thinner layer and less viscous containing of less dead granular sludge.

These observations confirmed the initial proposal that the formation of the sludge layer was related to the composition of the grain wastewater and that the causative agent appeared to be related to the TSS content of this wastewater. However, although drum filtering of the wastewater appeared to reduce the problem, it did not eliminate it.

7.3 System performance

Detailed daily results are listed in Appendix A. In Fig 4.2 the COD loading versus time for unfiltered COD analysis are shown. In order to have a "standard" reference, organic loadings were calculated in terms of the mass of substrate COD fed per day per sludge bed volume (kgCOD/m^3 sludge volume/d).

In Fig 4.3 % COD removal for unfiltered COD samples are shown. COD removal was calculated from the unfiltered influent and effluent COD. From Fig 4.3 it is apparent that the system shows signs of failure during two separate periods:

(i) From day 12 the % unfiltered COD removal dropped from >80 % to 20 % by day 15; from day 15 the % unfiltered COD removal recovered very slowly to

>80 % by day 36.

(ii) From day 82 the % unfiltered COD removal dropped from >94 % to 19 % by day 86; from day 86 the % unfiltered COD removal recovered slowly to >80 % by day 98.

From the above and Fig 4.3 it is evident that recovery from failure was a slow process, taking 10 and 11 days respectively. It was concluded that the possible reasons for this failure were:

1. Uncontrolled heating: For the first failure on day 12, the temperature at the bottom of the reactor was higher than 45°C because of overheating from the heating wire. This was corrected and the system slowly recovered.

2. Sludge rinsed: For the second failure on day 82, the sludge was drained from the reactor and rinsed with tap water on day 82 to remove all the fine grain particles in the sludge that had accumulated on feeding the unfiltered grain. This corresponds directly with the failure and the system recovered slowly after this.

During periods where the system was operating successfully, % COD removal was good at 91-96 % based on unfiltered COD with both centrifuged and filtered grain wastewater as influent indicating that, despite the formation of the sludge layer, the grain wastewater could be treated successfully in the UASB system. However, the periods of failure do indicate that the system is prone to upset. Furthermore, as noted above, the formation of the sludge layer severely impacts full-scale system operation.

7.4 Bio-gas production

Daily biogas production is shown plotted in Fig 4.4. Comparing the biogas production (Fig 4.4) with % COD removal (Fig 4.3), as expected biogas production follows % COD removal closely, with reduced biogas production during the two periods of failure identified above.

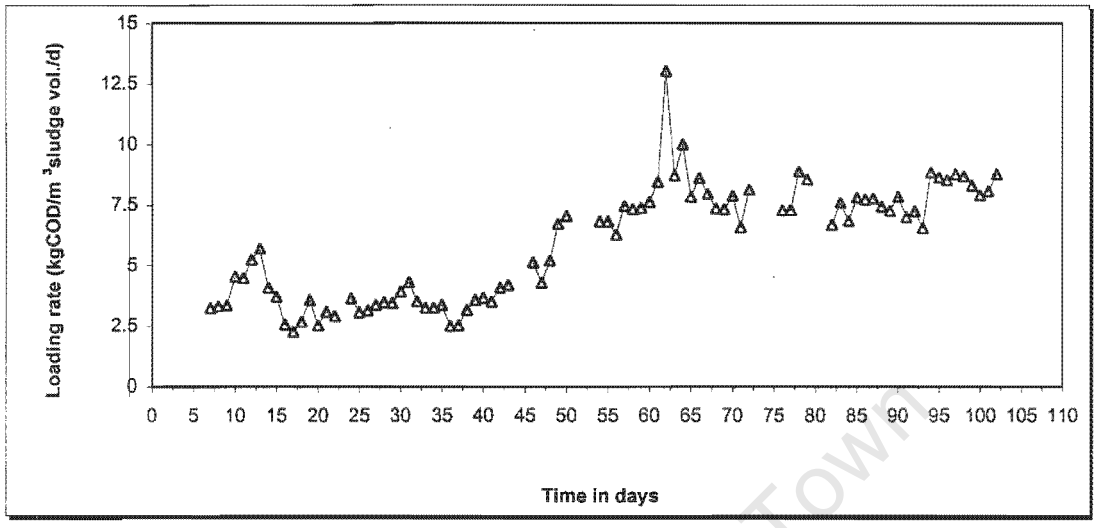

Fig 4.2 COD loading versus time for unfiltered COD analysis.

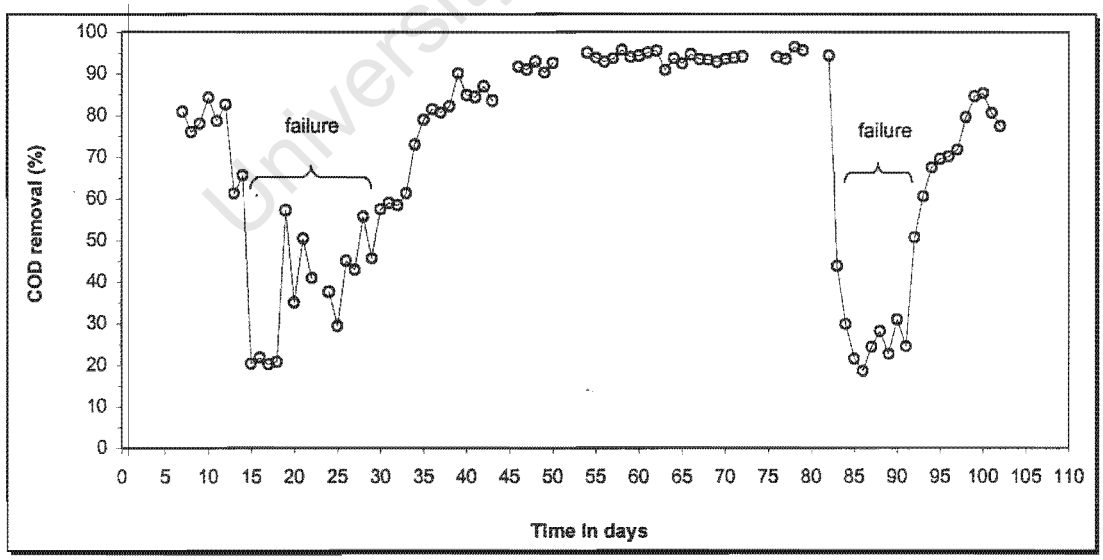

Fig 4.3 % COD removal versus time for unfiltered COD analysis.

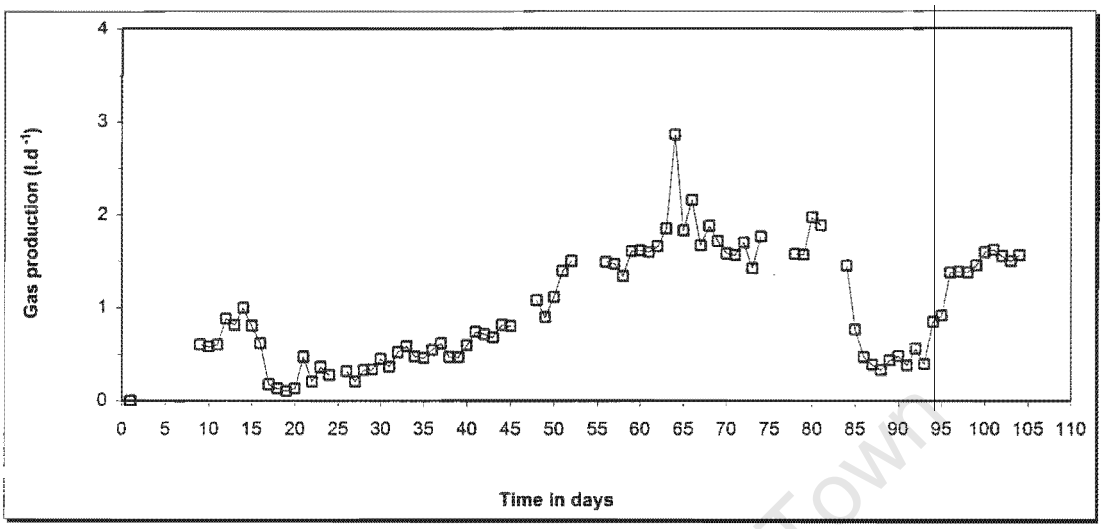

Fig 4.4 Daily biogas production (ℓ. d^{-1}).

8. CONCLUSIONS

From the results obtained during the preliminary investigation the following conclusions could be made:

- A sludge layer was formed on the liquid surface of the laboratory-scale UASB system, appearing as a thick gelatinous mass covered by a thin crust. This confirmed that the problem identified at full-scale could be reproduced at laboratory scale, validating the experimental protocol.

- The sludge layer above was present when both the centrifuged (high TSS) and drum filtered (low TSS) grain wastewaters served as influent. However, the sludge layer was very much reduced with the filtered grain wastewater compared to the centrifuged grain wastewater. This indicated that the causative agent for the sludge layer did appear to be related to the TSS content of the grain wastewater.

However, although drum filtering of the wastewater appeared to reduce the problem, it did not eliminate it.

- During periods of successful operation, % COD removal of >90 % could be achieved with both the centrifuged and filtered grain wastewater. However, the system was prone to upsets with relatively long recovery periods, of about 11 days.

The success in reproducing the sludge layer observed at full-scale in the laboratory-scale system prompted a more detailed investigation into this operational problem, and the behaviour of the UASB system when treating grain distillation wastewater, see Chapter 5.

CHAPTER 5

MAIN INVESTIGATION INTO TREATMENT OF GRAIN WASTEWATER IN A UASB SYSTEM AT SFW WELLINGTON DISTILLERY

1.1 INTRODUCTION

The full-scale UASB bioreactor at the SFW Wellington Distillery was designed and implemented to treat all wastewater types produced during the distillation processes at this distillery. However, in operation of the UASB system, two main problems were encountered (see Chapter 2), namely accumulation of a sludge layer on top of the UASB reactor at the overflow weirs during treatment of grain wastewater, and struvite formation during treatment of wine wastewater (struvite formation will be discussed in more detail in Chapter 6).

With regard to the sludge layer, in Chapter 4 a preliminary investigation into this phenomenon was presented. From this investigation it was concluded *inter alia* that, with grain wastewater as influent the sludge layer could be reproduced at laboratory-scale validating the experimental protocol, and that the accumulation of the sludge layer appeared related to the nature of the grain wastewater, in particular to the TSS content of this wastewater. In this Chapter, this experimental investigation will be extended with specific objectives:

- To confirm that the sludge layer is specific to the grain wastewater and is not related to distillery wastewaters in general, that is, to demonstrate that the layer does not accumulate with wine wastewater,

- To confirm the findings in Chapter 4 that the accumulation of the sludge layer is related in some fashion to the TSS content of the grain wastewater,

- To establish whether blending the grain wastewater with wine wastewater will eliminate the sludge layer problem,

- To compare UASB system performance with wine and grain wastewaters, and a blend of the two wastewaters, and

- To investigate the effect of substrate change on system performance, i.e. the effect of changing from wine to grain wastewaters, or a blend of these.

1.2 EXPERIMENTAL APPOACH

Two identical laboratory-scale UASB reactors were set up and operated in parallel, one as an experimental unit (Reactor 1) and the other as a control (Reactor 2). Thereafter:

- To acclimatise the biomass in both UASB systems and to establish identical performance in the systems, both were fed equal quantities and concentrations of wine wastewater as influent.

- The control system was maintained on wine wastewater as influent, and the experimental system switched to grain wastewater as influent, fed as a blend with wine wastewater and on its own.

- System performance of the experimental and control systems were monitored and compared with respect to sludge layer accumulation, COD removal and profiles of short chain fatty acids (SCFA), pH, COD, soluble phosphorus and FSA along the axis of flow through the UASB reactor.

2. EXPERIMENTAL METHODS

2.1 Reactor set-up

The two laboratory-scale UASB reactors used in this investigation were identical and were based on the reactor design used by Sam-Soon *et al.* (1989) for investigating pelletization in the upflow anaerobic sludge bed (UASB) reactor. The reactors

differed from Sam-Soon's design only in inner diameter and consequently reactor volume (due to the availability of perspex tube used to construct the reactors).

The laboratory-scale UASB reactors were transparent perspex cylinders (Fig 5.1). The inside diameter of the reactor is 120 mm and the height 1 600 mm, giving a total effective reactor volume of 10.2 litres. The bottom of the reactor is flat with four inlet ports evenly spaced around the circumference discharging in a horizontal direction. At the top of the reactor is the gas/liquid/solid separator. Gas collection is by means of a hollow inverted cone; rising gas bubbles are defected into the cone by a collar around the inside wall of the reactor below the cone. The gas passes from the cone, along a gas line, through a conical flask which served as a liquid trap to prevent carry over of liquid in the gas line, to a gas meter.

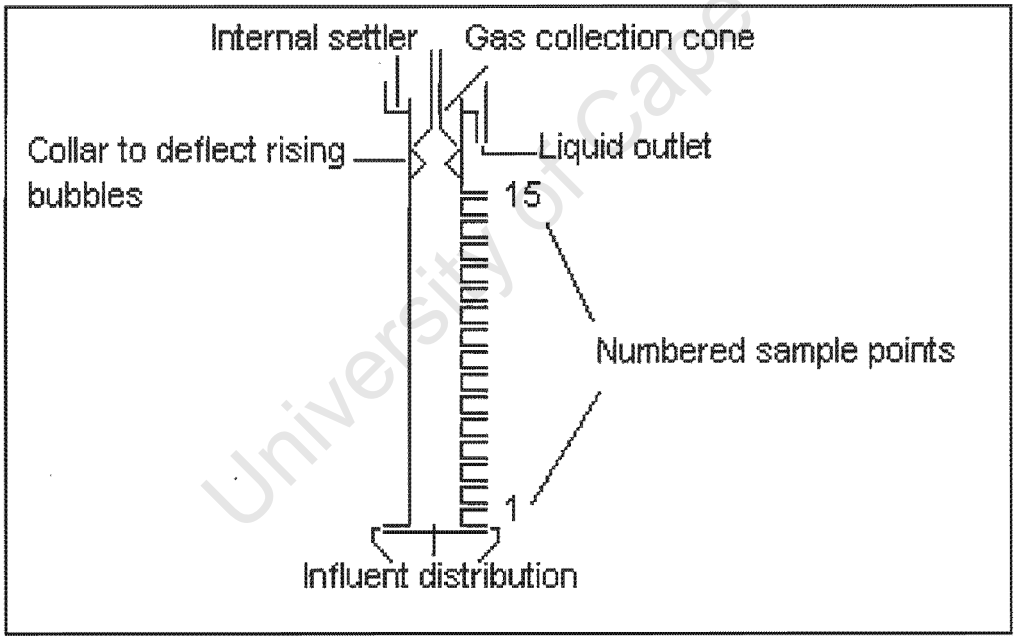

Fig 5.1 Schematic diagram of one of the laboratory-scale UASB reactors.

The volume of the effluent gas is measured by a wet gas meter (model No. DM3A, Alexander Wright, London). Effluent discharge is via an annular space between the gas collection cone and the reactor wall to enter a small solid/liquid separator (volume approximately 600 mℓ). Clarified liquid flows over a launder (v-shaped weirs) to the collection vessel while solids, which settle out, are returned into the reactor by gravity. Fifteen sampling ports are evenly spaced along the length of the reactor. Temperature in the reactor was maintained at 35°C (±1°C) by a thermostat controlled electrical heating tape wrapped around the reactor.

Both reactors were operated in a flow through mode with no recycle for alkalinity recovery (Wentzel *et al.*, 1994), since the objective was not to investigate pH control and the flow through system is simple to operate.

To prevent channelling in the sludge beds and to ensure free movement of gas through the sludge bed, the reactor contents were stirred by means of a slow internal stirrer (2 rpm) driven by a magnetic stirrer motor.

2.2 Wastewater characteristics

The influent feed stock was of three types:

1. Wine wastewater.
2. Unsettled grain wastewater.
3. Settled grain wastewater.

The wine and unsettled grain wastewater were those fed to the full-scale UASB system. These were collected from the SFW Wellington Distillery in 25 litre plastic canisters. The grain wastewater was collected after the decanting and centrifugation pre-treatment stages and the wine wastewater after centrifugation (see Chapter 2). The wastewaters were transported to the laboratory and stored in a refrigerated room at 4°C.

For the grain wastewater, to investigate the effects of the TSS content of this wastewater on sludge layer accumulation, a grain wastewater with high (>1 000 mg/ℓ) and low (<1 000 mg/ℓ) TSS content was used as influent feed to the laboratory-scale UASB systems. The decanted and centrifuged grain wastewater had TSS >1 000 mg/ℓ and this served as the high TSS grain wastewater feed, termed "unsettled grain wastewater". For the low TSS content grain wastewater, in Chapter 4 the grain wastewater was drum filtered to reduce the TSS. However, the drum filter was no longer available and could not be used to produce low TSS grain wastewater for this part of the investigation. Preliminary experiments indicated that extended settling (>2 days) reduced the TSS content of the grain wastewater to <1 000 mg/ℓ. Accordingly, to produce low TSS grain wastewater, the grain wastewater was settled for 3 days and the supernatant decanted to serve as influent feed to the laboratory-scale UASB reactors, termed "settled grain wastewater". The characteristics of the wastewaters are listed in Table 5.1.

Table 5.1 Wastewater characteristics.

Type	COD (mg/ℓ)	TKN (mgN/ℓ)	P (mgP/ℓ)	TSS (mg/ℓ)
Wine	20,000-30,000	300-350	180-200	100-500
Unsettled grain	25,000-30,000	170-180	270-300	>1 000
Settled grain	20,000-25,000	170-180	270-300	<1 000

The daily feed to the two laboratory-scale reactors were drawn from the appropriate concentrated feed stock, and diluted with tap water to the desired COD concentration. Where the experimental and control systems received the same influent, this was made up together and divided between the two systems. The pHs of the concentrated and diluted effluent were generally in the region of pH 4.0-4.5; i.e. highly acidic with a low buffer capacity. Accordingly, alkalinity was added in the form of 100-200 mg $NaHCO_3$ per 20 litres diluted feed to increase the pH and prevent the pH in the reactor from falling below the levels that inhibits methanogenesis (pH<6.8, Wentzel *et al.*,

1994). This caused the pH in the UASB reactors sludge beds to stabilise in the region of 7.

2.3 Feeding regime

Table 5.2 shows a record of the feeding regime and loading rates implemented over the entire study.

2.4 Analytical methods

The following parameters were measured to assess the reactor performance.

1. Unfiltered influent and effluent COD
2. pH in influent and settler
3. Gas production
4. Substrate flowrate
5. Effluent short chain fatty acids (SCFA) :- third period
6. Effluent H_2CO_3* alkalinity :-third period
7. Individual SCFA, pH, COD, soluble phosphorus and FSA profiles along the length of the reactors:- third period

COD's and FSA's were measured in accordance with Standard Methods (1985). Total soluble phosphorus was measured on 0.45 μm filtered samples, using persulphate digestion followed by molybdate vandate colourimetric reaction (Standard Methods, 1985).Gas production was measured by means of a wet gas meter (model No. DM3A, Alexander Wright, London). Gas monitoring did not give consistent and accurate readings due to a faulty gas flow meter, but rinsing bubbles in the gas collection cone gave a qualitative indication of gas production. The pH was measured with a portable Hanna pH meter (HI 9025) fitted with an epoxy combined pH electrode (Hanna HI 1230). SCFA and H_2CO_3* alkalinity were measured with the simple 5-point titration method described by Moosbrugger *et al.* (1992). Individual SCFA species were determined by gas chromatography using a Varian Model 3700

gas chromatograph equipped with a flame ionization detector (FID) and a Nukol™ fused silica capillary column (30 x 0.53 mm in diameter and 0.5 μm film thickness) (Supelco, Inc., Bellefonte). The column temperature was initially held at 105°C for 2 min, then increased at a rate of 8°C per min. to 190°C. The injector temperature was set at 130°C, while the detector was set at 300°C. Nitrogen was used as carrier gas at a rate of 6.1 mℓ min^{-1}. A sample volume of 0.5 $\mu\ell$ was introduced via the injector port. A calibration was made up of acetic, propionic, i-butyric, n-butyric, i-valeric and n-valeric acids added to 0.5 mℓ 0.1 N HCl with an internal standard of n-hexanol (26 %). The internal standard was chosen because its polarity and boiling point allowed it to be closest to the fatty acid peaks. The results were recorded and integrated on Borwin™ (JMBS Developments, Grenoble) integration software.

3. RESULTS

Three distinct periods of operation were identified, and are described separately below.

3.1 Period 1: Start-up

Granular anaerobic sludge taken from the full-scale UASB reactor at the SFW Wellington Distillery was used to seed the two laboratory-scale UASB systems. The two reactors were inoculated with approximately 4 litres of sludge respectively which formed a well-defined sludge bed. Prior to seeding, the sludge was rinsed with tap water in order to remove dead debris and fine particles, and the seed sludge contained well-structured granules, 1-2 mm in diameter. The operating temperature was set at 35°C (±1°C).

The COD loading and COD removal are shown plotted in Fig 5.2 and 5.3 respectively for both reactors 1 and 2. Detailed results are listed in Appendix B.

For the first 48 hours, only water was fed to the reactors while heating commenced. This was to ensure that the UASB seed sludge was thoroughly washed before the

Table 5.2 Details of the feeding regime.

REACTOR 1						REACTOR 2					
feeding periods day no.'s	average values during feeding periods: COD in (mg/ℓ)	flowrate (ℓ/d)	loading rate kgCOD/m³s-vol*/d	substrate feeding	comments	feeding periods day no.'s	average values during feeding periods: COD in (mg/ℓ)	flowrate (ℓ/d)	loading rate kgCOD/m³s-vol*/d	substrate feeding	comments
Period 1											
1-2				start-up: water	4ℓ sludge bed,no tests	1-2				start-up: water	4ℓ sludge bed,no tests
3-5				wine waste	4ℓ sludge bed,no tests	3-5				wine waste	4ℓ sludge bed,no tests
6-8	2123	8	4.2	wine waste	4ℓ sludge bed	6-8	2234	8	4.5	wine waste	4ℓ sludge bed
9-35	3524	9	7.9	wine waste	4ℓ sludge bed	9-35	3585	11	9.8	wine waste	4ℓ sludge bed
36-53	4210	8	8.4	wine waste	4ℓ sludge bed	36-53	4255	12	12.8	wine waste	4ℓ sludge bed
54-66	4324	8	8.6	wine waste	4ℓ sludge bed	54-84	4672	12	14.0	wine waste	4ℓ sludge bed
67-84	4925	11	13.5	wine waste	4ℓ sludge bed						
Period 2: *Restart systems with new wine wastewater feedstock; Reactor 1 experimental, Reactor 2 control*											
88-99	3767	4	7.5	start-up:new wine	2ℓ sludge bed	88-99	3784	4	6.1	start-up: wine	2.5ℓ sludge bed
100-106	5101	4	10.2	new winewaste	2ℓ sludge bed	100-106	5053	4	8.1	new winewaste	2.5ℓ sludge bed
107-125	4744	5	11.9	new winewaste	2ℓ sludge bed	107-131	4611	6	11.1	new winewaste	2.5ℓ sludge bed
126-131	4244	6	12.7	new winewaste	2ℓ sludge bed	132-157	5224	8	16.7	new winewaste	2.5ℓ sludge bed
132-177	4954	7	17.3	new winewaste	2ℓ sludge bed	158-247	5098	9	18.4	new winewaste	2.5ℓ sludge bed
178-185	4662	7	16.3	unsettled grain+wine	2ℓ sludge bed						
186-202	4864	8	19.5	unsettled grain+wine	2ℓ sludge bed						
203-204	3978	7	13.9	settled grain+wine	2ℓ sludge bed						
205-217	4153	8	16.6	settled grain	2ℓ sludge bed						
218-247	5470	8	21.9	unsettled grain	2ℓ sludge bed						
Period 3: *Restart systems; Reactor 1 control, Reactor 2 experimental*											
312-322	2494	7	4.5	start-up new wine	4ℓ sludge bed	312-322	2545	7	4.5	start-up new wine	4ℓ sludge bed
323-338	3624	7	6.3	new winewaste	4ℓ sludge bed	323-338	3572	7	6.3	new winewaste	4ℓ sludge bed
339-343	Clean unit; reduce sludge bed volume					339-343	Clean unit; reduce sludge bed volume				
344-394	5120	7	14.3	new winewaste	2.5ℓ sludge bed	344-395	5108	7	14.3	new winewaste	2.5ℓ sludge bed
395-141	6334	7	17.7	new winewaste	2.5ℓ sludge bed	396-414	4441	7	12.4	settled grain	2.5ℓ sludge bed

*s-vol = sludge bed volume

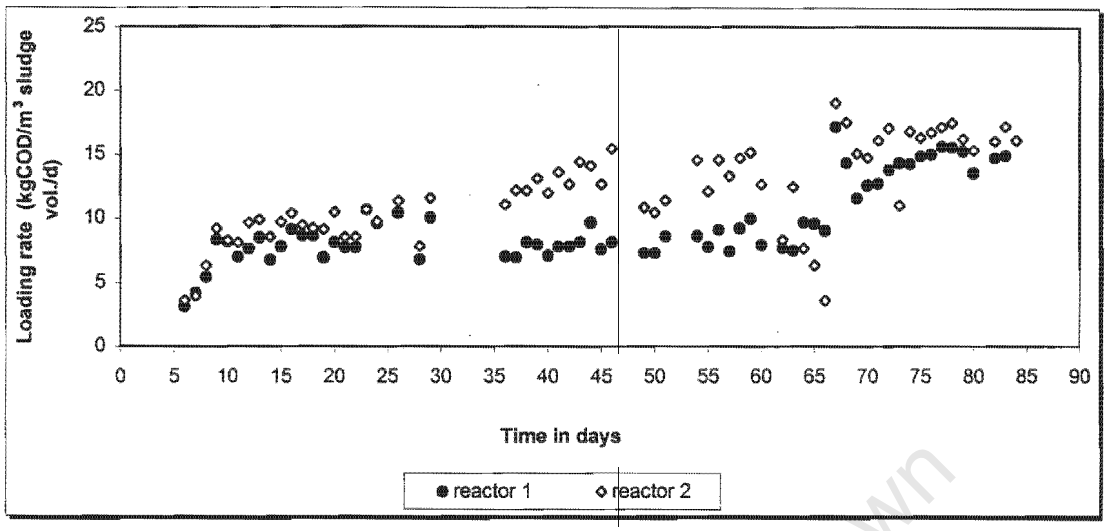

Fig 5.2 COD loading rate versus time for reactors 1 and 2 respectively – Period 1.

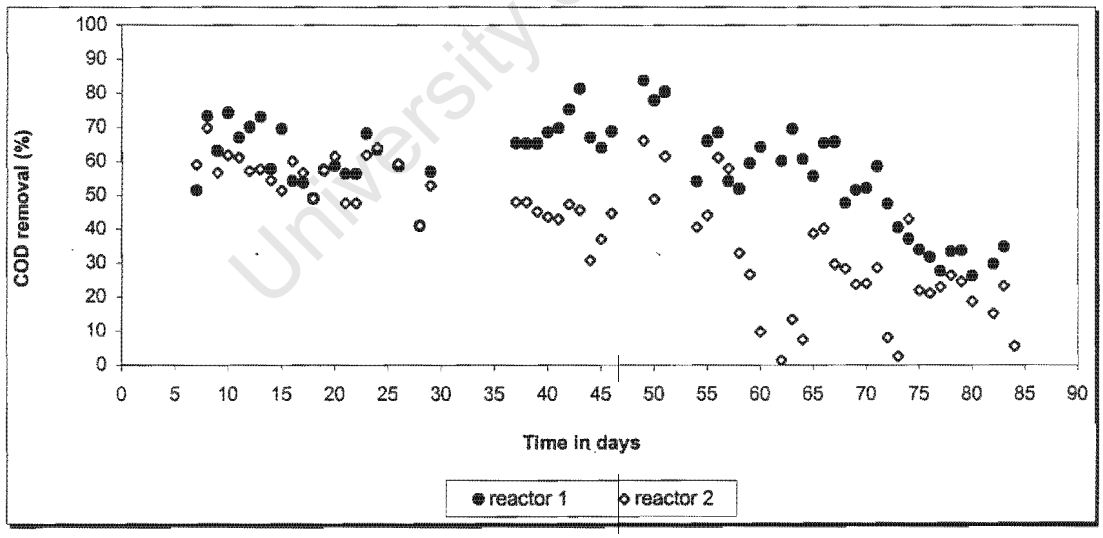

Fig 5.3 % COD removal versus time for reactors 1 and 2 respectively – Period 1.

investigation commenced. On the third day low concentrations of diluted wine wastewater were fed to both reactors for the next 3 days and by then the UASB reactors had attained the desired operating temperature (±1°C).

On the sixth day the diluted feed COD concentrations were measured at COD concentration of ±1 570 mg/ℓ for reactor 1 and 1 800 mg/ℓ for reactor 2 respectively. The flow rate for both units was set at 8 ℓ per day, giving a loading rate of 3 kgCOD/m^3 sludge volume/d for reactor 1 and 4 kgCOD/m^3 sludge volume/d for reactor 2 respectively. The COD removal obtained in both units was above 50 percent.

The first objective was to continue feeding both units with diluted wine waste until 90 percent or greater COD removal efficiencies were attained, indicating that the biomass had fully acclimatised, as accepted by Sam-Soon *et al.* (1989). However, the COD removal in both units remained poor, <70 % (see Fig 5.3). Accordingly, the substrate to the experimental unit could not be changed. Removal efficiencies decreased gradually, to well below 50 percent for both units towards the end of the first period (see Fig 5.3). Due to the poor COD removals it was decided to terminate the investigation on day 84. A definitive explanation for the poor COD removal behaviour of the UASB systems could not be identified at that stage. However, from results obtained during the start up for the second period (see below), it was concluded that the poor reactor performance during the first period was related to the wine wastewater "stock" used as feed for this period. This was confirmed by the fact that when "new" wine wastewater was collected from the distillery and fed to the units only 3 days after termination of the first period, the laboratory-scale units immediately showed vastly improved COD removal within the first week of start up, i.e. 90 percent COD removal was reached for both reactors. Figure 5.3 shows the COD removal versus time for reactors 1 and 2 during the first period; system failure is clearly illustrated.

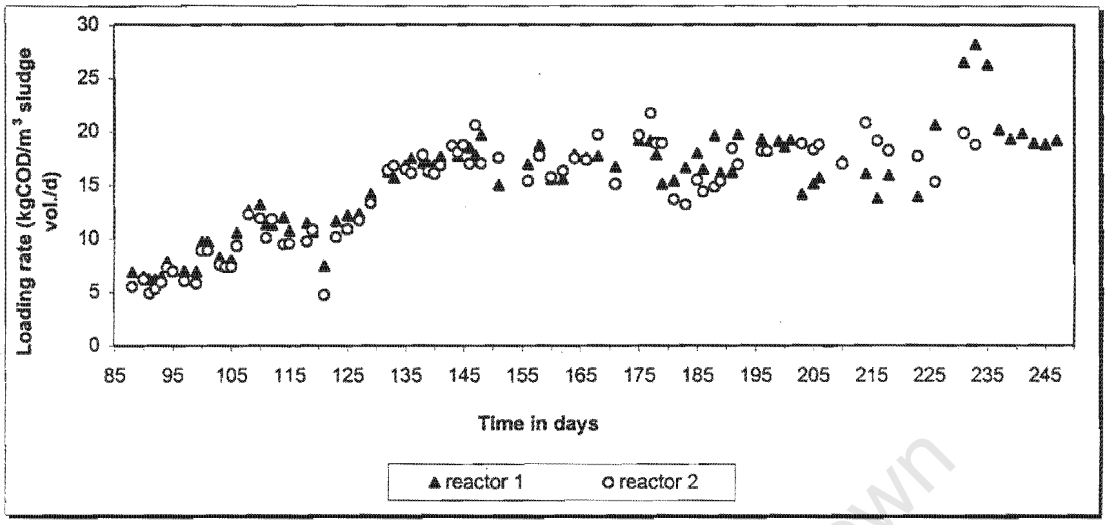

Fig 5.4 COD loading rate versus time for reactors 1 and 2 respectively – Period 2.

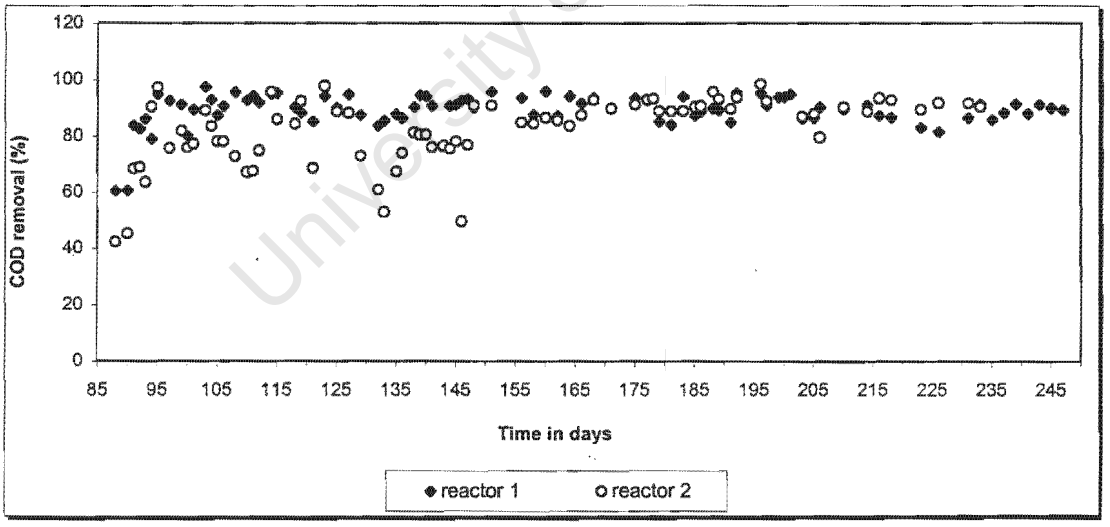

Fig 5.5 % COD removal versus time for reactors 1 and 2 respectively – Period 2.

3.2 Period 2

3.2.1 Start-up

The start up of the second period commenced on day 88 with "new" wine wastewater and reduced sludge volumes. The sludge beds in the reactors were drained to approximate 2.0 and 2.5 litres for reactor 1 and reactor 2 respectively. To acclimatise the sludge, diluted wine wastewater was fed initially to both units, at a COD of 3 441

mg/ℓ for both reactors 1 and 2 (Table 5.2). The flow rate employed was set at 4 ℓ per day for both units, i.e. COD loading rate of 7 kgCOD/m^3 sludge volume/d and 6 kgCOD/m^3 sludge volume/d for reactor 1 and 2 respectively. The loading rate was kept constant for both reactors and after one week COD removal efficiencies of 90 percent were obtained. Once it was accepted that the sludge beds in both units were fully acclimatised to the wine wastewater the main study commenced.

3.2.2 Loading rate

For the second period, loading rates for reactors 1 and 2 are shown in Fig 5.4. The loading rate was gradually increased from an initial loading rate of 7 kgCOD/m^3 sludge volume/d for reactor 1 and 6 kgCOD/m^3 sludge volume/d for reactor 2 respectively. Acceptable organic loadings were achieved in both systems, at about 18 kgCOD/m^3 sludge volume/d.

In order to have a "standard" reference, organic loading were calculated in terms of the mass of substrate COD fed per day per sludge bed volume (kgCOD/m^3 sludge volume/d).

3.2.3 Substrate feed

During this investigation period (period 2) the main objective was to implement substrate changes to the experimental unit (reactor 1) and compare its performance against the control unit (reactor 2). On day 178 the feed to the experimental reactor was changed from wine wastewater to a 1:1 blend of unsettled grain and wine wastewaters. This blend was maintained for 24 days until day 202 when another feed change was made. A 1:1 blend of settled grain and wine wastewater was fed to the

experimental unit for two days, thereafter only settled grain wastewater was fed for 13 days, from day 205 to day 217. On day 218 the final feed change was made and only unsettled grain wastewater was fed for a further 30 days until the termination of the investigation on day 247.

3.2.4 System performance

In Fig 5.4 COD loading and Fig. 5.5 the COD removal versus time are shown for reactors 1 and 2 respectively during the second period. In Table 5.2, the substrate feeds applied are shown. Detailed results are listed in Appendix B.

From Fig 5.5, for the first 90 days the influent feed was wine wastewater. Within 8 days of start up (day 95) reactor 1 achieved COD removals >90 % and these removals were maintained throughout the investigation. For reactor 2, initially COD removals were very variable due to problems in operation of the laboratory-scale system, but after about 60 days (day 148) removals >90 % were achieved and maintained for the rest of the investigation. This indicated that the sludge masses were fully acclimatised to the operating conditions. Also, both systems were able to accommodate the increase in loading rate (see Figs 5.4) without deterioration in effluent quality. Accordingly, the substrate changes (see 3.2.3 above) were implemented for reactor 1. For reactor 1 removals >90 % were achieved with influent feed of wine wastewater, 1:1 blend of wine and unsettled grain wastewater and settled and unsettled grain wastewater only. Furthermore, following a substrate change no deterioration in system performance was experienced. These observations confirmed the conclusions from the preliminary investigation in Chapter 4 that system performance with grain wastewater in all forms is good. Also, very little or no adaptation is necessary in switching from one feed type to the other. Furthermore, the grain wastewater in all forms maintained the well-defined pelletized sludge bed, with pellets of diameter ±2 mm.

These results confirm the conclusions drawn in Chapter 4, that grain wastewater can be successfully treated in the UASB system, provided sludge layer accumulation (see below) can be accommodated. It was noted that a better quality effluent was obtained when treating wine wastewater, compared to the other substrates. The effluent quality of the mixed wine and unsettled grain wastewaters, unsettled and settled grain

wastewaters, did contain some turbidity due to grain solids. However, since COD removals were calculated from the unfiltered influent COD and unfiltered effluent COD for all the wastes, this turbidity did not contribute significantly to effluent COD. Figure 5.6 shows effluent pH values over the second period for the experimental unit compared to the control unit. No additional alkalinity was required at each feed change other than that referred to previously.

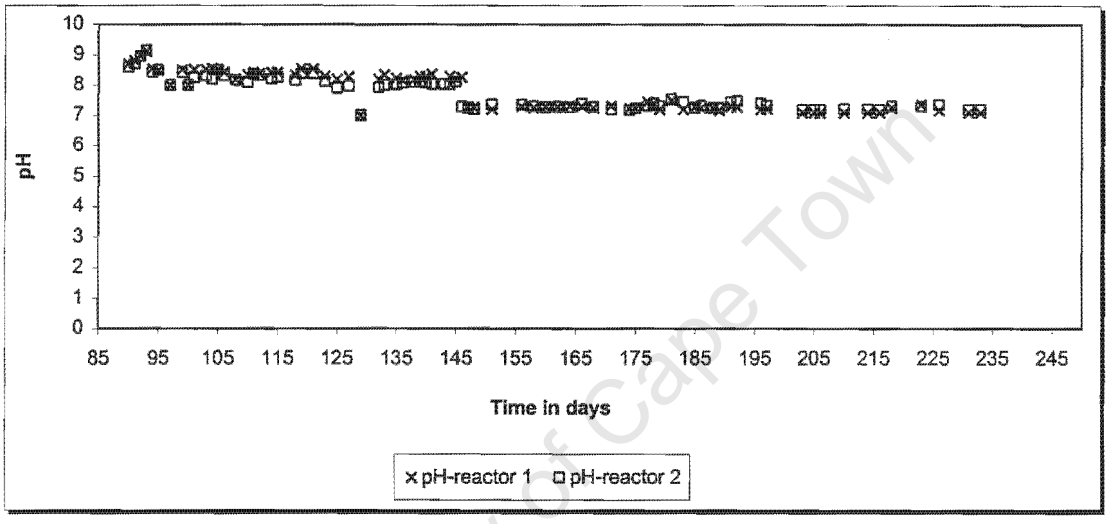

Fig 5.6 Effluent pH values for reactor 1 and 2 respectively – Period 2.

3.2.5 Sludge layer accumulation

Both reactors treated wine wastewater for the first 90 days from start up of the second period. Optimum COD removal, i.e. 90 percent efficiencies, were obtained in both reactors after one week from start up, though some operational problems were experienced with reactor 1, see above. Removal efficiencies of 90 percent or greater were an indication that the sludge masses were fully acclimatised to the substrate feed. Some foaming was observed at optimum COD removal efficiencies, but did not prove problematic and was caused by extensive gas production.

Accumulation of the sludge layer was evaluated daily. With the wine wastewater, sludge layer accumulation was never observed. However, with the grain wastewater in any form, i.e. blend, settled or unsettled, the sludge layer accumulated; if physically removed, the layer redeveloped within 24 hours. These observations confirm that the sludge layer accumulation is a property of the grain wastewater and not distillery wastewaters in general. The sludge layer accumulation was most severe with the unsettled grain wastewater, and reduced in the blend and settled grain wastewaters. This confirmed the findings in Chapter 4, that the sludge layer accumulation was linked to the solids content of the grain wastewater. However, blending the grain wastewater with wine wastewater, or settling the grain wastewater reduced but did not prevent sludge layer accumulation. This is in agreement with the result on the drum filtered grain wastewater (see Chapter 4). Therefore, settling or drum filtering the grain wastewater prior to treatment in the UASB system can reduce, but not eliminate the sludge layer accumulation.

3.3 Period 3

3.3.1 Introduction

The third period commenced after a long shutdown period of 64 days. Once it was established that sludge layer accumulation is a phenomenon common to the treatment of any type of the grain wastewater (centrifuged, filtered, settled, or blended) this was investigated in more detail. The main objective of this part of the investigation was to understand in more detail UASB reactor behaviour when treating a grain wastewater compared to a UASB reactor treating wine wastewater. This involved comparing the concentration profiles along the line of flow of the UASB reactor when treating grain and wine wastewaters.

The study was divided into the following tasks, to:

- Set up two laboratory-scale UASB reactors in parallel (see Section 2.1 above).
- Acclimatise both units on wine wastewater and monitor performance.

- Replace the feed of the one reactor with settled grain wastewater and monitor and compare the performance.

- Compare the concentration profiles along the line of flow between both units.

3.3.2 Start–up

On day 312, the third investigation period commenced with the following changes introduced. "New" sludge was collected from the UASB system at the SFW Wellington Distillery. In the experimental unit, the "new" sludge was used to replace the "old" sludge from the second period with an effective volume of 4 litres. The sludge was replaced because during period 2 this system had received grain wastewater; both systems were to be started on wine wastewater. Since the full-scale UASB reactor was receiving wine wastewater, the sludge was not rinsed as previously done. Some "new" sludge was also added to the control unit, to increase the volume to ±4 litres. The same wine wastewater that served as influent during the second period was used as substrate feed. Diluted wine wastewater was fed to both units to acclimatise the seeding sludges. The initial loading rates were 3 kgCOD/m^3 sludge volume/d and 4 kgCOD/m^3 sludge volume/d for reactor 1 and 2 respectively.

Reactor 1, which operated as the experimental unit during the second period, was operated as the new control unit and visa versa.

3.3.3 Operation

Figure 5.8 show COD loading versus time for reactors 1 and 2 respectively over the third period of the study.

The loading rates were gradually increased to 8 kgCOD/m^3 sludge volume/d before both units were shut down on day 338 and cleaned. Sludge from both units was drained leaving a balance of ±2.5 litres sludge in both.

Thereafter, the loading rates were immediately increased from 8 to 13 kgCOD/m^3 sludge volume/d for the control unit and to 14 kgCOD/m^3 sludge volume/d for the experimental unit respectively. On day 396 the feed to the experimental unit was changed to diluted settled grain wastewater (see Section 2.3 above).

During the study the following parameters for both systems were measured:

- In the influent: Unfiltered COD and pH.
- In the effluent: Unfiltered COD, pH and total SCFA and H_2CO_3* alkalinity (occasionally).
- Occasional profile measurement of COD, FSA, SCFA species, pH along the line of flow in the reactor.

Samples from the reactor ports down the reactors were taken by means of a special device that allowed the sample to be extracted and pH measured without loss of dissolved gases, particularly CO_2; loss of CO_2 causes change in pH but does not influence alkalinity (Loewenthal *et al.*, 1989). The sampling device is shown schematically in Figure 5.7.

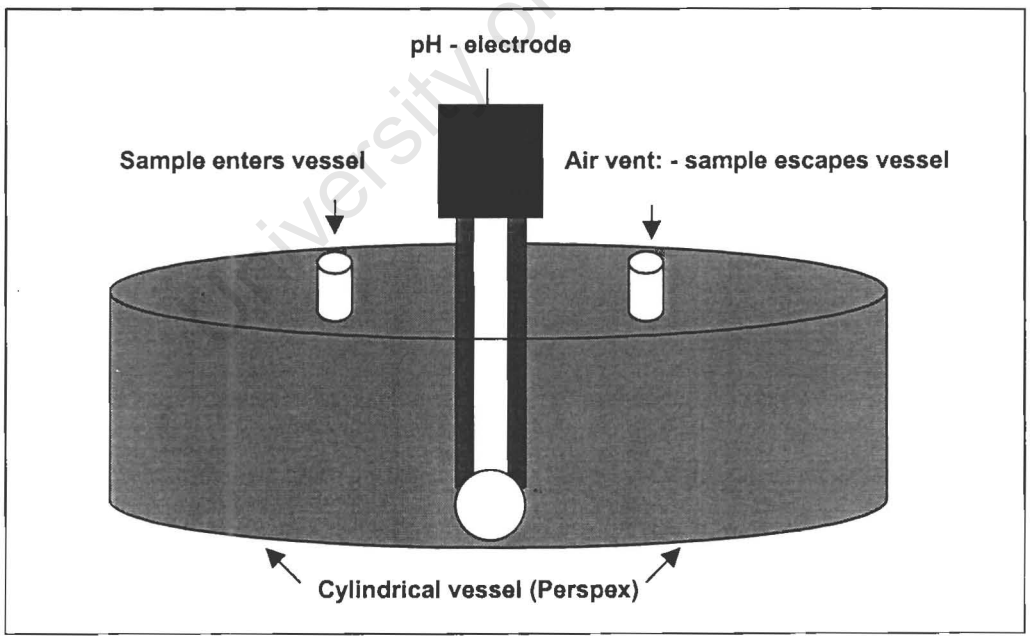

Fig 5.7 Schematic diagram of the pH sampling vessel.

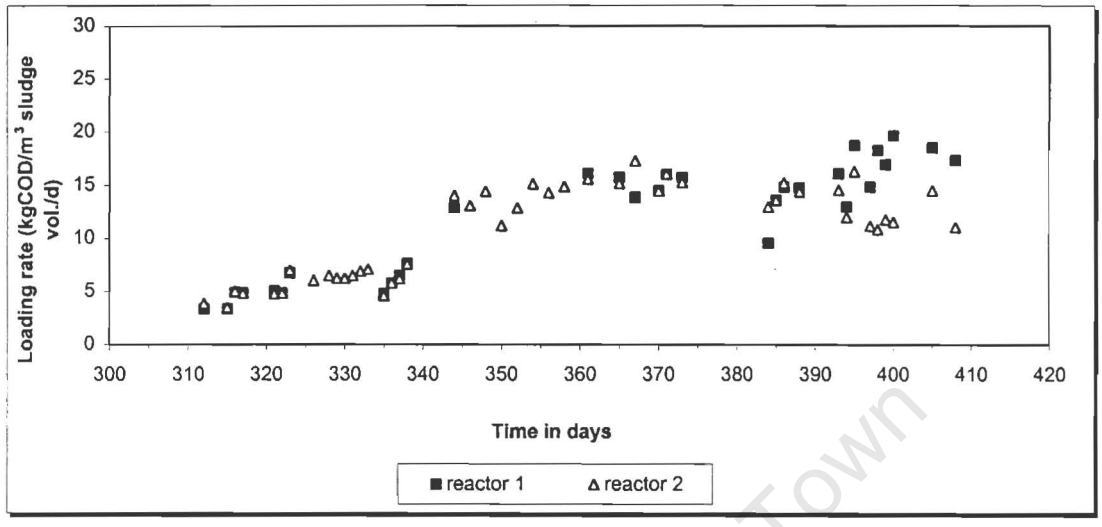

Fig 5.8 COD loading rate versus time for reactors 1 and 2 respectively – Period 3.

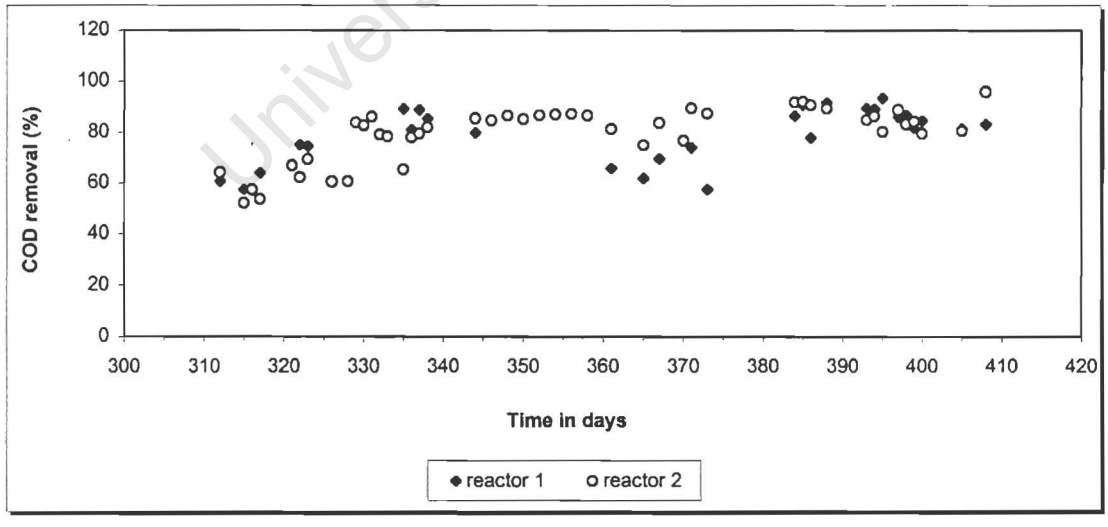

Fig 5.9 % COD removal versus time for reactors 1 and 2 respectively – Period 3.

3.3.4 System performance

In Fig 5.8 COD loading and in Fig 5.9 COD removal versus time for reactors 1 and 2 are shown respectively during the third period. In Table 5.2, the substrate feeds applied are shown. Detailed results are listed in Appendix B.

From Fig 5.9, for the first 27 days the influent feed was wine wastewater. Both UASB systems achieved COD removals of >80 %. On day 339, the units were shutdown for 1 day for cleaning, and the sludge in each unit was drained to an effective volume of 2.5 litres. On day 344, both reactors were started up on wine wastewater again at higher loading rates (see Fig 5.8). From Fig 5.9 it can be seen that the COD removals in both systems respectively increased gradually with time. For reactor 1, COD removals >80 % were achieved on day 384 and these removals were maintained for the rest of the investigation. For reactor 2, COD removals >80 % were also achieved, but decreased slightly when settled grain wastewater was fed to reactor 2 from day 396 (see Fig 5.8). However, COD removals >80 % were maintained for the rest of the investigation (see Fig 5.9).

Fig 5.10 (a) and Fig 5.10 (b) shows the effluent SCFA concentrations and H_2CO_3* alkalinity concentrations respectively for reactor 1 and 2, for the period from day 393 to day 400. Fig 5.10 (a) and (b) also shows the substrate change for reactor 2 during this period.

From Fig 5.10 (a) it is noted that the effluent SCFA concentrations for reactor 2 decreased when this reactor was switched from wine wastewater to settled grain wastewater, from 200 to 400 mg/ℓ as HAc to values as low as 0 mg/ℓ as HAc. Fig 5.10 (b) shows alkalinity generated for reactor 2 when settled grain wastewater was treated, is lower than when wine wastewater was treated, but started increasing as the sludge adapted to the settled grain wastewater.

With regard to the effluent SCFA, the reduction in concentration on switching from wine wastewater to settled grain wastewater indicates a notable change in behaviour; this is confirmed and dealt with in more detail when comparing the bed profiles with the two wastewaters, see Section 3.3.5 below.

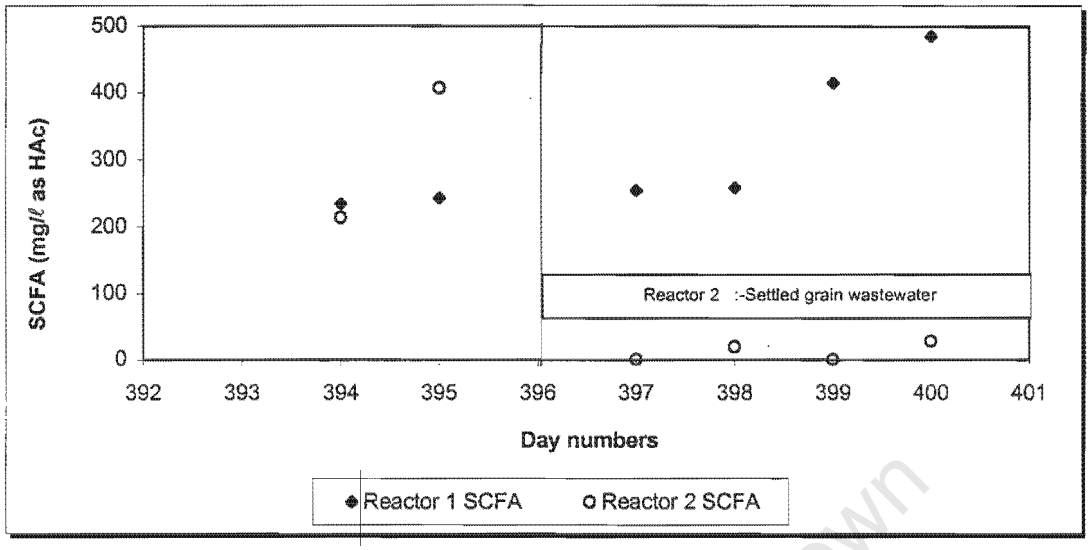

Fig 5.10 (a) Effluent SCFA concentrations for reactors 1 and 2 respectively – Period 3 at specific days.

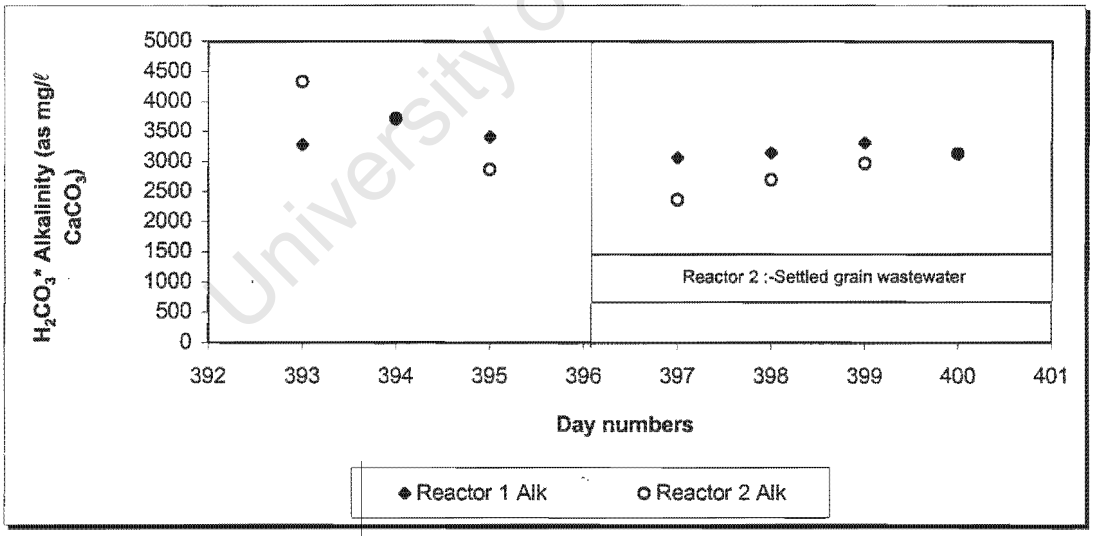

Fig 5.10 (b) Effluent Alkalinity (as mg/ℓ $CaCO_3$) for reactors 1and 2 respectively – Period 3 at specific days.

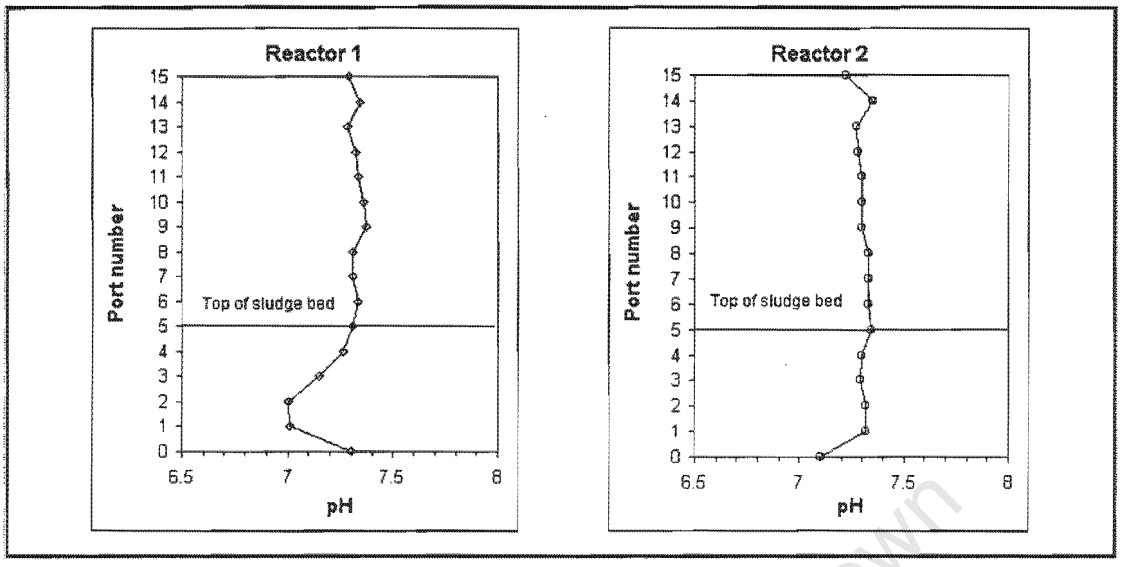

Fig 5.11 (a) Comparison of pH profiles observed in the UASB system treating wine wastewater (Reactor 1) and grain wastewater (Reactor 2) respectively.

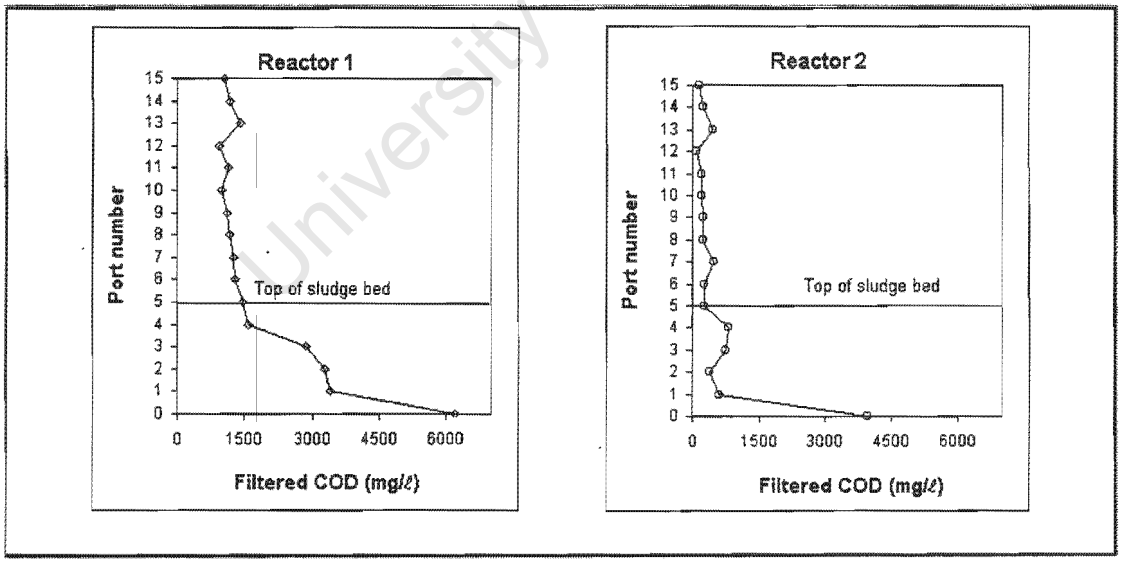

Fig 5.11 (b) Comparison of filtered COD concentration profiles observed in the UASB system treating wine wastewater (Reactor 1) and grain wastewater (Reactor 2) respectively.

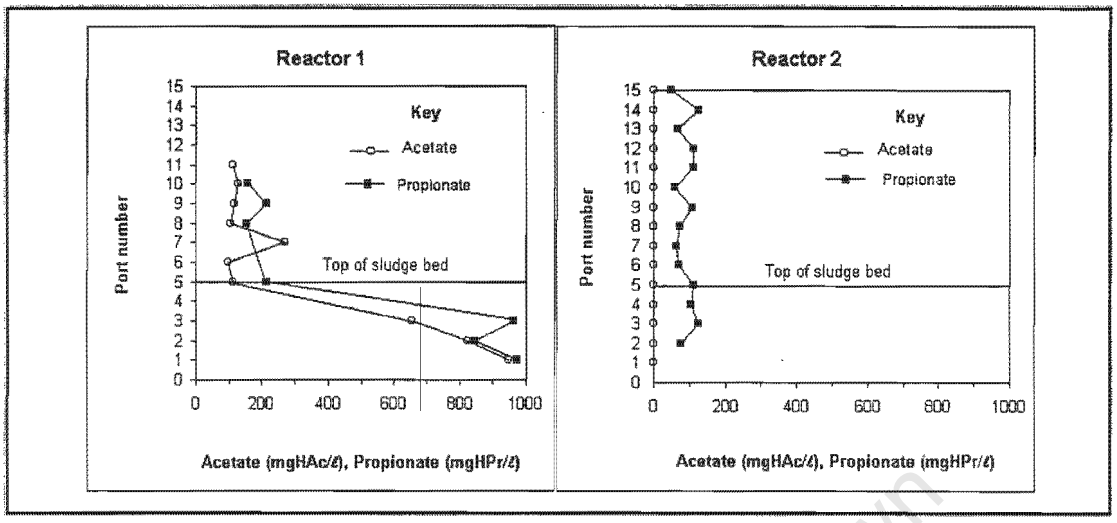

Fig 5.11 (c) Comparison of HAc and HPr concentration profiles observed in the UASB system treating wine wastewater (Reactor 1) and grain wastewater (Reactor 2) respectively.

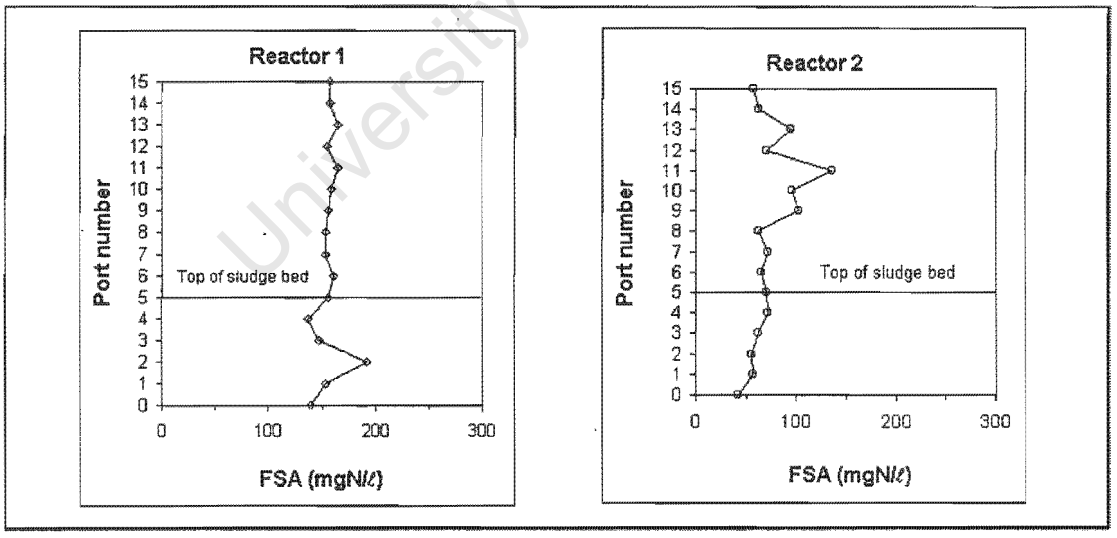

Fig 5.11 (d) Comparison of FSA concentration profiles observed in the UASB system treating wine wastewater (Reactor 1) and grain wastewater (Reactor 2) respectively.

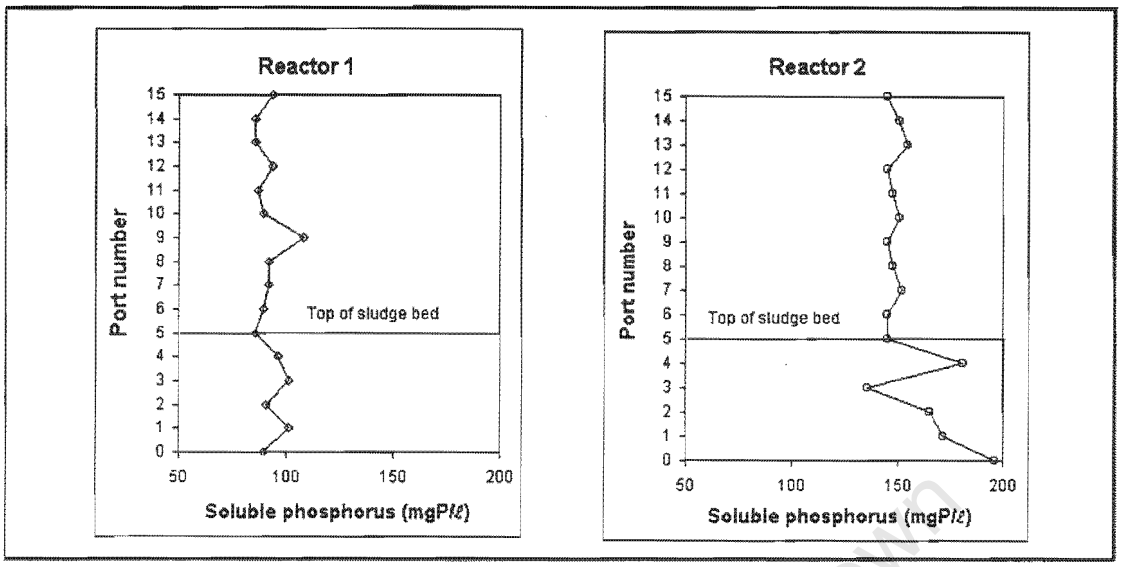

Fig 5.11 (e) Comparison of soluble phosphorus concentration profiles observed in the UASB system treating wine wastewater (Reactor 1) and grain wastewater (Reactor 2) respectively.

3.3.5 Concentration profiles

Fig 5.11(a, b, c, d and e) shows concentrations profiles taken on day 408 along the length of reactors 1 and 2 respectively for pH, COD, FSA, P_T and SCFA species concentrations. On day 408, reactor 1 treated "new" wine wastewater and reactor 2 settled grain wastewater.

With regard to the profiles measured with wine wastewater (Reactor 1), these conform to profiles measured previously with apple juice wastewater (Sam-Soon *et al.*, 1987), glucose (Sam-Soon *et al.*, 1990), protein (Moosbrugger *et al.*, 1990), brewery wastewater (Moosbrugger *et al.*, 1993a) and wine distillery wastewater (Moosbrugger *et al.*, 1993b):

pH: From Fig 5.11(a), the pH declines in the lower part of the sludge bed to a minimum pH=7 at Port 2. This indicates that influent alkalinity was sufficient to buffer the pH above the minimum value of 6.6 suggested by Sam-Soon *et al.* (1987)

and Wentzel *et al.* (1994). This decline in pH coincides with the increase in acetic (HAc) and propionic (HPr) acids, see Fig 5.11(c). Above Port 2, the pH increases to reach pH=7.33 by Port 5 (top of the sludge bed) and thereafter stabilizes at approximately this value. This increase in pH corresponds to the decrease in HAc and HPr due to biological consumption, see Fig 5.11 (c).

COD: From Fig 5.11 (b) the COD profile (supernatant COD after settling pellets) shows a decrease in the lower part of the sludge bed to reach a value of about 3 272 mgCOD/ℓ by Port 1. Thereafter, the COD decreases more slowly, to reach 1 500 mgCOD/ℓ by Port 5 (top of sludge bed), and 970 mgCOD/ℓ by Port 10.

HAc: From Fig 5.11 (c), HAc increases in the lower part of the sludge bed to reach a maximum of about 950 mgHAc/ℓ by Port 2. Thereafter, HAc concentration decreases to reach about 100 mgHAc/ℓ by Port 5, and remains at approximately this value through the rest of the sludge bed.

HPr: From Fig 5.11 (c), HPr conforms to the HAc profile, reaching a maximum of approximately 950 mgHPr/ℓ in the lower part of the sludge bed and decreasing to a minimum of 150 mgHPr/ℓ in the top part of the sludge bed.

Free and saline ammonia (FSA): From Fig 5.11 (d), FSA initially increases to reach about 195 mgN/ℓ at Port 2, due to deamination of organic N present in the influent. Thereafter, FSA exhibits a decrease to reach a minimum of about 155 mgN/ℓ through the rest of the bed, due to uptake of FSA for cell and pellet polymer synthesis.

Soluble phosphorus: From Fig 5.11 (e) phosphorus exhibits only a small decrease through the sludge bed due to the uptake for cell synthesis.

As noted earlier, this behaviour conforms to that observed by Sam-Soon and co-workers. To explain the behaviour, they proposed that three distinct zones can be identified (Wentzel *et al.*, 1994):

- *A lower active zone* in which concentrations of the SCFAs, propionate and acetate, increase to maxima, soluble COD reduces to less than half its influent value, and pH declines to a minimum. – Ports 0 to 2 here.

- *An upper active zone* in which the propionate and acetate concentrations decrease to minima, COD decreases to a near minimum, NH_3-N remains near constant, and pH increases to a stable value. – Ports 2 to 4 here.

- *An upper inactive zone* in which no observable biokinetic activity is observed. – Ports 4 to 5 here.

From the biochemistry of digestion process (McInerney *et al.*, 1979), Sam-Soon and co-workers identified microorganism behaviour in the three zones as follows (Wentzel *et al.*, 1994):

- *In the lower active zone* – acidogens generate SCFA, principally acetic (HAc) and propionic (HPr), carbon dioxide (CO_2) and hydrogen (H_2) from the influent substrate. The hydrogen is generated at such a rate that a high hydrogen partial pressure (high pH_2) is created; this is indicated by the observed increase in HPr which is produced only under high pH_2 ($>10^{-3.7}$ atm). Hydrogenotrophic methanogens generate methane (CH_4) from H_2 and CO_2; Acetoclastic methanogens convert some HAc to CH_4 and CO_2; Acetogens are inactive due to the high pH_2.

- *In the upper active zone* – the pH_2 has been reduced to, and maintained at, such low values due to action of hydrogenotrophs that; acetogens can convert HPr to HAc, H_2 and CO_2; acetoclastic methanogens convert all the HAc to CH_4 and CO_2.

- *In the upper inactive zone* – no observable biological activity takes place.

From the above, it is apparent that the differentiation of the sludge bed into lower and upper active zones is based on whether HPr generation takes place (lower active, high pH_2) and whether HPr oxidation to HAc occurs (upper active, low pH_2) or not (lower

active, high pH_2); HPr is generated by acidogens only under high pH_2 and oxidized to HAc by acetogens only under low pH_2.

From the observations made here, these proposals apply also to the UASB system treating wine wastewater. However, the profiles for the UASB system treating grain wastewater differ markedly from those for the UASB system treating wine wastewater:

pH: From Fig 5.11 (a), the pH profile does not exhibit the characteristic decrease in the lower part of the sludge bed followed by an increase in the upper part of the bed, but shows an initial increase from the influent value of 7.1 to 7.34 by Port 1. Thereafter pH remains approximately constant at pH=7.34 throughout the sludge bed.

COD: From Fig 5.11(b), the COD decreases from the influent value of 3 959 mgCOD/ℓ to about 600 mgCOD/ℓ at Port 1, and thereafter decreases slowly to about 280 mgCOD/ℓ by Port 5 and remains at this value throughout the rest of the reactor.

HAc: From Fig 5.11 (c), negligible HAc were measured throughout the sludge bed. This conforms with measurements made on effluent samples, Section 3.3.4 above.

HPr: From Fig 5.11 (c), the HPr is constant through the sludge bed at a low value of about 80 mgHPr/ℓ.

FSA: From Fig 5.11 (d), the FSA shows slight increase through the sludge bed, probably due to deamination of organic-N from the influent.

Soluble phosphorus: From Fig 5.11 (e), soluble phosphorus shows a small decrease through the sludge bed due to uptake for cell synthesis.

The profile for the UASB system treating grain wastewater indicates that with this wastewater the three zones of behaviour identified for the system treating wine wastewater (and other similar wastewaters, Wentzel *et al.*, 1994) do not develop to any marked extent. A possible explanation for this is that the grain wastewater

contains considerable suspended solids. The rate of acidogenesis with suspended solids as substrate would be limited by the rate of hydrolysis. Typically, hydrolysis rates would be much slower than acidogenesis rates with a soluble substrate. The net effect is to lower the overall rate of acidogenesis. With the lower acidogenic rates, as fast as the short chain fatty acids are produced they would be consumed in the subsequent reactions, and no significant short chain fatty acids would be observed. Also, the low rate of acidogenesis implies that the rate of H_2 production is low so that a high pH_2 zone does not develop in the sludge bed.

The absence of a differentiation of the behaviour in the UASB pelletized bed into three distinct zones when treating grain wastewaters raises the question of the long term viability of a UASB system treating grain wastewater. In developing their hypothesis for pelletization in UASB systems, Sam-Soon *et al.* (1987) proposed that partial phase separation of the anaerobic processes and development of a zone with a high hydrogen partial pressure were essential for pellet formation (Wentzel *et al.*, 1994). In the UASB system treating grain wastewater here, observations (no HAc and little HPr) indicate that these prerequisites for pellet formation are not achieved. If this is true, according to the hypothesis of Sam-Soon *et al.* pellet growth will not occur, or will be greatly reduced. This indicates that, in the long term in switching from wine wastewater (where pellet growth has occurred) to grain wastewater there will be a gradual loss of the pelletized sludge bed, until the pelletized bed declines to such low values that the system will fail. It is probable that the laboratory-scale systems here receiving grain wastewater as influent were not operated for periods long enough for the loss of sludge bed to be noticeable. Some loss of pelletized bed was observed, with pellet debri accumulating in the sludge layer on the liquid surface, but pellet break-up and loss is a feature common in UASB systems. The systems would have to be operated for longer periods to determine whether sludge bed loss is significant.

The investigation here does indicate that when switching from wine wastewater, where a well-defined pelletized sludge bed has been developed, to grain wastewater, the grain wastewater can be effectively treated in the short term. However, most likely the sludge bed will diminish with time. To re-establish the pelletized bed, the system will have to be switched back to wine wastewater for a period.

4. CONCLUSIONS

From the results obtained in this investigation the following conclusions could be made:

- In conformity with the conclusions made in the preliminary investigation (Chapter 4); when treating grain wastewater, a sludge layer was formed on the liquid surface of the laboratory-scale UASB system, appearing as a thick gelatinous mass. This confirmed that the problem identified at full-scale could be reproduced at laboratory scale, validating the experimental protocol.
- The sludge layer above was present with the grain wastewater in any form, i.e. blended with wine wastewater, settled or unsettled grain wastewater only. The sludge layer accumulation was most severe with unsettled grain wastewater, and reduced in the blend and settled grain wastewater – blending the grain wastewater with wine wastewater or settling the grain wastewater reduced, but did not eliminate sludge layer accumulation.

- With wine wastewater, sludge layer accumulation was never observed.

- The observations above indicate that sludge layer accumulation is a property of the grain wastewater, and not distillery wastewaters in general. Also, in conformity with the conclusions made in Chapter 4, the sludge layer accumulation is linked to the solids content of the grain wastewater. Reducing the solids content by drum filtration (Chapter 4), or settling or blending (Chapter 5) can reduce but not eliminate the sludge layer accumulation.

- The bed profiles measured for the UASB system treating wine wastewater conform to those measured previously with apple juice wastewater (Sam-Soon *et al.*, 1987), glucose (Sam-Soon *et al.*, 1990), protein (Moosbrugger *et al.*, 1990), brewery wastewater (Moosbrugger *et al.*, 1993a) and wine distillery wastewater (Moosbrugger *et al.*, 1993b). In these profiles the typical three distinct zones of behaviour can be identified, namely lower active, upper active and upper inactive zones. The action of microorganisms in these zones conforms to the proposals of Sam-Soon and co-workers (Wentzel *et al.*, 1994).

- For the UASB system treating grain wastewater, the bed profile differs markedly from that above. The three zones of behaviour do not develop to any marked extent. A possible explanation proposed for this behaviour is that the grain wastewater contains considerable suspended solids. The rate of acidogenesis with suspended solids as substrate, would be limited by the rate of hydrolysis. Typically, hydrolysis rates would be much slower than acidogenesis rates with a soluble substrate. The net effect is to lower the overall rate of acidogenesis. With the lower acidogenic rates, the short chain fatty acids would be consumed in subsequent reactions as fast as they are produced, with the result that the short chain fatty acids concentrations would remain low throughout the UASB system.

- With grain wastewater, the absence of a differentiation into the three zones of behaviour raises the question of the long term viability of a UASB system treating this type of wastewater. In developing their hypothesis for pelletization in UASB systems, Sam-Soon *et al.* (1987) proposed that partial phase separation of the anaerobic processes and development of a zone with a high hydrogen partial pressure were essential for pellet formation (Wentzel *et al.*, 1994). In the UASB system treating grain wastewater here, observations (no HAc and little HPr) indicate that these prerequisites for pellet formation are not achieved. If this is true, according to the hypothesis of Sam-Soon *et al.* pellet growth will not occur, or will be greatly reduced. This indicates that, in the long term in switching from wine wastewater (where pellet growth has occurred) to grain wastewater there will be a gradual loss of the pelletized sludge bed, until the pelletized bed declines to such low values that the system will fail. This aspect requires further investigation.

- The investigation here does indicate that when switching from wine wastewater, where a well-defined pelletized sludge bed has been developed, to grain wastewater, the grain wastewater can be effectively treated in the short term. However, most likely the sludge bed will diminish with time. To re-establish the pelletized bed, the system will have to be switched back to wine wastewater for a period.

CHAPTER 6

EQUILIBRIUM CHEMISTRY AND KINETICS OF STRUVITE PRECIPITATION AT 37^{o}C

1. INTRODUCTION

At the full-scale UASB system at the SFW Distillery at Wellington, one major operational problem experienced was precipitation of struvite ($MgNH_4PO_4$) when treating wine wastewater (see Chapter 2). The struvite formed within the effluent collection pipework, mostly where pressure changes occurred, for example at pipe bends, as reported by Loewenthal *et al.* (1994). The mass of precipitant formed was so extensive that it caused substantial narrowing of the pipework, from diameter 90 mm to less than 20 mm within two weeks. This restricted flows, eventually leading to operational failure and system shutdown (see Chapter 2). Physical removal of the precipitant with high-pressure jet sprays and scraping equipment were unsuccessful. Furthermore, the structural design and layout of the effluent discharge pipe network limited access for cleaning. Laboratory tests on dissolving struvite with various strong acids and bases were conducted at SFW Laboratories at Stellenbosch. These indicated that a 30-40 % solution of concentrated caustic soda dissolved the struvite crystal to form a slurry that could be easily removed with high pressure water. On implementing this scheme at the full-scale UASB system, it was found successful provided the caustic soda was continually circulated through the pipework by pumping, to promote contact with the struvite deposits. A caustic soda pumping system was installed and is currently in use. However, this strategy requires shutdown of the plant and the caustic soda and disposal of the resultant struvite/caustic soda slurry are expensive. This stimulated an investigation into the causes for struvite precipitation, to identify possible methods to reduce or even eliminate struvite precipitation.

2. RESEARCH OBJECTIVES

From Chapter 2 and above, one operational problem experienced at the full-scale UASB

system at the SFW Wellington Distillery, is the precipitation of struvite in the effluent discharge pipe network. The uncontrolled precipitation of the mineral struvite is a major problem in many wastewater conveyance and treatment systems, for example in anaerobic treatment of wine distillery and piggery wastewaters and sludge waste derived from biological excess phosphorus removal activated sludge systems (Loewenthal *et al.*, 1994). The pipe networks transporting the treated effluents in these and similar anaerobic digesters, are particularly prone to scaling and clogging as a result of struvite precipitation, since in these wastes ammonium, magnesium and phosphate are present at relatively high concentrations.

One solution to the struvite precipitation problem is its physical removal, as practised at the SFW Wellington Distillery, see above. However, this requires shutdown of the wastewater treatment system, which is highly undesirable. Alternative approaches would be to prevent the struvite from precipitating, or to stimulate its precipitation in a controlled environment thereby overcoming precipitation in the effluent pipe network. Of these two options, the latter, i.e. controlled precipitation, holds the most promise for development.

The controlled precipitation of struvite at the Wellington UASB reactor would have the following advantages.

- Reduce maintenance costs by reducing scaling problems in pipelines and pumps (Momberg, 1992).

- Continuous spirit distillation from wine and anaerobic treatment of its effluents could be implemented, i.e. not necessary to shut the plant down for physical removal.

- Quantitatively reduce phosphate and ammonia concentrations in the reactor's effluent (Momberg, 1992), thereby reducing discharge of these nutrients to the local municipal wastewater treatment works.

- Make phosphates, ammonia and magnesium available to the agricultural sector as a slow release fertiliser for plant growth (Momberg, 1992).

With the controlled precipitation of struvite it is envisaged that struvite would be stimulated to precipitate in a reactor specifically designed for this purpose. This will enable the precipitated struvite to be readily removed. Further, the controlled precipitation of the struvite will reduce the ionic product of the struvite components (i.e. $[Mg^{2+}][NH_4^+][PO_4^{3-}]$) in the UASB reactor to sufficiently low values that precipitation within the UASB effluent pipework will be greatly reduced or even eliminated.

To implement this scheme it is necessary for the purposes of process control to be able to:

1. Predict the conditions under which struvite will precipitate.
2. Predict the mass of struvite that will precipitate under any condition.
3. Predict the struvite precipitation rate.
4. Stimulate the precipitation/crystallisation of struvite under controlled conditions in a reactor designed for that purpose so that precipitation will be negligible in critical areas of the system.

Of these objectives, 1 and 2 above have already been largely met (using equilibrium chemistry). Algorithms have been formulated for solving a number of pH related problems arising in anaerobic digestion, including struvite precipitation (Loewenthal *et al.*, 1994). Loewenthal (1997), Loewenthal, and Morrison (1997, 1998) have developed a user friendly computer program, STRUVITE 3.1, for the practical implementation of the algorithms for struvite precipitation. However, STRUVITE 3.1 is restricted to 25°C as no solubility product measurements for struvite have been made at other temperatures. In making use of STRUVITE 3.1, it would be essential to have a solubility product value at 37°C, as most anaerobic reactors, including the UASB system at Wellington, operate at this temperature since anaerobic fermentation is optimum at this temperature.

The precipitation rate (3 above) of struvite available in literature was determined from laboratory studies conducted on supernatant from a UASB digester treating wine wastewater, but is restricted to 20°C, Musvoto *et al.* (1998, 2000). Similar information for 37°C is not available and needs to be determined.

The design of a struvite precipitation reactor (4 above) will depend on the technical information derived from future pilot-scale studies performed at the full-scale UASB reactor at the SFW Wellington Distillery.

Thus, the objectives of this investigation were divided in two parts, i.e.

Part 1: Literature review: A summary of the relevant literature dealing with equilibrium chemistry and kinetics of struvite precipitation, in particular the equilibrium based algorithms formulated for solving a number of pH related problems in anaerobic digestion as reported by Loewenthal *et al.* (1994); control of pH and fouling due to struvite and calcium carbonate in anaerobic digestion, Loewenthal and Morrison (1998); and the development of the kinetic model for struvite and other calcium and magnesium mineral precipitation, Musvoto *et al.* (1998).

Part 2: Experimental measurements: Measure the struvite solubility product at 20°C and 37°C in distilled water, to validate the value at 20°C in distilled water obtained from the literature and develop a value for 37°C. Evaluate the deviation of the 20°C distilled water value from the 37°C distilled water value. Determine the struvite solubility product at 37°C in UASB digester supernatant. Determine from aeration batch tests on the UASB digester supernatant and modelling the test results, the types of minerals that precipitate, the concentrations of the different minerals that form, the specific mineral precipitation rates and the time taken for complete precipitation.

3. LITERATURE REVIEW OF STRUVITE PRECIPITATION THEORY

3.1 Introduction

Struvite is a mineral with formula $MgNH_4PO_4 \cdot 6H_2O$ and a molecular mass of 254.3 g/mole. It commonly precipitates in anaerobic systems, because effluents from these systems contain higher than usual concentrations of magnesium, ammonia and phosphate ions, which form the main components of struvite.

Struvite precipitation in anaerobic fermentation systems occurs mainly in two areas (Loewenthal *et al.*, 1994). First, within the pipe network transporting the treated effluent, particularly where pressure changes occur, for example, at bends and inlets to pumps. Second, on surfaces close to the inlet and outlet of the secondary settler effecting separation of the treated effluent.

Loewenthal *et al.* (1994) postulated that in both the above instances of struvite precipitation, it would appear that the trigger mechanism is a reduction of the partial pressure of carbon dioxide, pCO_2. Reduction of pCO_2 may cause expulsion of CO_2 from the aqueous phase and a concomitant increase in pH, giving rise to a state of supersaturation with respect to struvite that is sufficiently high so as to cause precipitation of this mineral (Loewenthal *et al.*, 1994).

In this section the literature is reviewed to describe the above in more detail. Following from the objectives for this investigation (part 1 above), the literature selected and presented include the following: (i) equilibrium modelling of struvite precipitation in anaerobic treatment systems, Loewenthal *et al.* (1994); Loewenthal and Morrison (1998) and (ii) the development of a kinetic model for struvite precipitation, Musvoto *et al.* (1998).

3.2 Principles of struvite precipitation

3.2.1 Struvite saturation state

The mineral struvite ($MgNH_4PO_4$) will either precipitate or dissolve into solution (provided the mineral is present) until equilibrium is reached between the magnesium, ammonium and phosphate species in the aqueous and solid phases, i.e. at equilibrium:

$$(MgNH_4PO_4)_{SOLID} \leftrightharpoons Mg^{2+} + NH_4^{+} + PO_4^{3-} \qquad (6.1)$$

At equilibrium the product of the equilibrium concentrations of the aqueous species $[Mg^{2+}]_{eq}$, $[NH_4^{+}]_{eq}$ and $[PO_4^{3-}]_{eq}$ equals the thermodynamic solubility product, i.e.

$$[Mg^{2+}]_{eq}\,[NH_4^{+}]_{eq}\,[PO_4^{3-}]_{eq} = K'_{spm} \qquad (6.2)$$

where

K'_{spm} = thermodynamic solubility product for struvite adjusted for Debye-Hückel ionic effects.

The product of the aqueous species of $[Mg^{2+}]$, $[NH_4^+]$ and $[PO_4^{3-}]$ is termed the ionic product. When the ionic product of the aqueous species concentrations exceeds K'_{spm}, the solution is supersaturated with respect to struvite and the mineral will precipitate from solution, and when the ionic product is less than K'_{spm} the solution is undersaturated and the mineral (if present) will tend to dissolve into solution, i.e.

$$[Mg^{2+}]\,[NH_4^+]\,[PO_4^{3-}] > K'_{spm} \qquad \text{precipitation} \qquad (6.3)$$

$$[Mg^{2+}]\,[NH_4^+]\,[PO_4^{3-}] < K'_{spm} \qquad \text{dissolution} \qquad (6.4)$$

3.2.2 Assessment of saturation state

From the above, to determine whether struvite will precipitate or dissolve from solution, the saturation state of the solution needs to be assessed, that is, the concentrations of Mg^{2+}, NH_4^+ and PO_4^{3-} need to be determined and hence the ionic product calculated and compared to the solubility product. For Mg^{2+}, this concentration is available from direct measurement (Standard Methods, 1985). For NH_4^+ and PO_4^{3-}, these are species in the weak acid/base systems of ammonia and phosphate respectively. If the total species concentrations for the ammonia (N_T) and phosphate (P_T) are available from measurement and a value for pH measured, then the individual weak acid/base system species concentrations can be calculated (see below and Appendix C). Hence, the ionic product can be calculated and compared to the solubility product and the saturation state assessed. However, this assessment is qualitative only, and does not provide a measure of the mass of the precipitant that can form, nor does it facilitate the development of a predictive approach to estimate change in precipitation potential with chemical dosing, either prescribed (e.g. acid dosing) or inadvertent (e.g. CO_2 loss from solution). To overcome these deficiencies, Loewenthal *et al.* (1994) developed an equilibrium chemistry based model to predict struvite precipitation, see Section 3.3 below.

3.3 Equilibrium chemistry based model for struvite precipitation, Loewenthal *et al.* (1994).

3.3.1 Introduction

In the precipitation of struvite, the weak acid/base species NH_4^+ and PO_4^{3-} form part of the struvite precipitant. Hence, the saturation state of struvite is dependant on the pH, since the weak acid/base species concentrations are pH dependant. Furthermore, since the precipitating mineral removes weak acid/base species from solution, the precipitation of struvite itself will influence the pH, which in turn will influence the saturation state. Accordingly, in developing an equilibrium chemistry based model for struvite precipitation, weak acid/base chemistry needs to be incorporated.

3.3.2 Weak Acid/Base Equilibrium Chemistry in Anaerobic Digesters

The pH in anaerobic systems is controlled by weak acid/base chemistry involving a number of weak acid/base subsystems simultaneously present in solution, typically the carbonate, phosphate, ammonia, acetate and water subsystems. The influence of pH on each of these subsystems is described by a set of aqueous phase equilibrium and mass balance equations.

Equilibrium equations (aqueous phase):

$$(H^+)[HCO_3^-]/[H_2CO_3^*] = K_{c1}/f_m = K'_{c1} \quad \text{} \textbf{Carbonate subsystem} \quad (6.5)$$

$$(H^+)[CO_3^{2-}]/[HCO_3^-] = K_{c2}f_m/f_d = K'_{c2} \quad \text{} \quad (6.6)$$

$$(H^+)[H_2PO_4^-]/[H_3PO_4] = K_{p1}/f_m = K'_{p1} \quad \text{} \quad (6.7)$$

$$(H^+)[HPO_4^{2-}]/[H_2PO_4^-] = K_{p2}f_m/f_d = K'_{p2} \quad \text{} \textbf{Phosphate subsystem} \quad (6.8)$$

$$(H^+)[PO_4^{3-}]/[HPO_4^{2-}] = K_{p3}f_d/f_t = K'_{p3} \quad \text{} \quad (6.9)$$

$$(H^+)[NH_3]/[NH_4^+] = K_n f_m = K'_n \quad \text{} \textbf{Ammonia subsystem} \quad (6.10)$$

$$(H^+)[Ac^-]/[HAc] = K_a/f_m = K'_a \quad \text{} \textbf{Acetate subsystem} \quad (6.11)$$

Mass balance equations:

$$C_T = [H_2CO_3^*] + [HCO_3^-] + [CO_3^{2-}] \quad (6.12)$$

$$P_T = [H_3PO_4] + [H_2PO_4^-] + [HPO_4^{2-}] + [PO_4^{3-}] \quad (6.13)$$

$$N_T = [NH_4^+] + [NH_3] \quad (6.14)$$

$$A_T = [HAc] + [Ac^-] \quad (6.15)$$

where

(X) = activity of species X (mol ℓ^{-1})

[X] = molarity of species X (mol ℓ^{-1})

f = activity coefficient, subscripts m, d and t refer to mono-, di-.and tri-protic states

K_x = thermodynamic equilibrium constant of species X

K'_x = thermodynamic equilibrium constant of species X, adjusted for Debye-Hückel ionic effects

For the water subsystem the activity product equilibrium equation is given by:

$$(H^+)[OH^-] = K_w/f_m = K'_w \quad (6.16)$$

3.3.3 Characterisation of weak acid/base subsystems

Calculation of the ionic product for struvite requires values for specific weak acid/base species concentrations, namely PO_4^{3-} and NH_4^+, see Section 3.2.1 above. Examination of the sets of equations above for weak acid/base systems indicates that in order to speciate a solution (i.e. determine the concentration each of the weak acid species), a value for a parameter for each of the weak acid/base subsystems must be known (Loewenthal *et al.*, 1989). That is, the system needs to be characterised via some selected set of measurements, with one measurement for each weak acid/base subsystem. In the struvite example, if total weak acid/base species concentrations C_T, P_T, N_T and A_T constitute the characterisation parameters for carbonate, phosphate, ammonia and acetate subsystems respectively, and pH for the water subsystem, then it is possible to develop a general solution for each of the species concentrations as a function of pH from Eqs (6.5) to (6.15) above. This is illustrated in the log [species]-

pH plot shown in Figure 6.1 where for given total species concentrations the concentration of individual weak acid/base species are plotted against pH.

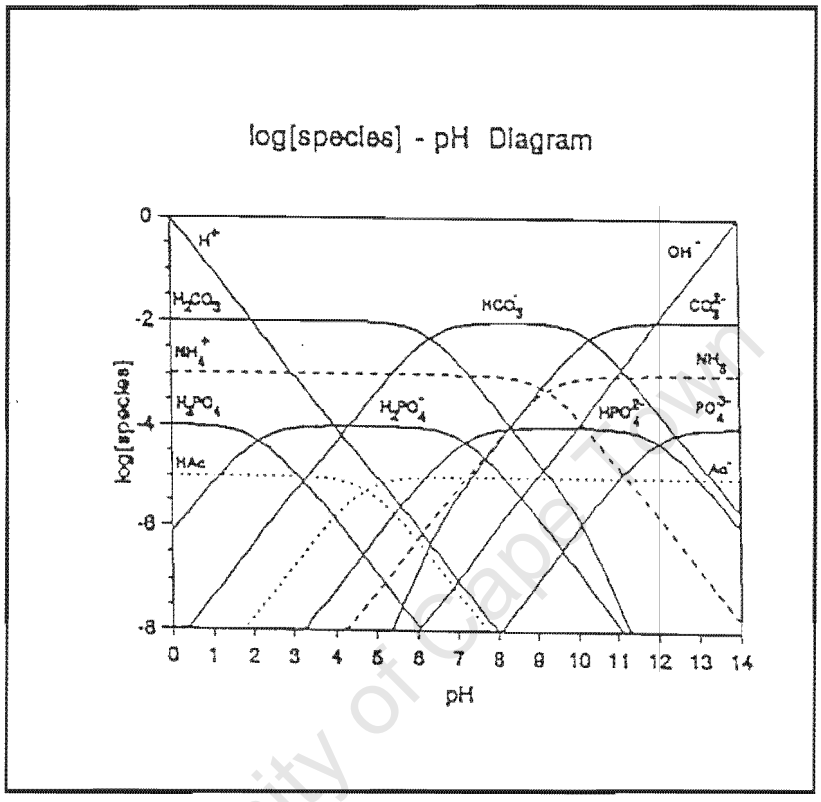

Fig 6.1 Typical log {species} – pH plot for $C_T=10^{-2}$ mol ℓ^{-1}, $P_T=10^{-4}$ mol ℓ^{-1}, $N_T=10^{-3}$ mol ℓ^{-1} and $A_T=10^{-5}$ mol ℓ^{-1} (Loewenthal *et al.*, 1994).

3.3.4 Capacity parameters

The above set of equations and parameters from a convenient basis for characterising weak acid/base subsystems and speciating them. However, they do not form a convenient basis for dealing with problems involving determination of change of state due to some chemical perturbation, (deliberate or inadvertent) particularly because the pH (which is central in the equations) does not change in a simple stoichiometric fashion with the chemical perturbation. To circumvent this problem, Loewenthal *et al.* (1991) showed that a number of capacity parameters are useful. These are:

i) Proton accepting/donating parameters relative to selected reference species for each of the weak acid/base subsystems in solution, termed the subsystem alkalinities/acidities.

ii) Solution proton accepting/donating capacity parameters, termed the solution alkalinities/acidities, equal to the sum of subsystem alkalinities/acidities.

The solution capacity parameters have a central role in the formulation of algorithms for solving problems associated with change in state, for two reasons. First, certain of these parameters are amenable to measurement in the laboratory by simple acid/base titration. Second, these parameters change in a simple stoichiometric fashion with chemical dosing.

For an aqueous solution containing the carbonate, phosphate, ammonia and acetate subsystems, an equation for total alkalinity (with weak acid/base reference species all in the most protonated form) can be formulated using a proton balance, yielding:

$$\textbf{Total alk.} = \textbf{H}_2\textbf{CO}_3, \textbf{H}_3\textbf{PO}_4, \textbf{NH}_4^+, \textbf{HAc alkalinity} \qquad (6.17a)$$

The total (or solution) alkalinity equals the sum of the weak/base subsystem alkalinies:

$$\textbf{Total alk.} = \textbf{Alk H}_2\textbf{CO}_3 + \textbf{Alk H}_3\textbf{PO}_4 + \textbf{Alk NH}_4^+ + \textbf{Alk HAc} + \textbf{Alk H}_2\textbf{O} \qquad (6.17b)$$

Each of the weak acid/base subsystem alkalinities can be expressed in terms of weak acid/base species concentrations, as follows:

$$\textbf{Total alk.} = 2[CO_3^{2-}]+[HCO_3^-]+3[PO_4^{3-}]+2[HPO_4^{2-}]+[H_2PO_4^-]+[NH_3]+ [A^-]+[OH^-]+[H^+] \qquad (6.17c)$$

Using a similar approach, solution alkalinity and acidity equations can be formulated for any selected set of reference species. The solution alkalinity and acidity have the advantage that, provided the correct reference species are chosen (i.e. includes the species of the chemical being dosed), then these change in a simple stoichiometric

fashion with dosing. This enables the solution state after dosing to be determined (Loewenthal *et al.*, 1991).

3.3.5 Determination of C_T for carbonate system

In anaerobic digestion difficulties are encountered in direct measurement of total inorganic carbon species concentration, C_T, (due to loss of CO_2 on sampling and the non-availability and expense of inorganic carbon analysers, Loewenthal *et al.*, 1991) and alternative parameters for this subsystem are either the partial pressure of carbon dioxide, pCO_2, and/or the solution total alkalinity. Determination of C_T from solution total alkalinity measurements (in place of C_T from direct measurement) is set out fully by Loewenthal *et al.* (1991); determination from CO_2 measurement is as follows:

In anaerobic digesters, the carbonate species in aqueous and gaseous phases are in equilibrium, which can be depicted by Henry's law expression:

$$[H_2CO_3^*] = K_H pCO_2 \tag{6.18}$$

where

K_H = Henry's law constant

Determination of each of the carbonate species concentrations in terms of pH and CO_2 using the relevant weak acid/base equilibrium equations gives:

$$C_T = pCO_2\{K_H + K_H K'_{c1}/(H^+) + K'_{c1}.K'_{c2}.K_H/(H^+)^2\} \tag{6.19}$$

Thus, knowing pCO_2 and the pH, the carbonate subsystem total species concentration can be calculated, i.e. the carbonate subsystem is completely characterised. Having described how weak acid/base speciation is effected, problems involving saturation state, change in state with dosing and mineral precipitation potential can now be addressed.

3.3.6 Struvite saturation State

As noted above, struvite ($MgNH_4PO_4$) will either precipitate or dissolve into solution (provided the mineral is present) until an equilibrium situation occurs between

magnesium, ammonium and phosphate species in the aqueous and solid phases, i.e. at equilibrium,

$$(MgNH_4PO_4)_{SOLID} \rightleftharpoons Mg^{2+} + NH_4^+ + PO_4^{3-} \quad (6.20)$$

At equilibrium the product of the equilibrium concentrations of the aqueous species $[Mg^{2+}]_{eq}$, $[NH_4^+]_{eq}$ and $[PO_4^{3-}]_{eq}$ equals the thermodynamic solubility product, i.e.

$$[Mg^{2+}]_{eq}\,[NH_4^+]_{eq}\,[PO_4^{3-}]_{eq} = K'_{spm} \quad (6.21)$$

where

K'_{spm} = thermodynamic solubility product for struvite adjusted for Debye-Hückel ionic effects

When the ionic product of the species concentrations exceeds K'_{spm}, the solution is supersaturated with respect to struvite and the mineral will precipitate from solution, and when the ionic product is less than K'_{spm} the mineral will tend to dissolve into solution.

To assess the saturation state of a solution, concentrations of Mg^{2+}, NH_4^+ and PO_4^{3-} and hence the ionic product needs to be determined. For Mg^{2+} this is effected by direct measurement (Standard Methods, 1985). For NH_4^+ and PO_4^{3-}, these would be determined from the measured total species concentrations and pH, via speciation of the ammonia and phosphate weak acid/base systems, as set out above. The ionic product of species concentrations is compared with K'_{spm} yielding a qualitative description of the saturation state. As the mineral is composed of weak acid/base species (NH_4^+, PO_4^{3-}), the concentrations of which are affected by both the precipitation/dissolution phenomenon and the resultant pH change, this technique cannot reflect the mass concentration of mineral that can precipitate out of solution. In this regard, from a practical point of view the struvite precipitation potential is of fundamental importance.

3.3.7 Struvite Precipitation Potential

The precipitation potential of a mineral is the mass concentration of the mineral that will precipitate from solution to establish an equilibrium state between species in the

aqueous and solid phases. Loewenthal *et al.* (1976, 1986) showed that where the carbonate and water subsystems are the only weak acid/base subsystems present, the precipitation potential for carbonate minerals can be determined relatively easily from the initial characterised state (initial pH, Alkalinity and calcium concentrations). Their algorithm is based on two fundamentals. First, if an aqueous calcium carbonate solution is known to be saturated with respect to calcite ($CaCO_3$), values for only two parameters need to be known at saturation to characterise the solution. In this regard total acidity and total alkalinity minus twice calcium molarity (AM2C), are parameters that remain unchanged with calcite precipitation, so that the values for these parameters at saturation equals the initial known values. Second, for a fixed total acidity, the total alkalinity varies monotonically with pH. This latter observation allows for a rapid successive approximation technique to determine the saturation state. Unfortunately an analogous algorithm cannot be applied to determine the struvite precipitation potential because this mineral is composed of both proton donating and accepting species (NH_4^+ and PO_4^{3-} respectively) so that the solubility of the mineral does not necessarily vary monotonically with pH.

An approach to determine the struvite precipitation potential is one of successive approximation applied directly to the precipitation potential. In this approach struvite is considered infinitely soluble, and the value assumed for the precipitation potential is considered equal to the dosage of struvite. A dosage of struvite is then applied to (or removed from) the solution and the solution characterised in the new state allowing determination of the new species ionic product ($[Mg^{2+}][NH_4^+][PO_4^{3-}]$). The dosage is then adjusted, the solution characterised and the species ionic product recalculated. This is repeated until the species ionic product equals the appropriate solubility product K'_{spm}.

In this regard the nub of the problem is to characterise the new state of a solution for a known applied dose of struvite. This is, in essence, a single aqueous phase conditioning problem, the solution of which can be obtained using principles for chemical conditioning of solutions comprised of mixtures of weak acid/base subsystems (Loewenthal *et al.*, 1991). Using this approach, Loewenthal *et al.* (1994) formulated algorithms to (i) determine change in state with addition/removal of a specific molar mass of struvite, (ii) determine the dosage to obtain saturation with respect to struvite,

and (iii) determine the change in struvite precipitation potential arising from some external perturbation applied to the system either by change in pCO_2 or generation/abstraction of volatile acids (i.e. acetic acid). These algorithms were validated by comparing predicted and experimental results for struvite precipitation from pure water solutions.

3.3.8 Computer program STRUVITE 3.1

Loewenthal and Morrison (1998) coded the above equilibrium algorithms for struvite into a user friendly computer programme called STRUVITE 3.1.

3.3.9 Effect of pH on struvite precipitation potential

From the above mentioned algorithms and computer programme developed by Loewenthal and co-workers, it is possible to develop a visual explanation for precipitation of struvite in UASB systems (See Fig 6.2, Loewenthal *et al.*, 1994).

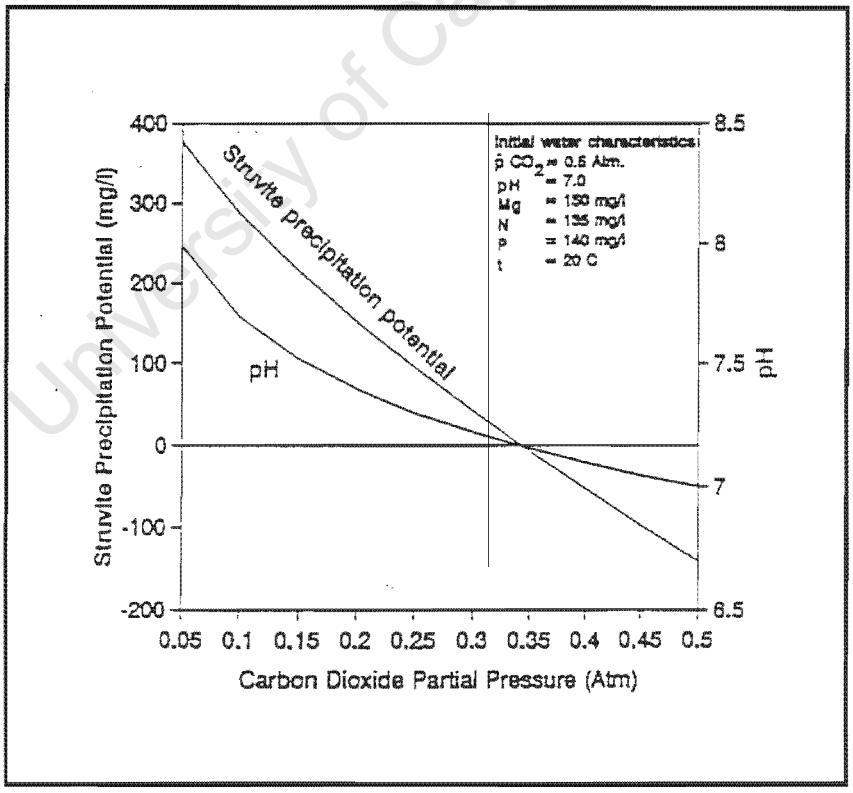

Fig 6.2 A plot of struvite precipitation potential and pH after reaching equilibrium with CO_2, but before struvite precipitaion against pCO_2 (Loewenthal *et al.*, 1994).

From Fig 6.2 we see, a loss of CO_2 and a resultant decrease in pCO_2 causes the pH to increase. From Fig 6.1, an increase in pH causes a shift in weak/base species: For the phosphate subsystem, this causes an increase in $[PO_4^{3-}]$ and for the ammonia subsystem it causes a decrease in $[NH_4^+]$. The increase in $[PO_4^{3-}]$ exceeds the decrease in $[NH_4^+]$ and, since $[Mg^{2+}]$ remains constant, the struvite ionic product ($[Mg^{2+}][NH_4^+][PO_4^{3-}]$) increases. This causes the struvite precipitation potential to increase (Fig 6.2), when the struvite ionic product exceeds the solubility product the solution becomes supersaturated with respect to struvite; the struvite precipitation potential becomes positive and struvite will precipitate.

3.3.10 Struvite kinetics

The approach to resolving struvite precipitation above of Loewenthal and co-workers is based on equilibrium chemistry. Difficulties with the equilibrium chemistry approach are that:

(i) solution procedures are tedious
(ii) kinetic (rates) of precipitation are not considered
(iii) situations where more than one mineral precipitates, i.e. multi-mineral precipitation, cannot be addressed
(iv) loss of CO_2 from the solution, or the final pH serves as input – the time dependent loss of CO_2 and its influence on pH cannot be determined.

To resolve *inter alia* the difficulties above, Musvoto *et al.* (1997, 1998) developed a kinetic based approach to simulate systems with multi weak acid/bases, multi-phases (solid/liquid/gas) and multi-mineral precipitation. Following this approach, a kinetic model was developed to simulate the reactions that occur on anaerobic digester liquor (ADL) aeration (Musvoto *et al.*, 2000). This model incorporates:

- Forward and reverse dissociation reactions for the weak acid/base systems water, carbonate, phosphate, ammonium and short chain fatty acids.
- Precipitation of the minerals struvite ($MgNH_4PO_4 \cdot 6H_2O$), amorphous calcium phosphate (ACP, $Ca_3(PO_4)_2 \cdot xH_2O$), newberyite ($MgHPO_4 \cdot 3H_2O$), calcite ($CaCO_3$) and magnesite ($MgCO_3$); from the literature and experimental investigations, these are the minerals most likely to precipitate on aeration of ADL.

- Gas stripping of NH_3 and gas exchange of CO_2.
- Ion pairing reactions for $CaOH^+$, $CaCO_3(aq)$, $CaHCO_3^+$, $CaPO_4^-$, $CaHPO_4(aq)$, $CaH_2PO_4^+$, $MgOH^+$, $MgCO_3(aq)$, $MgHCO_3^+$, $MgHPO_4(aq)$ and $MgPO_4^-$; from the literature, these are the ion pairs commonly found in systems dominated by the various carbonate, Mg, Ca, P and N species at pHs typical of ADL.

The model was validated by means of aeration batch tests on upflow anaerobic sludge bed (UASB) liquors and sewage sludge ADL (Musvoto *et al.*, 1998, 2000). The weak acid/base dissociation constants, ion pairing stability constants and mineral solubility products were kept constant at typical literature values. By curve fitting the predicted and the measured experimental batch test results for inorganic carbon (C_T), Mg, Ca, free and saline ammonia (FSA), orthoP and pH over 24h or longer, the mineral precipitation and gas stripping rates were determined for the UASB and sewage sludge ADL. From the simulations, a deeper understanding of the processes operating in the batch tests could be developed, to identify *inter alia* the dominant precipitation minerals, the conditions that cause these minerals to precipitate and rates of precipitation of the minerals.

From the above, the kinetic model forms a useful analytical tool to evaluate multi-phase multi-mineral precipitation problems. Since it was not certain whether precipitation from the UASB supernatant at the SFW Wellington Distillery was due to struvite alone, or a multi-mineral precipitation phenomenon, it was proposed to apply the kinetic model of Musvoto *et al.* to the UASB system at the SFW Wellington Distillery. For this, batch tests similar to those conducted by Musvoto *et al.* (2000) were to be conducted and the results compared to kinetic model simulations.

4. EXPERIMENTAL INVESTIGATION

4.1 Introduction

In the algorithms of Loewenthal *et al.* (1994), the computer program STRUVITE (Loewenthal and Morrison, 1997) and the kinetic model of Musvoto *et al.* (1998, 2000) above for struvite precipitation, the solubility product for struvite is an essential parameter. From the literature, the thermodynamic solubility product value quoted for

struvite is pK_{sp}=12.6 to 13.26 at 25°C and infinitive dilution, i.e. in distilled water, see Table 6.1 (Musvoto *et al.*, 2000). Furthermore, Loewenthal and Morrison (1998) also determined a thermodynamic solubility product value for struvite with distilled water and activated sludge effluent as background solutions at 20°C that agreed favourably with the literature value, see Table 6.2. From Table 6.2, the pK_{sp} values for activated sludge effluent were higher than those for distilled water. Musvoto *et al.* (1998) determined the solubility product and precipitation rate for struvite at 20°C for effluent from a UASB reactor treating wine distillery wastewater, as pK_{sp}=13.16 and precipitation rate =3000 $g/m^3.d$, see Table 6.3. This solubility product value and precipitation rate was determined from simulations of three batch tests in which the UASB reactor effluent was aerated; the pK_{sp} value fell within the range of values given in the literature, i.e. pK_{sp}=12.6–13.26, see Table 6.1 and 6.3, however, no values for struvite precipitation rates are available in the literature.

The solubility product values quoted in Tables 6.1, 6.2 and 6.3 are all restricted to temperatures not encountered in anaerobic digestion. A study (part 2 of this investigation) was therefore undertaken to experimentally determine the solubility product for struvite at 37°C with distilled water as background solution (i.e. infinite dilution). To collect the relevant data, batch tests were conducted at 20 and 37°C in which struvite was stimulated to precipitate in distilled water (Section 4.2.1).

The investigation was extended, to determine the struvite solubility product at 37°C with UASB reactor supernatant as background solution, and also the struvite precipitation rate and whether any other minerals (e.g. calcium phosphate, calcite) can be expected to precipitate. For this, the experimental method of Musvoto *et al.* (1998, 2000) was followed – two aerobic batch tests were performed at the SFW Wellington Distillery, on effluent from the full-scale UASB reactor treating wine wastewater (Section 4.2.2).

The data obtained from the aerobic batch tests were used in a kinetic based mixed weak acid/base chemical precipitation model (Musvoto *et al.*, 1998, 2000), to determine the struvite pK_{sp}, precipitation rate for struvite at 37°C, and other possible mineral precipitants (Section 5).

Table 6.1 Solubility product pK_{sp} for struvite at 25°C and infinitive dilution from literature.

Value	Reference
12.6	Stumm and Morgan (1981)
13.16	JESS (Murray and May, 1996)
12.6	Butler (1964)
12.72	Abbona *et al.* (1982)
13.15	Taylor *et al.* (1963) cited by Scott *et al.* (1991)
13	Mamais *et al.* (1994)
13.26	Ohlinger *et al.* (1998)

Table 6.2 Solubility product pK_{sp} for struvite at 20°C (Loewenthal and Morrison, 1998).

Experimental determination of thermodynamic solubility product of struvite in distilled water and in activated sludge effluent at 20°C.						
Background electrolyte	Addition of:			μ	pH	pK_{sp}
	P_T mg/ℓ	N_T mg/ℓ	Mg^{2+} mg/ℓ			
Distilled water	400	300	300	0.088	6.725	12.82
Distilled water	500	300	300	0.091	6.768	12.83
Distilled water	500	300	400	0.100	6.653	12.85
Activated sludge effluent	500	300	500	0.137	6.495	12.97
Activated sludge effluent	500	500	400	0.121	6.653	12.88
Activated sludge effluent	500	300	300	0.102	6.773	12.92

Table 6.3 Solubility product and Precipitation rate of struvite for aerated UASB wine wastewater at 20°C (Musvoto *et al.*, 1998).

Constant	Batch Test 16	Batch test 17	Batch test 18	Literature value
-Log Solubility product (pK_{sp})	13.16	13.16	13.16	12.6-13.26
Rate of precipitation ($g/m^3.d$)	3000	3000	3000	-

4.2 Materials and Methods

Experiments were undertaken to determine: 4.2.1 Struvite solubility product in distilled water at 20 and 37°C and 4.2.2 Struvite and other mineral solubility products and precipitation kinetics in full-scale UASB reactor supernatant at 37°C; see below.

4.2.1 Struvite solubility product in distilled water at 20 and 37°C

Experimental set-up

For the study, a ±2.5 litre reactor was constructed from a transparent perspex cylinder of 120 mm diameter, 600 mm high, sealed at the bottom and with a flange on top to allow a stirrer motor to be mounted securely. The perspex allows the reactor to be robust, easy to work with and allows the contents to be visible from the outside.

The electric motor was fixed to a plate that could be screwed to the flange on top of the reactor. A stainless steel shaft ran from the motor, through the plate and was long enough to reach to the bottom of the reactor. A stirrer blade was attached to the shaft and this allowed continuous mixing of the contents in the reactor. By using this method, the motor did not come into contact with the reactor's contents, preventing failure of the motor as well as allowing for easy maintenance.

The reactor was placed in a water bath filled with water. The water was heated by means of an element, in the same way as a kettle. The temperature was set at the desired temperature, i.e. 20 or 37°C, and controlled via a thermostat that was attached to the side of the bath. Figure 6.3 shows a schematic diagram of the reactor and water bath.

pH and temperature electrodes respectively were inserted half way into the reactor contents via a hole in the flange. These electrodes were connected to a portable Hanna pH meter (HI 9025) and used for continuous pH monitoring. The hole also allowed for sampling with a 50 mℓ long tip pipette.

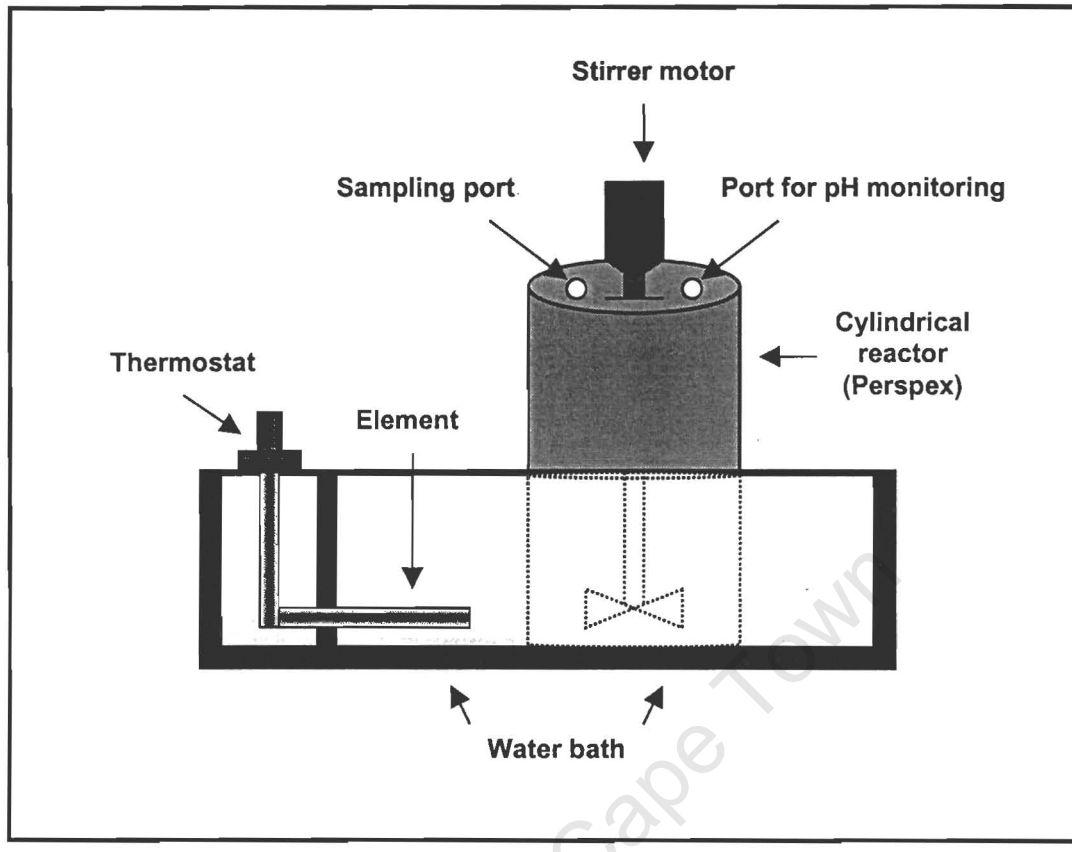

Fig 6.3 Schematic diagram of the reactor and water bath.

Experimental procedure

A known volume of de-ionised distilled water (usually 1.4 ℓ) was added to the clean dry reactor and allowed to attain the temperature of 37°C (or 20°C). Known molar masses of magnesium (via addition of $MgCl_2$), ammonium species (via addition of NH_4Cl) and phosphate species (via addition of K_2HPO_4) were added one at a time, using a 100 mℓ beaker to dilute the samples before adding to the reactor (calculation of the masses of chemicals to be added is set out in Appendix C). The magnesium chloride was added last and the remaining water added to achieve the 2 litre volume. The pH meter was calibrated using standardised buffer solutions at pH 4 and 7 before each test. The stirrer was switched on for mixing the reactor contents after the temperature, pH and time were recorded, and the experiment was left to run until completion. After 24 hours, the precipitation reaction was assumed complete and the stirrer was switched off and the

reactor contents allowed to settle for 10-20 minutes. A 50 mℓ supernatant sample was immediately filtered through Whatman GF/C glassfibre filter paper and the filtrate divide into two. To the one filtrate sample, a few drops (±1.5 mℓ) of concentrated sulphuric acid were added to reduce the pH to below 2 so that no further precipitation could occur. The acidified sample was analysed for Mg by emission spectroscopy using the inductively coupled plasma (ICP) method (Standard Methods, 1985).

The second filtrate sample was not acidified and 5 ml of it was diluted 5 times with de-ionised water for more accurate testing and analysed for FSA and orthophosphate (Standard Methods, 1985).

4.2.2 Aerobic batch tests at 37°C using full-scale UASB reactor effluent

Experimental set up and procedure

Aerobic batch tests were conducted on effluent from the full-scale UASB reactor (in operation treating wine wastewater) at the SFW Wellington Distillery. Treated effluent was drawn directly from a sample port in the UASB effluent discharge line into a 25 litre perspex bucket, serving as the reactor. The reactor was allowed to overflow displacing any oxygen present. This UASB reactor is operated at a temperature of 37°C (±1°C), and the effluent was at this temperature. During the test, the temperature decreased to ±31°C by the end, giving an average temperature of 35°C. The batch test commenced by aerating the contents for at least 2 hours immediately after two initial samples of 10 mℓ and 100 mℓ respectively were drawn from the reactor for analysis. At intervals, additional 10 mℓ and 100 mℓ samples were drawn from the reactor and analysed. The pH in the reactor was monitored throughout the experiment using a Hanna pH meter (Hanna HI 9321) fitted with a Hanna epoxy combined pH electrode.

Following the experimental procedure as conducted by Musvoto *et al.* (1998), immediately after sampling and before filtration the 10 mℓ sample was analysed for Free and saline ammonia (FSA) using the Spectroquant ready-to-use test range which can be measured with the SQ 118 photometer (Manual, Photometer SQ 118, MERCK). The 100 mℓ sample was immediately filtered through Whatman GF/C glassfibre filter paper and the filtrate divided into two. To one filtrate sample, a few drops (1.5 mℓ) of

concentrated nitric acid (HNO_3) were added to reduce the pH to below 2 and so prevent further precipitation. The acidified sample was analysed for the following:

- Ca, Fe and Mg by the AA (atomic absorption) method.

- Total phosphate species (P_T): Persulphate digestion followed by molybdate/vandate colour reaction and/or ICP method (Standard methods, 1985).

The second filtered sample was not acidified and was analysed for:

- Total inorganic carbon species (C_T): This parameter was calculated after directly measuring the H_2CO_3* alkalinity and pH using the 5-point titration method of Moosbrugger *et al.* (1992).

- Short chain fatty acids (SFCA): 5-point titration method of Moosbrugger *et al.* (1992).

4.3 Calculation of struvite solubility product

Once the struvite solubility product tests (Section 4.2.1) were completed, the differences between the initial and final molar concentrations were calculated as these should be closely equal; For struvite, from the empirical formula the molar ratio for Mg, FSA and phosphate is 1:1:1 (Momberg, 1992). If the difference between initial and final concentrations did not agree, the results were discarded. If agreement was obtained for the results, these were used to calculate the solubility product with the equation:

$$\mathbf{K'_{sp} = [Mg^{2+}][NH_4^{+}][PO_4^{3-}]} \qquad (6.22)$$

In this formula, values are required for $[Mg^{2+}]$, $[NH_4^{+}]$ and $[PO_4^{3-}]$. Values available from measurement are $[Mg^{2+}]$, FSA (i.e. $[NH_4^{+}] + [NH_3]$, as N) and orthophosphate (i.e. $[H_3PO_4]+[H_2PO_4^{-}]+[HPO_4^{2-}]+[PO_4^{3-}]$, as P). For the FSA with pK=9.3, in the pH ranges of the tests ($6.5<pH<7$, Tables 6.4 and 6.5) the concentration of NH_3 is very small compared to NH_4^{+} and can be neglected. Therefore, the FSA measurement can be taken as equal to $[NH_4^{+}]$ as N. However, for the phosphorus, the concentrations of non-

$[PO_4^{3-}]$ species are not negligible and need to be taken into account, i.e. the phosphate system need to be speciated and $[PO_4^{3-}]$ determined. This can be done from equilibrium chemistry, see Appendix C. With $[Mg^{2+}]$, $[NH_4^+]$ and $[PO_4^{3-}]$ available, these can be inserted into Eq (6.22) above and K'_{sp} determined. This is the apparent solubility product for struvite and needs to be corrected for ionic strength effects to determine the true solubility product K_{sp}, for struvite at infinite dilution. To do this, K'_{sp} is multiplied by the relevant activity coefficients, i.e.

$$\mathbf{K_{sp} = K'_{sp}.f_t.f_d.f_m} \qquad (6.23)$$

where

f_t, f_d, f_m = tri-, di- and mono-valent activity coefficients, for PO_4^{3-}, Mg^{2+} and NH_4^+ respectively. See Appendix C for more detail.

From K_{sp}, the pK_{sp} for struvite can be calculated:

$$\mathbf{pK_{sp} = -\log K_{sp}} \qquad (6.24)$$

4.4 Experimental results

4.4.1 Struvite solubility product in distilled water at 20 and 37°C

Table 6.4 and Table 6.5 give the values determined for the true solubility product for struvite at 20 and 37°C respectively with distilled water as background solution. Detailed results are given in G. Randall (1998).

From Tables 6.4 and 6.5, the average pK_{sp} values for struvite at 20°C and 37°C were 12.66 (sample standard deviation 0.08) and 12.46 (sample standard deviation 0.194) respectively. The pK_{sp} value at 20°C falls within the range of values recorded in the literature (Table 6.1), indicating the experimental protocol and data are acceptable. The pK_{sp} value at 37°C is lower than the value at 20°C and this difference is statistically significantly at the 95 % confidence interval.

Thus, it would appear that the effect of an increase in temperature is to decrease the pK_{sp} value for struvite. However, this effect is relatively small, with the 17°C increase in temperature causing the pK_{sp} to decrease by only 0.2 units.

Table 6.4 Experimental determination of the thermodynamic solubility product of struvite pK_{sp} in distilled water at 20°C.

Experimental determination of thermodynamic solubility product of struvite in distilled water at 20°C.						
Test no.	**Addition of:**			μ	**pH**	**pK_{sp}**
	P_T mg/ℓ	**N_T mg/ℓ**	**Mg^{2+} mg/ℓ**			
1	300	400	300	0.0604	6.68	12.55
2	300	400	300	0.0485	6.78	12.54
3	300	500	300	0.0493	6.67	12.67
4	300	500	300	0.0492	6.66	12.69
5	300	500	300	0.0490	6.68	12.62
6	300	500	400	0.0583	6.57	12.73
7	300	500	400	0.0602	6.58	12.67
8	300	500	300	0.052	6.60	12.73
9	400	500	300	0.053	6.57	12.77
			Average			12.66
			Sample standard deviation			0.08

Table 6.5 Experimental determination of the thermodynamic solubility product of struvite pK_{sp} in distilled water at 37°C.

Experimental determination of thermodynamic solubility product of struvite in distilled water at 37°C.						
Test no.	**Addition of:**			μ	**pH**	**pK_{sp}**
	P_T mg/ℓ	**N_T mg/ℓ**	**Mg^{2+} mg/ℓ**			
1	300	400	300	0.0403	6.77	12.42
2	300	400	300	0.0601	6.77	12.33
3	300	400	300	0.0505	6.77	12.50
4	300	400	300	0.050	6.66	12.68
5	300	400	300	0.0511	6.72	12.56
6	400	400	400	0.0717	6.68	12.34
7	300	500	300	0.0552	6.85	12.27
8	250	400	300	0.0503	6.81	12.46
9	300	400	200	0.0495	6.88	12.33
10	300	400	200	0.0630	6.97	12.16
11	350	400	250	0.0507	6.75	12.51
12	300	400	400	0.0653	6.73	12.44
13	250	350	200	0.0388	6.88	12.92
			Average			12.46
			Sample standard deviation			0.194

4.4.2 Aerobic batch tests at 37°C using full-scale UASB reactor effluent

Two aeration batch tests were conducted on effluent from the UASB reactor at SFW Wellington Distillery treating wine wastewater. Table 6.6 shows the initial and final

concentrations for these two aerobic batch tests. Detailed results are given in Appendix D. The batch test data are shown plotted in Figs 6.4 (a to d) and 6.5 (a to d) respectively.

Table 6.6 Initial and final concentrations for the two aerobic batch tests on effluent from the SFW Wellington Distillery UASB system.

Parameter	Batch test 1		Batch test 2	
	Initial	Final	Initial	Final
Calcium (mg/ℓ)	48	24	53	22
Magnesium (mg/ℓ)	98	34	96	28
Phosphate (mgP/ℓ)	93.7	13	75.9	2.4
FSA (mgN/ℓ)	150	145	150	84
Iron (mgFe/ℓ)	0.22	0.42	0.21	0.67
pH	6.8	9.32	6.8	9.09

pH: From Figs. 6.4 (a) and 6.5 (a), the initial pH in the two batch tests is pH=6.8. With aeration, the pH of the batch tests increases rapidly with time, to reach a value of pH=9.32 by the end of the first batch test (90 minutes) and pH=9.09 by the end of the second batch test (120 minutes). Within the UASB system, anaerobic processes acting on the wine wastewater cause evolution of CO_2 (see Chapter 3) which results in an increase in the partial pressure of CO_2. When the UASB effluent is aerated the aeration strips CO_2 from the effluent, decreasing acidity. The decrease in acidity causes the pH to increase.

Specific conductivity (SC): From Fig 6.4 (a) and 6.5 (a), conductivity, which is a measure of the ionic strength of the solution, shows little change as the test progresses. This indicates that the precipitation of minerals as the test progresses has negligible influence on conductivity.

SCFA, $H_2CO_3^*$ alkalinity and C_T: From Figs 6.4 (b) and 6.5 (b), the SCFA at the start of the tests are relatively low (60-70 mg/ℓ as HAc) and remains approximately constant throughout the tests. The low SCFA concentrations indicate that the full-scale UASB system is functioning correctly. That these concentrations do not decrease in the batch tests with aeration indicates the absence of biological activity in the batch tests, probably due to the absence of aerobic microorganisms. The C_T concentrations decrease throughout the batch tests, due to loss of CO_2 by gas stripping.

Fe: From Figs 6.4 (c) and 6.5 (c), Fe is present at low concentrations and does not change appreciably. This indicates that this species did not participate significantly in the precipitation reactions.

Mg: From Figs 6.4 (c) and 6.5 (c), Mg concentrations decrease rapidly with aeration in both batch tests. With aeration, as the pH increases struvite (and possibly magnesite, $MgCO_3$) are increasingly supersaturated and precipitate from the solutions. Supersaturation is induced with increase in pH because for struvite the relative concentration of PO_4^{3-} species increases, and for magnesite the relative concentration of CO_3^{2-} species increases. In the first batch test (98 – 34) = 64 mgMg/ℓ = 2.7 mmolMg/ℓ precipitates and for the second batch test (96 – 28) = 68 mgMg/ℓ = 2.8 mmolMg/ℓ precipitates.

Ca: From Figs 6.4 (c) and 6.5 (c), Ca concentrations decrease rapidly with aeration and pH increase. This decrease in Ca concentration most likely is due to calcium phosphate precipitation; for the pH where Ca precipitates (pH 6.8 to ±8.3), calcite ($CaCO_3$) is unlikely to precipitate as this precipitates significantly only at higher pHs. In the first batch test, (48 – 24) = 24 mgCa/ℓ = 0.60 mmolCa/ℓ precipitates, and for the second batch test (53 – 22) = 31 mgCa/ℓ = 0.78 mmolCa/ℓ precipitates.

P: From Figs 6.4 (d) and 6.5 (d), P concentrations decrease rapidly with aeration in both batch tests. This decrease corresponds with the decreases in Mg and Ca above, and confirms that the Mg and Ca are principally precipitating with phosphates. For the first batch test (94 – 13) = 81 mgP/ℓ = 2.6 mmolP/ℓ precipitates and for the second batch test (76 – 2.4) = 74 mgP/ℓ = 2.4 mmolP/ℓ precipitates.

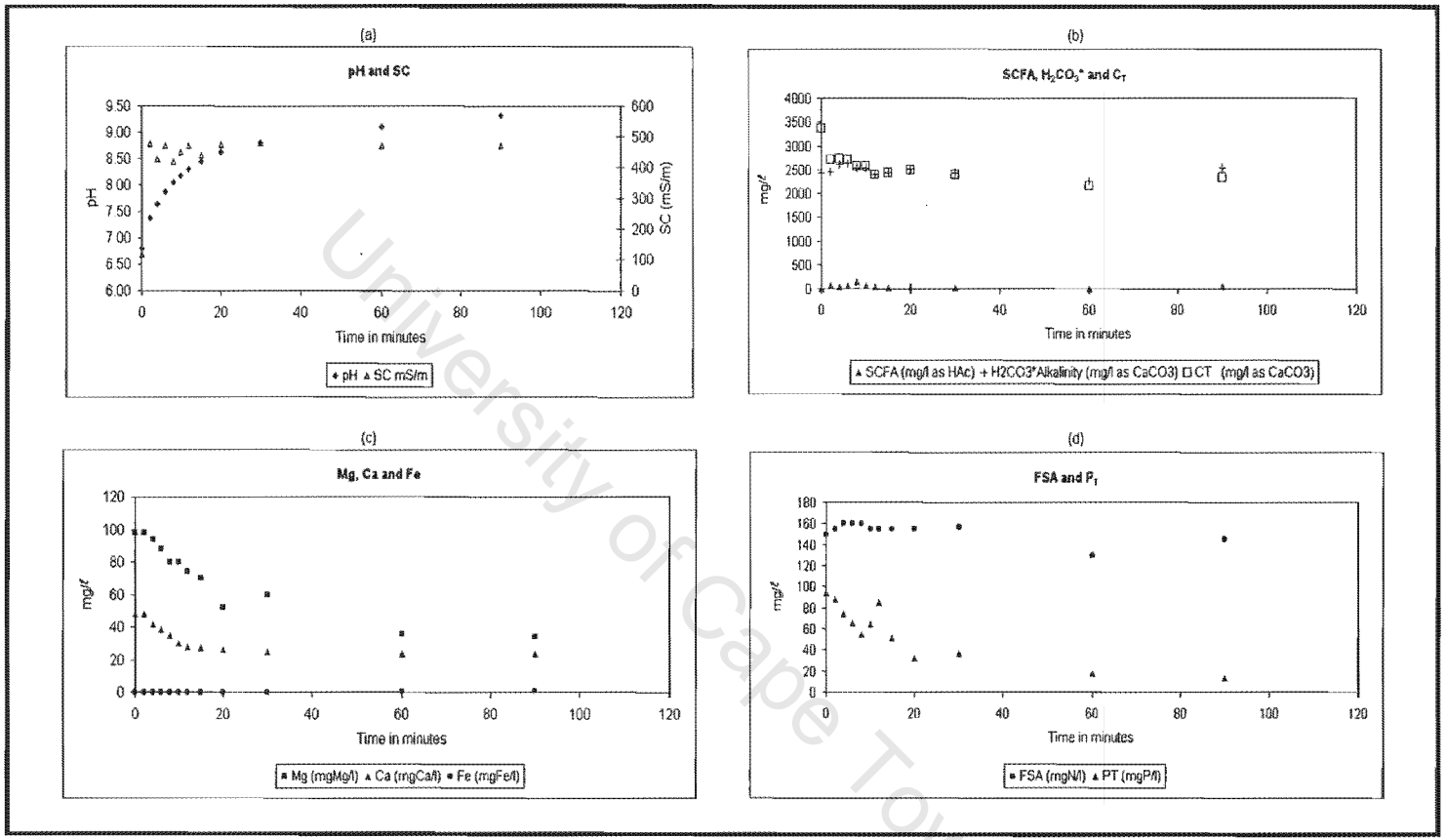

Fig 6.4 Measured (a) pH, specific conductivity (SC) and soluble concentrations for (b) SCFA, H_2CO_3* alk, total carbonate, C_T; (c) Mg, Ca, Fe; (d) free and saline ammonia (FSA), total soluble phosphate, P_T; in aerobic batch test on anaerobic digester supernatant from UASB reactor at SFW Wellington Distillery; Batch Test 1, Table D.1.

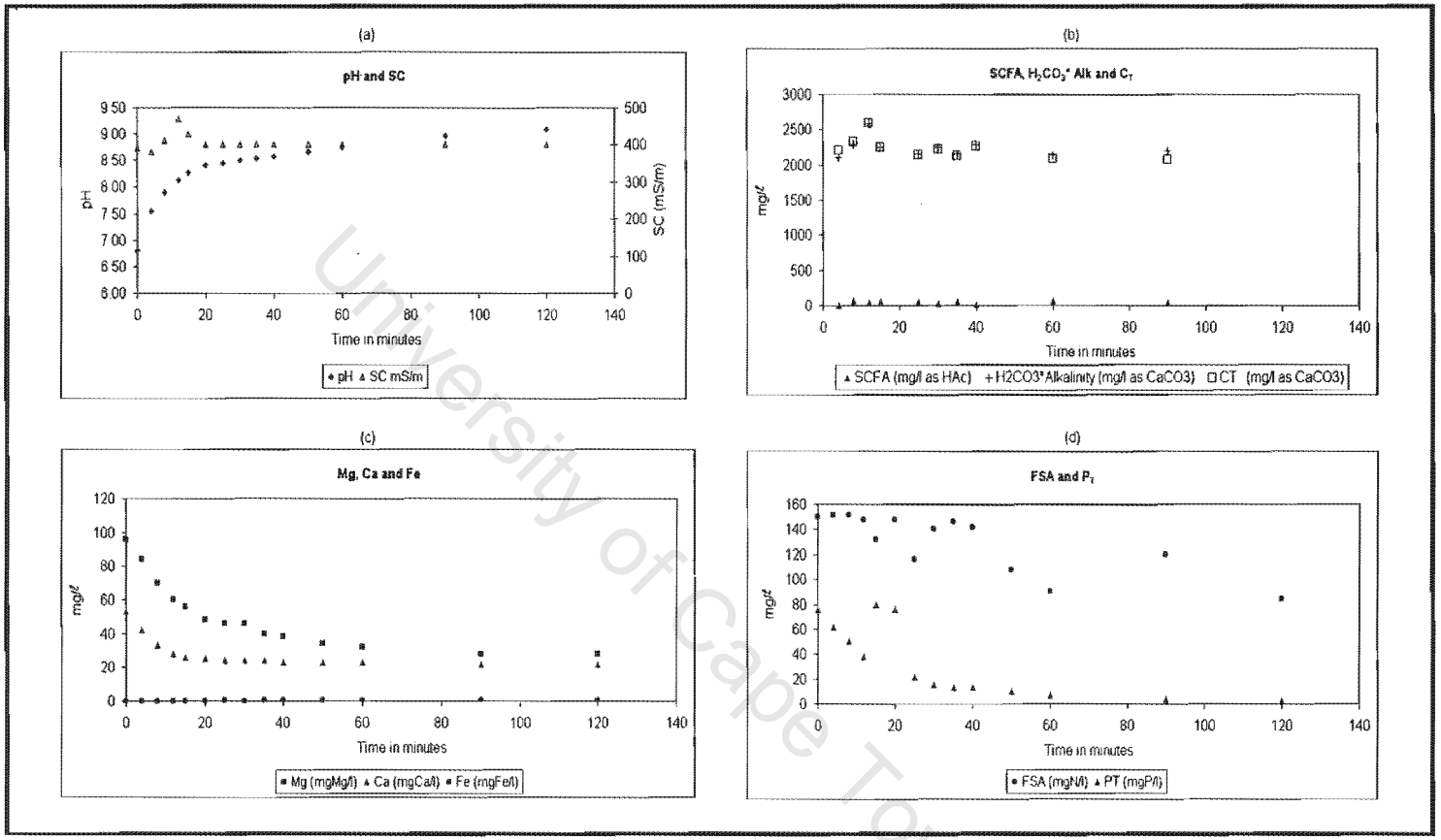

Fig 6.5 Measured (a) pH, specific conductivity (SC) and soluble concentrations for (b) SCFA, H_2CO_3* alk, total carbonate, C_T; (c) Mg, Ca, Fe; (d) free and saline ammonia (FSA), total soluble phosphate, P_T; in aerobic batch test on anaerobic digester supernatant from UASB reactor at SFW Wellington Distillery; Batch Test 2, Table D.2.

FSA: From Figs 6.4 (d) and Figs 6.5 (d), in both batch tests FSA concentrations decrease. However, the data are erratic and absolute values for the decreases cannot be determined.

Minerals precipitating: From the results above, minerals most likely precipitating are struvite, calcium phosphate and magnesite. Due to common species in these minerals, the amounts of these minerals that precipitate cannot be determined. This will be determined from the theoretical simulations with the kinetic multi-precipitation weak acid/base model (see Section 5 below). However, an indication of the precipitation potential can be obtained by assuming that all the Mg precipitates as struvite ($MgNH_4PO_4 \cdot 6H_2O$) and all the Ca as amorphous calcium phosphate (ACP, $Ca_3(PO_4)_2 \cdot xH_2O$). For the struvite, in the first batch test 2.7 x 245 = 662 mg/ℓ as $MgNH_4PO_4 \cdot 6H_2O$ precipitates, and in the second batch test 2.8 x 245 = 686 mg/ℓ as $MgNH_4PO_4 \cdot 6H_2O$. For the ACP, the water of hydration is unknown and cannot be taken into account. Accepting this deficiency, in the first batch test 0.6 x 310 = 186 mg/ℓ as $Ca_3(PO_4)_2$ precipitates and in the second batch test 0.78 x 310 = 242 mg/ℓ as $Ca_3(PO_4)_2$. These represent substantial precipitation potentials.

Time taken to reach equilibrium: From Figs 6.4 (d) and 6.5 (d), Ca reaches the equilibrium value after 30 minutes aeration in the first batch test, and 25 minutes in the second batch test. From Fig 6.4 (d) and 6.5 (d), Mg does not appear to reach equilibrium in the first batch test, but reaches equilibrium after 90 minutes in the second batch test. However, due to the simultaneous precipitation of multiple minerals it is not possible to determine when equilibrium is reached for the specific minerals. This will be addressed in more detail in the theoretical simulations of the batch test results (see Section 5 below).

5. APPLICATION OF KINETIC MODEL TO AEROBIC BATCH TESTS

The multi-precipitant weak acid/base kinetic model of Musvoto *et al.* (1998, 2000) was applied to the aerobic batch tests at 37°C on effluent from the UASB reactor at SFW

Wellington Distillery (Section 4.4.2 above). All simulations were with the computer programme AQUASIM (Reichert, 1994).

5.1 Model preparation

The model was given as input:

- The eight dissociation constants (pK) and their sensitivities for the sixteen forward and reverse dissociation processes for the water, carbonate, phosphate, SCFA and ammonia weak acid/base systems (Table 1, Musvoto *et al.*, 1997) from Table 2c in Musvoto *et al.* (1997). Musvoto *et al.* obtained these values from the literature.

- The specific rates constants for the eight reverse dissociation reactions (K_r) for the weak acid/base systems above from Table 2a in Musvoto *et al.* (1997), but in time units /d due to instability in AQUASIM with time units /s. This change in time units does not influence the predictions as these rates are several orders of magnitude faster than the mineral precipitation rates.

- The specific rate constants for the eight forward dissociation reactions for the weak acid/base systems above (K_f) are calculated by the AQUASIM programme from the input pK and K_r values above, as set out in Table 2a in Musvoto *et al.* (1997).

- The 11 stability constants (pK_{ST}) for the 22 forward and reverse dissociation processes for the ion pairs (Table 3, Musvoto *et al.*, 2000) from Table 1a in Musvoto *et al.* (2000). Musvoto *et al.* obtained these values from the literature.

- The specific rate constants for the 11 reverse dissociation reactions (K_r) for the ion pairs above from Table 1c in Musvoto *et al.* (2000).

- The specific rate constants for the 11 forward dissociation reaction for the ion pairs above (K_f) are calculated by the AQUASIM programme for the input pK_{ST} and K_r values above, as set out in Table 1c in Musvoto *et al.* (2000).

- The solubility product (pK_{sp}) values for the five minerals identified to precipitate (Table 2, Musvoto *et al.*, 2000) from Table 7 in Musvoto *et al.* (2000). Musvoto *et al.* obtained these values from the literature.

Initially, the pK, pK_{ST}, pK_{sp} and K_r (with calculated K_f) above were accepted as model constants (not changed). With the measured initial conductivity, also given as input and converted internally in the model to an ionic strength value with the formulae given by Loewenthal *et al.* (1989) (ionic strength μ = conductivity·$1.68 \cdot 10^{-4}$), the input pK, pK_{ST} and pK_{sp} values were internally corrected for ionic strength with the appropriate mono-, di- and trivalent ion activity coefficients, as indicated in the above mentioned tables. The input pK values were also internally adjusted for the input measured temperature (35°C); the pK_{ST} and pK_{sp} values could not be adjusted, as information on temperature sensitivities for these is not available in the literature. The initial total species concentrations (C_T, P_T, N_T, Ca and Mg) and pH values measured in the batch test were also given as input to the model, as initial conditions.

5.2 Model calibration

In validating their model, Musvoto *et al.* (2000) changed only the precipitation rate constants (K'_{ppt}) for the five minerals included in the model and the specific gas stripping rate constants (K'_r) for CO_2 and NH_3; these seven rate constants were determined by trial and error fitting of theoretical model predictions to the experimental data. In the initial simulations of the two batch tests reported here, the values for these constants found by Musvoto *et al.* (2000) were accepted, but with the gas stripping rate for CO_2 adjusted for aeration conditions for the batch test (see below). However, the correlation between predicted and measured results was poor. Accordingly, a calibration exercise was undertaken to improve this correlation. Values for the various constants are set out in Table 6.7.

Weak acid/base pK values and specific rates

The pK values for the weak acid/bases are well established, as well as their sensitivity to temperature. Accordingly, the values and temperature sensitivities obtained from the literature by Musvoto *et al.* (1997) were not changed. Also, the specific rate constants for the weak acid/base forward dissociation reactions from Musvoto *et al.* (1997) were

Table 6.7 Values for constants used in kinetic model simulation of aeration batch tests on full-scale UASB system supernatant at the SFW Wellington Distillery.

Description	Symbol	Value			Units	Source
		Default	Batch Test 1	Batch Test 2		
Weak acid/base – pK values						
Ammonia, carbonate, phosphate, SCFA, water	pK_x	Table 2c	default	default		Musvoto *et al.* (2000)
Weak acid/bases – specific rate constants for forward dissociation						
Ammonia, carbonate, phosphate, SCFA, water	K_{rx}	10^7-10^{15}	default	default	($g/m^3.d$)	Musvoto *et al.* (1997)
Ion pairs – pK_{ST} values						
$CaOH^+$	$pK_{ST,\ CaOH^+}$	-1.37	default	default		Musvoto *et al.* (2000)
$CaCO_3$ (aq)	$pK_{ST,\ CaCO3\ (aq)}$	-3.2	-3.37	default		Musvoto *et al.* (2000)
$CaHCO_3^+$	$pK_{ST,\ CaHCO3^+}$	-1.26	-0.59	-0.59		Calibration & Musvoto *et al.* (2000)
$CaPO_4^-$	$pK_{ST,\ CaPO4^-}$	-6.46	-5.9	-5.9		Loewenthal and Marais (1984)
$CaHPO_4$ (aq)	$pK_{ST,\ CaHPO4\ (aq)}$	-2.73	default	Default		Musvoto *et al.* (2000)
$CaH_2PO_4^+$	$pK_{ST,\ Ca2PO4^+}$	-1.41	default	Default		Musvoto *et al.* (2000)
$MgOH^+$	$pK_{ST,\ MgOH^+}$	-2.2	default	Default		Musvoto *et al.* (2000)
$MgCO_3$ (aq)	$pK_{ST,\ MgCO3\ (aq)}$	-3.4	default	Default		Musvoto *et al.* (2000)
$MgHCO_3^+$	$pK_{ST,\ MgHCO3^+}$	-1.16	default	Default		Musvoto *et al.* (2000)
$MgHPO_4$ (aq)	$pK_{ST,\ MgHPO4\ (aq)}$	-2.5	-3.5	Default		Calibration & Musvoto *et al.* (2000)
$MgPO_4^-$	$pK_{ST,\ MgPO4^-}$	-3.13	default	Default		Musvoto *et al.* (2000)
Ion pairs – specific rate constants for forward association						
Ion pairs above	K_{rx}	10^7	default	Default	($g/m^3.d$)	Musvoto *et al.* (2000)
Specific gas stripping rates						
O_2	$K_{La,\ O2}$	calibration	1 300	1 300	(/d)	Calibration
NH_3	$K_{La,\ NH3}$	calibration	5.2	5.2	(/d)	Calibration
Precipitating minerals – pK_{sp} values						
ACP	$pK_{sp,\ ACP}$	25.46	default	default		Musvoto *et al.* (2000)
Calcite	$pK_{sp,\ CACO3}$	6.45	default	default		Musvoto *et al.* (2000)
Magnesite	$pK_{sp,\ MgCO3}$	7.00	6.43	6.43		Calibration in literature range
Newberyite	$pK_{sp,\ New}$	5.8	default	Default		Musvoto *et al.* (2000)
Struvite	$pK_{sp,\ Struv}$	13.16	default	Default		Musvoto *et al.* (2000)
Precipitating minerals – specific precipitation rate constants						
ACP	$K_{ppt,ACP}$	350	48 000	48 000	($g/m^3.d$)	Calibration
Calcite	$K_{ppt,CaCO3}$	0.5	default	Default	($g/m^3.d$)	Musvoto *et al.* (2000) – insensitive
Magnesite	$K_{ppt,MgCO3}$	50	1 000	1 000	($g/m^3.d$)	Calibration
Newberyite	$K_{ppt,New}$	0.05	Default	Default	($g/m^3.d$)	Musvoto *et al.* (2000) – insensitive
Struvite	$K_{ppt,Struv}$	3 000	3 000		($g/m^3.d$)	Calibration

retained, but in time units /d as noted above – the requirement for these is simply that the reactions are so fast that they essentially are at equilibrium.

Gas stripping rates

The gas stripping rates were adjusted to take account of the aeration conditions in the batch tests. In the simulations it was found that the gas stripping rate for CO_2 required adjustment. In the model this rate is calculated from the specific rate for O_2; the value for this rate had to be changed from the range 400-670/d reported by Musvoto *et al.* (2000) to 1 300/d for both batch tests. This change is not unexpected since the specific gas stripping rates depend on the aeration conditions (gas flow rates, mixing, solids, etc.) applied in the specific tests, and this differed between the two tests reported here and those reported by Musvoto *et al.* The simulations were relatively insensitive to the specific gas stripping rate of NH_3, and the measured TKN data were inadequate to calibrate this rate. Accordingly, this rate was calibrated by ensuring the ratio $K_{La}NH_3/K_{La}O_2$ was equal to the value reported by Musvoto *et al.* (2000), as 0.004. This gave specific gas stripping rate constant for NH_3 of 5.2/d.

Ion pair specific dissociation rates

Similarly to the weak acid/bases, the requirement for the specific rate constants for the forward dissociation of the 11 ion pairs included in the model is that the rates are so rapid that they essentially are at equilibrium. Accordingly, the values from Musvoto *et al.* (2000) were accepted unmodified.

Remaining constants

In calibrating the remaining constants, it was noted that the mineral precipitation rates and the mass of minerals precipitating depends on a number of interacting factors, including concentrations of the free species combining to form the precipitants, the mineral specific precipitation rate constants (K_{ppt}), and the solubility product pK_{sp} values for the specific minerals.

In turn, the concentrations of the free species combining to form the precipitants are strongly influenced by the amounts of ion pairs formed, which in the model are determined by the stability constants pK_{ST} for the ion pairs. Thus, in calibration the constants K_{ppt}, pK_{sp} and pK_{ST} all have an influence on the rate of precipitation and the

constants K_{ppt}, pK_{sp} and pK_{ST} all have an influence on the rate of precipitation and the mass of precipitant formed. Different sets of values for these constants can be found that will give predictions that are similar. To resolve this difficulty, no guidance could be obtained from the literature; no values for the different mineral specific precipitation rate constants have been reported for multi-mineral precipitation conditions, and no information on the sensitivities of the pK_{sp} and pK_{ST} to temperature is available (literature values are at 25°C and the batch tests were conducted at 35°C).

Accordingly, in calibrating the model it was decided to ensure that:

- the specific precipitation rate constants for both batch tests were the same,
- to use the default values for the pK_{sp} where possible and, if these are changed to keep the same values for both batch tests,
- to adjust the pK_{ST} values to get the best fit of predicted to measured data, if possible using the same values for both batch tests.

Following the above, the final values for the constants for both batch tests are listed in Table 6.7. It should be noted that, irrespective of which calibration procedure is followed (i.e. the procedure above, or some other);

- there is not complete freedom in changing the values for the constants, some changes will not be able to match predicted to measured data.
- to obtain reasonable correlation between predicted and measured data, the amount of the different minerals precipitating and their precipitation rates must be similar, i.e. the net precipitation is largely independent of the calibration approach followed.

5.3 Results

Predicted and measured concentrations for the two batch tests are shown plotted in Figs 6.6 (a to f) and 6.7 (a to f) respectively. Predicted concentrations of minerals

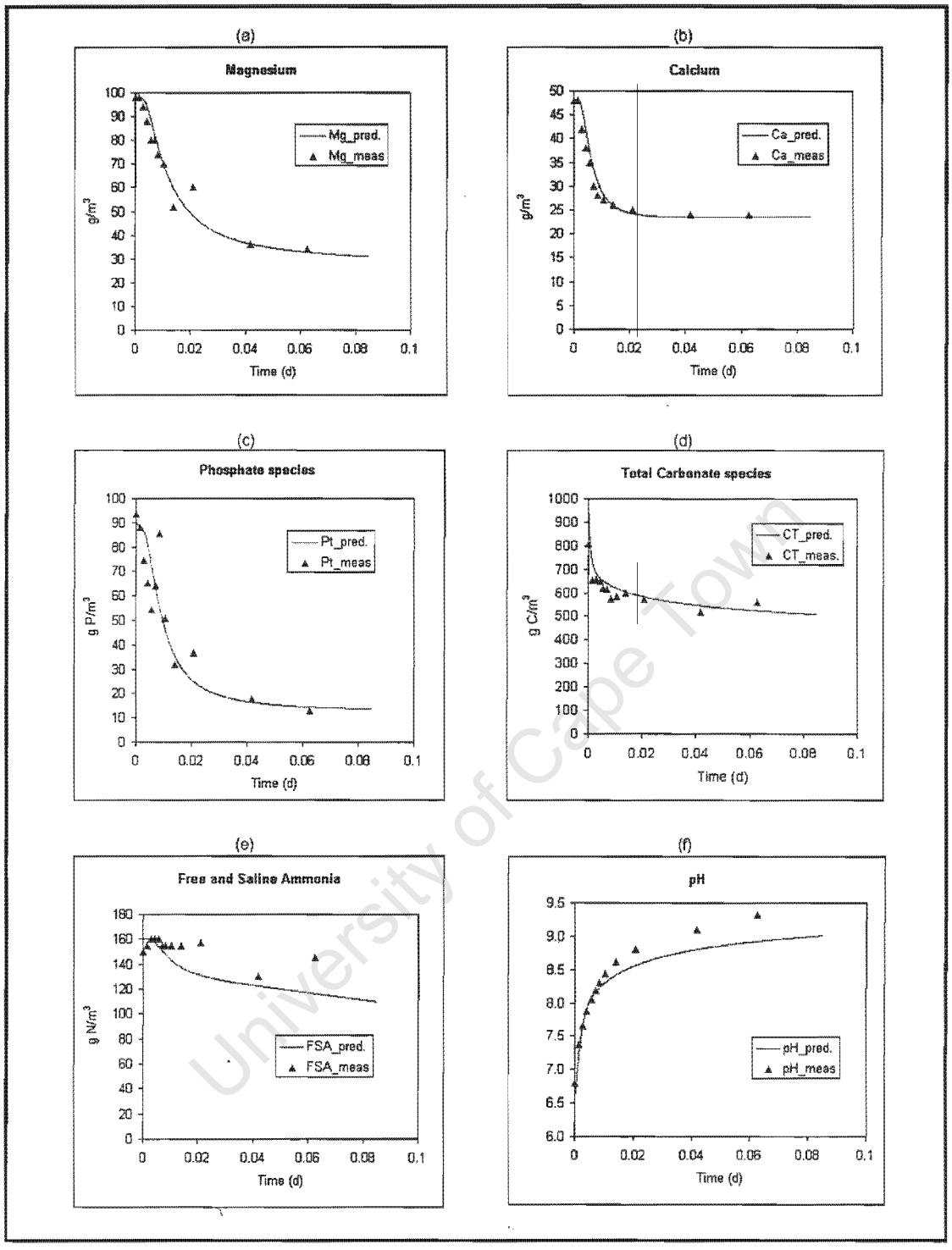

Fig 6.6 Predicted and measured soluble concentrations for (a) magnesium, (b) calcium, (c) total soluble phosphate, P_T, (d) total carbonate, C_T, (e) free and saline ammonia (FSA) and (f) pH; in aerobic batch test on anaerobic digester supernatant from the full-scale UASB reactor at SFW Wellington Distillery; Batch Test 1.

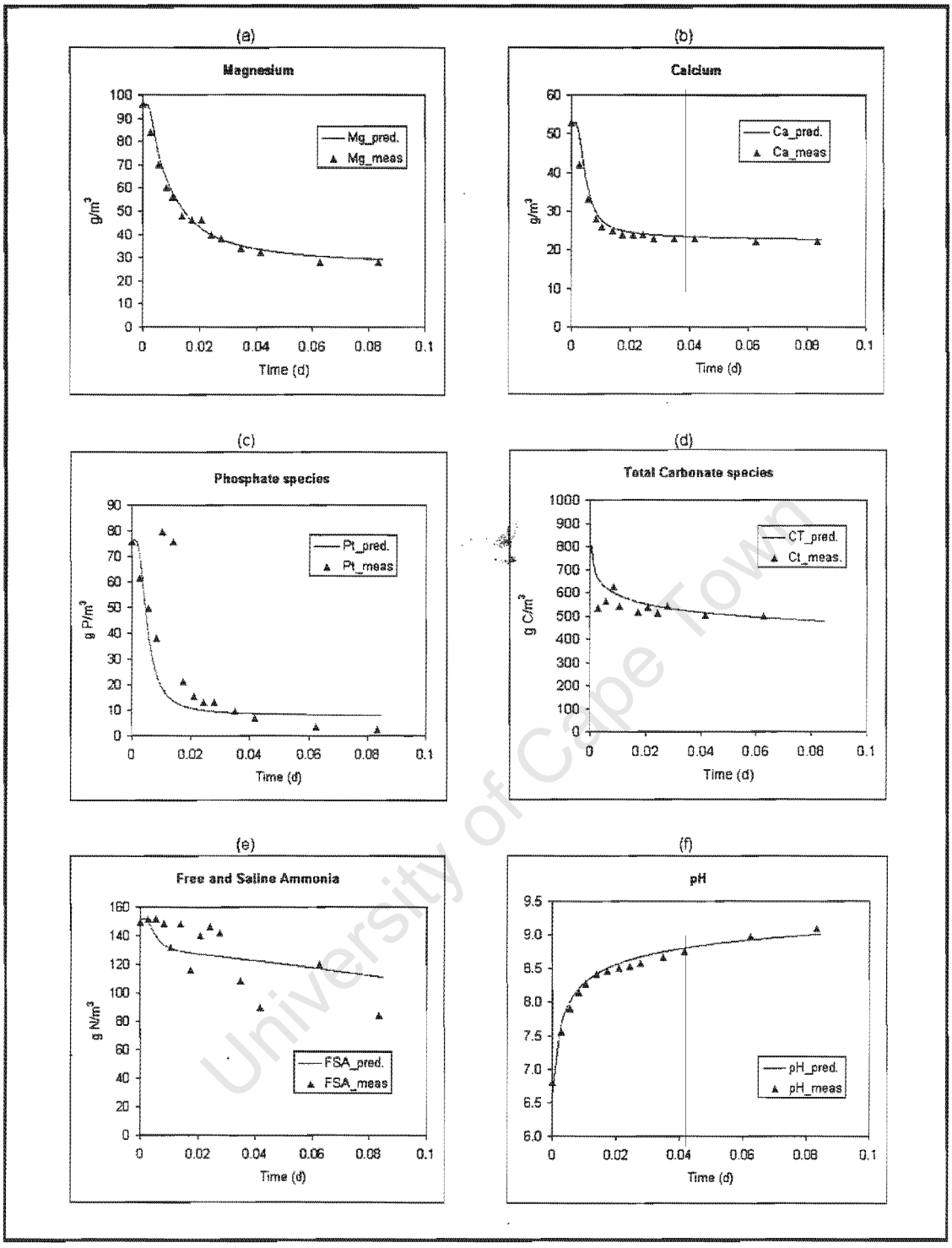

Fig 6.7 Predicted and measured soluble concentrations for (a) magnesium, (b) calcium, (c) total soluble phosphate, P_T, (d) total carbonate, C_T, (e) free and saline ammonia (FSA) and (f) pH; in aerobic batch test on anaerobic digester supernatant from the full-scale UASB reactor at SFW Wellington Distillery; Batch Test 2.

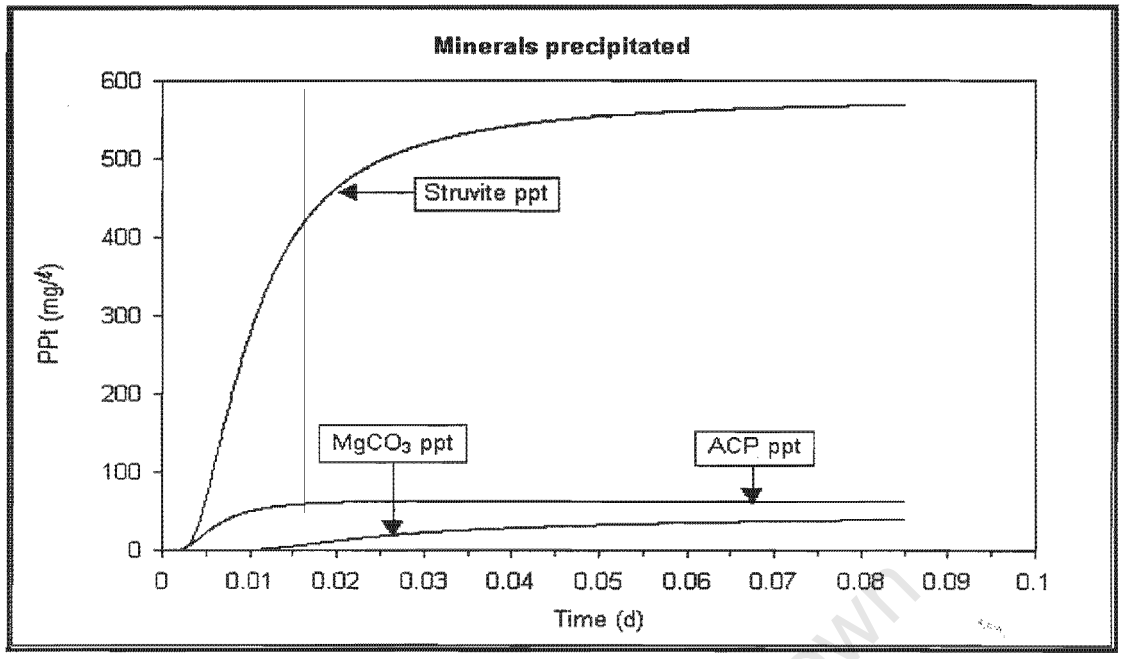

Fig 6.6 (g) Predicted concentrations of minerals precipitating in aerobic batch test on anaerobic digester supernatant from the full-scale UASB reactor at SFW Wellington Distillery; Batch Test 1.

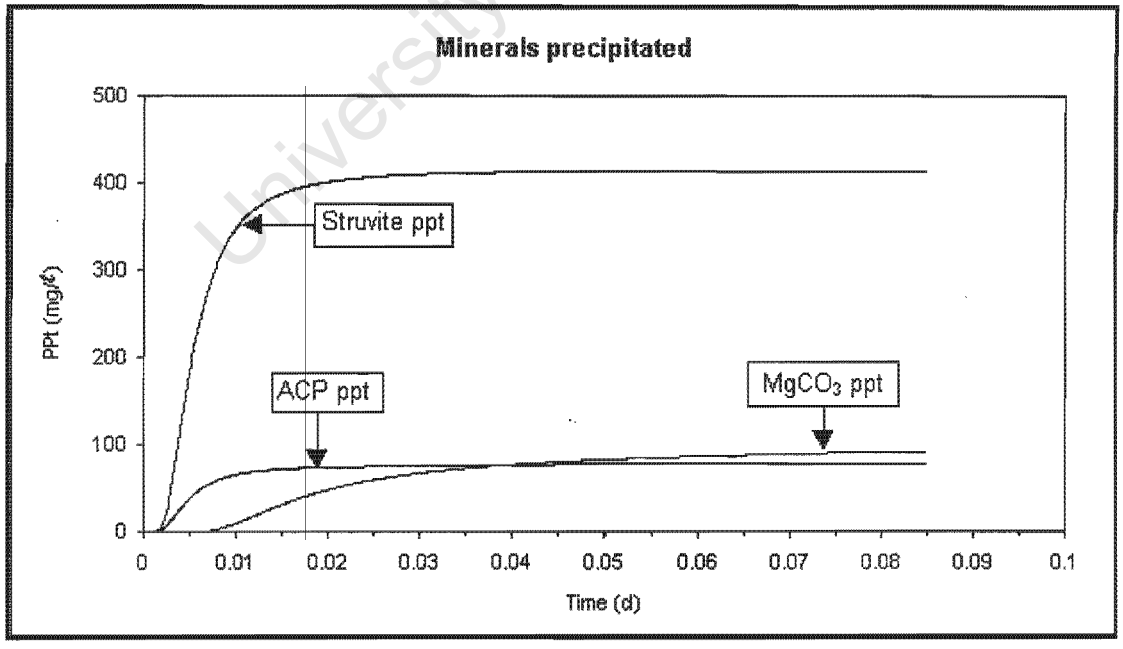

Fig 6.7 (g) Predicted concentrations of minerals precipitating in aerobic batch test on anaerobic digester supernatant from the full-scale UASB reactor at SFW Wellington Distillery; Batch Test 2.

precipitating are shown plotted in Figs 6.6 (g) and 6.7 (g) for batch tests 1 and 2 respectively.

Correlation between predicted and measured results

From Figs 6.6 (a-f) and 6.7 (a-f), predicted and measured results for both batch tests correlate closely, with the exception of pH for batch test 1 and phosphate for batch test 2. With regard to the pH in batch test 1, simulations were undertaken in which OH^- was dosed to the batch reactor, such that measured and predicted pHs matched very closely. However, this did not have any significant influence on predictions of mineral precipitation, and thus the lack of fit is not of importance in determining mineral precipitation. With regard to phosphate in batch test 2, improving the "fit" of predicted to measured phosphate caused the "fit" in Mg to be worse. Accordingly, the better Mg fit was accepted. However, the correlation between predicted and measured phosphate is not unacceptable.

Minerals precipitated

Accepting that the predictions are reasonable, the predicted concentrations of the different minerals that precipitate can be determined, see Figs 6.6 (g) and 6.7 (g) for batch tests 1 and 2 respectively. For both batch tests, the dominant mineral that precipitates is struvite, with some ACP and magnesite, and negligible newberyite and calcite. In batch test 1, after 90 minutes 562 mg/ℓ struvite as $MgNH_4PO_4 \cdot 6H_2O$ (=85 % of mass of precipitant) has precipitated, 63 mg/ℓ ACP as $Ca_3(PO_4)_2$ (=10 % of mass of precipitant) and 36 mg/ℓ magnesite as $MgCO_3$ (=5 % of mass of precipitant). In batch test 2, after 120 minutes 415 mg/ℓ struvite as $MgNH_4PO_4 \cdot 6H_2O$ (=71 % of mass of precipitant) has precipitated, 78 mg/ℓ ACP as $Ca_3(PO_4)_2$ (=13 % of mass of precipitant) and 92 mg/ℓ magnesite as $MgCO_3$ (=16 % of mass of precipitant). With the large volumes of flow passing through the UASB plant, this represents substantial precipitation potential. The exact amount of minerals that will precipitate in the UASB reactor will depend on the CO_2 loss and pH established.

Critical pH for precipitation

From Figs 6.6 (g) and 6.7(g), struvite and ACP start precipitating virtually immediately on aeration, after about 3½ and 2 minutes in batch tests 1 and 2 respectively. The pH

values at these times are 7.5 and 7.3 respectively. This indicates that the solution is initially slightly undersaturated with respect to these two minerals. However, with aeration the pH increases very rapidly to exceed the critical pH for precipitation where the minerals become supersaturated and hence precipitate. Magnesite only starts precipitating after about 13 and 10 minutes in batch test 1 and 2 respectively. The pH values at these times are 8.2 and 8.1 respectively. This indicates that initially magnesite is undersaturated, and remains undersaturated until the pH exceeds the critical pH of about 8.1. Thereafter, the solution is supersaturated with respect to magnesite and hence magnesite precipitates.

Time to complete precipitation

In batch test 2, from Fig 6.7 (g) both struvite and ACP precipitation are virtually complete after about 20 minutes – further aeration results in only small additional precipitation of these two minerals. In batch test 1, from Fig 6.6 (g) after 20 minutes ACP precipitation is virtually complete, but struvite continues precipitating and by about 30 minutes 90 % of the struvite that will precipitate has precipitated. In contrast magnesite continues precipitating throughout both batch tests.

It should be noted that the time to complete precipitation will depend on the aeration conditions applied; the greater the aeration, the faster the CO_2 stripping rate, the faster the increase in pH and hence the shorter the time to reach complete precipitation.

6. CONCLUSIONS

In this chapter, precipitation of minerals from the UASB system at the SFW Distillery at Wellington has been investigated. The investigation involved:

(1) Determination of the struvite solubility product in distilled water at 20°C and 37°C, to validate the value at 20°C obtained from the literature and the experimental protocol, and develop a value for 37°C.

(2) Aeration batch tests at 37°C on supernatant drawn directly from the UASB system, and kinetic modelling of these batch test results to develop a deeper understanding of the processes operating in the precipitation.

6.1 Struvite solubility product in distilled water

From 9 tests at 20°C and 13 at 37°C:

- The average struvite solubility products (pK_{sp}) in distilled water at 20°C and 37°C were 12.66 (sample standard deviation 0.08) and 12.46 (sample deviation 0.194) respectively.

- The pK_{sp} value at 20°C falls within the range of values recorded in the literature (pK_{sp}=12.6 to 13.26), indicating the experimental protocol and data are acceptable.

- The pK_{sp} value at 37°C is lower than the value at 20°C, and this difference is statistically significant at the 95 % confidence interval.

- Thus, it would appear that the effect of an increase in temperature is to decrease the pK_{sp} value for struvite. However, this effect is relatively small, with the 17°C increase in temperature causing the pK_{sp} to decrease by only 0.2 units.

6.2 Aeration batch tests and modelling

From this investigation, the following conclusions can be drawn:

- The dominant mineral that precipitates is struvite ($MgNH_4PO_4 \cdot 6H_2O$), with some amorphous calcium phosphate (ACP, $Ca_3(PO_4)_2$) and magnesite ($MgCO_3$), and negligible newberyite ($MgHPO_4 \cdot 3H_2O$) and calcite ($CaCO_3$).

- For the two batch tests conducted, from modelling respectively
  - 562 and 415 mg/ℓ struvite,
  - 63 and 78 mg/ℓ ACP,

- 36 and 92 mg/ℓ magnesite

precipitated. With the large volumes of flow passing through the UASB system, these represent substantial precipitation potentials.

- The precipitation of struvite is stimulated by the increase in pH when CO_2 is lost from the UASB supernatant. Within the UASB digester, the partial pressure of CO_2 is high due to anaerobic processes acting in the digester. When the supernatant leaves the digester it comes into contact with atmospheric conditions where the partial pressure of CO_2 is much lower than inside the digester. This causes CO_2 loss from the supernatant to the air, until equilibrium between the CO_2 concentration in the supernatant and the air is reached. Loss of CO_2, represents an increase in acidity which means that the pH of the supernatant will increase. This increase in pH causes struvite to become supersaturated, and hence it precipitates.

- When the supernatant leaves the digester, it is initially undersaturated with respect to struvite. Depending on the initial conditions in the supernatant, significant struvite starts precipitating when the pH increases above pH=7.3 to 7.5.

- With aeration, the critical pH for struvite precipitation is reached after 2 to 3½ minutes aeration. However, this time will depend on a number of factors, including aeration rate, initial pH, buffer capacity, initial P and Mg concentrations, etc.

- The increase in pH with aeration also stimulates precipitation of ACP. However, as noted above, the mass of ACP precipitating is relatively small compared with struvite. Similarly to struvite, ACP is initially undersaturated but starts precipitating after 2 to 3½ minutes aeration, when the critical pH for ACP precipitation of 7.3 to 7.5 is reached.

- The increase in pH with aeration also stimulates precipitation of magnesite. However, magnesite is significantly undersaturated at the start of the test and only starts precipitating after 10 to 13 minutes, when the critical pH for magnesite precipitation of 8.1 to 8.2 is reached.

- For struvite and ACP, the precipitations are essentially complete after 20 to 30 minutes aeration, and further aeration results in minor precipitation of these two minerals. For magnesite, this continues precipitating throughout both batch tests. It should be noted that the time to complete precipitation will depend on the aeration conditions applied – the greater the aeration, the faster the CO_2 stripping rate, the faster the increase in pH, and hence the shorter the time to reach complete precipitation.

- In the kinetic model, the pK_{sp} value for struvite was pK_{sp}=13.16. This value is the same as that of Musvoto *et al.* (2000) from similar batch tests and falls within the range of values reported in the literature (12.6 to 13.26). The value is larger than the value measured at 37°C in distilled water (12.46). This increase in value probably is due to the presence of organics and other compounds in the UASB supernatant. A similar increase was noted by Loewenthal and Morrison (1998) for activated sludge effluent (12.92) compared to distilled water (12.83) at 20°C. Furthermore, the effect of ion pair formation on struvite precipitation is taken into account in the kinetic model, but was not considered when calculating the pK_{sp} value in distilled water.

- In the simulations with the kinetic model, the specific rate constant for struvite precipitation was 3000 $g/m^3.d$. This is the same value found by Musvoto *et al.* (2000) for the same UASB ADL at 20°C.

6.3 Recommendations

The investigation here confirms that the precipitation problem experienced at the full-scale UASB system at SFW Wellington Distillery is predominantly due to struvite, and to a smaller extent ACP. The precipitation is stimulated by CO_2 loss which causes the pH to increase, which results in struvite and ACP supersaturation and hence precipitation. To limit struvite and ACP precipitation within the full-scale UASB system, the investigation has clearly demonstrated that stimulating struvite precipitation by aeration in a controlled environment is feasible. If introduced at the full-scale UASB system as a side-stream process, this controlled struvite precipitation possibly will reduce the Mg and P concentration sufficiently so that precipitation within the UASB effluent collection pipework will be reduced significantly. The calibrated AQUASIM

model can be applied to model the side stream flow through the reactor to determine reactor retention times and aeration rates to achieve a desired mineral removal. This proposal requires evaluation at pilot-scale on the full-scale UASB reactor at the SFW Wellington Distillery.

CHAPTER 7

CONCLUSIONS

The full-scale UASB system at the SFW Wellington Distillery treats two main types of wastewaters, grain wastewater generated in the distillation of grain products and wine wastewater generated in the distillation of grape wine. In operation of this system, a number of operational problems were encountered. Of these, the two main operating problems causing operational failure of the UASB system that remain unresolved are (i) sludge layer formation on treatment of grain wastewater and (ii) struvite precipitation on treatment of wine wastewater. This research project investigates both problems at a laboratory-scale to identify possible causes and solutions.

7.1 Sludge layer formation with grain wastewater

In a preliminary investigation, a laboratory-scale UASB system was operated with grain wastewater as influent, with or without prior filtration through a rotary drum filter. From the results obtained during this preliminary investigation, the following conclusions could be made:

- A sludge layer was formed on the liquid surface of the laboratory-scale UASB system, appearing as a thick gelatinous mass. This confirmed that the problem identified at full-scale could be reproduced at laboratory scale, validating the experimental protocol.

- The sludge layer above was present when both the centrifuged (high TSS) and filtered (low TSS) grain wastewaters served as influent. However, the sludge layer was very much reduced with the filtered grain wastewater compared to the centrifuged grain wastewater. This indicated that the causative agent for the sludge layer did appear to be related to the TSS content of the grain wastewater. However, although drum filtering of the wastewater appeared to reduce the problem, it did not eliminate it.

- During periods of successful operation, % COD removal of >90 % could be achieved with both the centrifuged and filtered grain wastewater. However, the system was prone to upsets with relatively long recovery periods, of about 11 days.

The success in reproducing the sludge layer observed at full-scale in the laboratory-scale system prompted a more detailed investigation into this operational problem. Two laboratory-scale UASB systems were operated in parallel. One system served as a control and received wine wastewater as influent. The other system served as the experimental system, and was switched from wine wastewater to grain wastewater as influent, either as a blend with the wine wastewater or on its own with and without prior settling. From the results obtained in this investigation, the following conclusions could be made:

- In conformity with the conclusions made in the preliminary investigation, when treating grain wastewater, a sludge layer was formed on the liquid surface of the laboratory-scale UASB system, appearing as a thick gelatinous mass. This confirmed that the problem identified at full-scale could be reproduced at laboratory scale, validating the experimental protocol.

- The sludge layer above was present with the grain wastewater in any form, i.e. blended with wine wastewater, settled or unsettled grain wastewater only. The sludge layer accumulation was most severe with unsettled grain wastewater, and reduced in the blend and settled grain wastewater – blending the grain wastewater with wine wastewater or settling the grain wastewater reduced, but did not eliminate sludge layer accumulation.

- With wine wastewater, sludge layer accumulation was never observed.

- The observations above indicate that sludge layer accumulation is a property of the grain wastewater, and not distillery wastewaters in general. Also, in conformity with the conclusions made in the preliminary investigation, the sludge layer accumulation is linked to the solids content of the grain wastewater.

Reducing the solids content by drum filtration, settling or blending can reduce but not eliminate the sludge layer accumulation.

- The bed profiles measured for the UASB system treating wine wastewater conform to those measured previously with apple juice wastewater (Sam-Soon *et al.*, 1987), glucose (Sam-Soon *et al.*, 1990), protein (Moosbrugger *et al.*, 1990), brewery wastewater (Moosbrugger *et al.*, 1993a) and wine distillery wastewater (Moosbrugger *et al.*, 1993b). In these profiles the typical three distinct zones of behaviour can be identified, namely lower active, upper active and upper inactive zones. The action of microorganisms in these zones conforms to the proposals of Sam-Soon and co-workers (Wentzel *et al.*, 1994).

- For the UASB system treating grain wastewater, the bed profile differs markedly from that above. The three zones of behaviour do not develop to any marked extent. A possible explanation proposed for this behaviour is that the grain wastewater contains considerable suspended solids. The rate of acidogenesis with suspended solids as substrate, would be limited by the rate of hydrolysis. Typically, hydrolysis rates would be much slower than acidogenesis rates with a soluble substrate. The net effect is to lower the overall rate of acidogenesis. With the lower acidogenic rates, the short chain fatty acids would be consumed in subsequent reactions as fast as they are produced, with the result that the short chain fatty acids concentrations would remain low throughout the UASB system.

- With grain wastewater, the absence of a differentiation into the three zones of behaviour raises the question of the long term viability of a UASB system treating this type of wastewater. In developing their hypothesis for pelletization in UASB systems, Sam-Soon *et al.* (1987) proposed that partial phase separation of the anaerobic processes and development of a zone with a high hydrogen partial pressure were essential for pellet formation (Wentzel *et al.*, 1994). In the UASB system treating grain wastewater here, observations (no HAc and little HPr) indicate that these prerequisites for pellet formation are not achieved. If this is true, according to the hypothesis of Sam-Soon *et al.* pellet growth will not occur, or will be greatly reduced. This indicates that, in the long term in switching from wine wastewater (where pellet growth has occurred) to grain wastewater there will

be a gradual loss of the pelletized sludge bed, until the pelletized bed declines to such low values that the system will fail. This aspect requires further investigation.

- The investigation here does indicate that when switching from wine wastewater, where a well-defined pelletized sludge bed has been developed, to grain wastewater, the grain wastewater can be effectively treated in the short term. However, most likely the sludge bed will diminish with time. To re-establish the pelletized bed, the system will have to be switched back to wine wastewater for a period.

7.2 Struvite precipitation with wine wastewater

Precipitation of minerals from the UASB system at the SFW Distillery at Wellington was also investigated. The investigation involved:

(1) Determination of the struvite solubility product in distilled water at 20°C and 37°C, to validate the value at 20°C obtained from the literature and the experimental protocol, and develop a value for 37°C.

(2) Aeration batch tests at 37°C on supernatant drawn directly from the UASB system, and kinetic modelling of these batch test results to develop a deeper understanding of the processes operating in the precipitation.

7.2.1 Struvite solubility product in distilled water

From 9 tests at 20°C and 13 at 37°C:

- The average struvite solubility products (pK_{sp}) in distilled water at 20°C and 37°C were 12.66 (sample standard deviation 0.08) and 12.46 (sample deviation 0.194) respectively.

- The pK_{sp} value at 20°C falls within the range of values recorded in the literature (pK_{sp}=12.6 to 13.26), indicating the experimental protocol and data are acceptable.

- The pK_{sp} value at 37°C is lower than the value at 20°C, and this difference is statistically significant at the 95 % confidence interval.

Thus, it would appear that the effect of an increase in temperature is to decrease the pK_{sp} value for struvite. However, this effect is relatively small, with the 17°C increase in temperature causing the pK_{sp} to decrease by only 0.2 units.

7.2.2 Aeration batch tests and modelling

From this investigation, the following conclusions could be drawn:

- The dominant mineral that precipitates is struvite ($MgNH_4PO_4 \cdot 6H_2O$), with some amorphous calcium phosphate (ACP, $Ca_3(PO_4)_2$) and magnesite ($MgCO_3$), and negligible newberyite ($MgHPO_4 \cdot 3H_2O$) and calcite ($CaCO_3$).

- For the two batch tests conducted, from modelling respectively
  - 562 and 415 mg/ℓ struvite,
  - 63 and 78 mg/ℓ ACP,
  - 36 and 92 mg/ℓ magnesite

  precipitated. With the large volumes of flow passing through the UASB system, these represent substantial precipitation potentials.

- The precipitation of struvite is stimulated by the increase in pH when CO_2 is lost from the UASB supernatant. Within the UASB digester, the partial pressure of CO_2 is high due to anaerobic processes acting in the digester. When the supernatant leaves the digester it comes into contact with atmospheric conditions where the partial pressure of CO_2 is much lower than inside the digester. This causes CO_2 loss from the supernatant to the air, until equilibrium between the CO2 concentration in the supernatant and the air is reached. Loss of CO_2, represents an increase in acidity which means that the pH of the supernatant will increase. This increase in pH causes struvite to become supersaturated, and hence it precipitates.

- When the supernatant leaves the digester, it is initially undersaturated with respect to struvite. Depending on the initial conditions in the supernatant, significant struvite starts precipitating when the pH increases above pH=7.3 to 7.5.

- With aeration, the critical pH for struvite precipitation is reached after 2 to 3½ minutes aeration. However, this time will depend on a number of factors, including aeration rate, initial pH, buffer capacity, initial P and Mg concentrations, etc.

- The increase in pH with aeration also stimulates precipitation of ACP. However, as noted above, the mass of ACP precipitating is relatively small compared with struvite. Similarly to struvite, ACP is initially undersaturated but starts precipitating after 2 to 3½ minutes aeration, when the critical pH for ACP precipitation of 7.3 to 7.5 is reached.

- The increase in pH with aeration also stimulates precipitation of magnesite. However, magnesite is significantly undersaturated at the start of the test and only starts precipitating after 10 to 13 minutes, when the critical pH for magnesite precipitation of 8.1 to 8.2 is reached.

- For struvite and ACP, the precipitations are essentially complete after 20 to 30 minutes aeration, and further aeration results in minor precipitation of these two minerals. For magnesite, this continues precipitating throughout both batch tests. It should be noted that the time to complete precipitation will depend on the aeration conditions applied – the greater the aeration, the faster the CO_2 stripping rate, the faster the increase in pH, and hence the shorter the time to reach complete precipitation.

- In the kinetic model, the pK_{sp} value for struvite was pK_{sp}=13.16. This value is the same as that of Musvoto *et al.* (2000) from similar batch tests and falls within the range of values reported in the literature (12.6 to 13.26). The value is larger than the value measured at 37°C in distilled water (12.46). This increase in value probably is due to the presence of organics and other compounds in the UASB supernatant. A similar increase was noted by Loewenthal and Morrison (1998)

for activated sludge effluent (12.92) compared to distilled water (12.83) at 20°C. Furthermore, the effect of ion pair formation on struvite precipitation is taken into account in the kinetic model, but was not considered when calculating the pK_{sp} value in distilled water.

- In the simulations with the kinetic model, the specific rate constant for struvite precipitation was 3000 $g/m^3.d$. This is the same value as that of Musvoto *et al.* (2000).

7.3 Future research

From this investigation two areas have been identified for further research:

(1) In the treatment of grain distillery wastewaters, this investigation has raised the question of the long term viability of a UASB system treating this type of wastewater. From the hypothesis for pelletization in UASB systems of Sam-Soon *et al.* (1987), it appears that with this wastewater the conditions may not be conducive for pellet formation. This aspect requires further investigation.

(2) The investigation here confirms that the precipitation problem experienced at the full-scale UASB system at SFW Wellington Distillery is predominantly due to struvite, and to a smaller extent ACP. The precipitation is stimulated by CO_2 loss which causes the pH to increase, which results in struvite and ACP supersaturation and hence precipitation. To limit struvite and ACP precipitation within the full-scale UASB system, the investigation has clearly demonstrated that stimulating struvite precipitation by aeration in a controlled environment is feasible. If introduced at the full-scale UASB system as a side-stream process, this controlled struvite precipitation possibly will reduce the Mg and P concentration sufficiently so that precipitation within the UASB effluent collection pipework will be reduced significantly. The calibrated AQUASIM model can be applied to model the side stream flow through the reactor to determine reactor retention times and aeration rates to achieve a desired mineral removal. This proposal requires evaluation at pilot-scale on the full-scale UASB reactor at the SFW Wellington Distillery.

APPENDIX A

PRELIMINARY INVESTIGATION – DETAILED RESULTS

Note: - values that are omitted, no analysis were done.

UASB DETAILED RESULTS:- PRELIMINARY INVESTIGATION

		unfiltered		filtered		load		% COD removal		COD removed	gasproduction			status	*feed
date	day	COD in	COD out	COD in	COD out	unfiltered	filtered	unfiltered COD	filtered COD	unfiltered COD	ℓ gas/d	ℓ gas rate per	ℓ gas/d		
		mg/ℓ	mg/ℓ	mg/ℓ	mg/ℓ	kgCOD/m^3 sludge vol./d				mg/ℓ		%COD removed			
06/08/1997	1													no test	US
07/08/1997	2													no test	US
08/08/1997	3													no test	US
09/08/1997	4													no test	US
10/08/1997	5													no test	US
11/08/1997	6													no test	US
12/08/1997	7	1615	307	1033	55	3.2	2.1	81	95	1308			0.60	no test	US
13/08/1997	8	1656	397	1012	133	3.3	2.0	76	87	1259			0.58	no test	US
14/08/1997	9	1677	368	1073	82	3.4	2.1	78	92	1309			0.60	sludge layer	US
15/08/1997	10	2270	356	1452	127	4.5	2.9	84	91	1914			0.88	sludge layer	US
16/08/1997	11	2239	478	1808	198	4.5	3.6	79	89	1761			0.81	sludge layer	US
17/08/1997	12	2617	453	1687	194	5.2	3.4	83	89	2164			1.00	sludge layer	US
18/08/1997	13	2852	1104	1891	590	5.7	3.8	61	69	1748			0.80	sludge layer	US
19/08/1997	14	2034	699	1063	556	4.1	2.1	66	48	1335			0.61	sludge layer	US
20/08/1997	15	1850	1472	981	826	3.7	1.9	20	14	378			0.17	sludge layer	S
21/08/1997	16	1280	1000	1199	951	2.6	2.4	22	21	280			0.13	sludge layer	S
22/08/1997	17	1128	900	1189	784	2.3	2.4	20	34	228			0.10	sludge layer	S
23/08/1997	18	1341	1061	894	654	2.7	1.8	21	27	280			0.13	sludge layer	S
24/08/1997	19	1788	764	1493	622	3.6	3.0	57	58	1024			0.47	sludge layer	S
25/08/1997	20	1260	817	1189	825	2.5	2.4	35	31	443			0.20	sludge layer	S
26/08/1997	21	1544	764	1544	630	3.1	3.1	51	59	780			0.36	sludge layer	S
27/08/1997	22	1449	855	1388	855	2.9	2.8	41	38	594			0.27	sludge layer	S
28/08/1997	23													sludge layer, no testing	S
29/08/1997	24	1819	1134	1758	1183	3.6	3.5	38	33	685			0.32	sludge layer	S
30/08/1997	25	1532	1081	1491	946	3.1	3.0	29	37	451			0.21	sludge layer	S
31/08/1997	26	1573	863	1480	744	3.1	3.0	45	50	710			0.33	sludge layer	S
01/09/1997	27	1686	962	1634	855	3.4	3.3	43	48	724			0.33	sludge layer	S
02/09/1997	28	1737	769	1696	835	3.5	3.4	56	51	968			0.45	sludge layer	S
03/09/1997	29	1727	937	1696	851	3.5	3.4	46	50	790			0.36	sludge layer	S
04/09/1997	30	1963	835	1922	695	3.9	3.8	57	64	1128			0.52	sludge layer	S
05/09/1997	31	2148	880	2066	645	4.3	4.1	59	69	1268			0.58	sludge layer	S
06/09/1997	32	1758	732	1604	600	3.5	3.2	58	63	1026			0.47	sludge layer	S
07/09/1997	33	1624	629	1460	534	3.2	2.9	61	63	995			0.46	sludge layer	S
08/09/1997	34	1622	438	1198	347	3.2	2.4	73	71	1184			0.54	sludge layer	US
09/09/1997	35	1684	355	1322	268	3.4	2.6	79	80	1329			0.61	sludge layer	US
10/09/1997	36	1249	231	1136	173	2.5	2.3	82	85	1018			0.47	sludge layer	US
11/09/1997	37	1260	244	1105	144	2.5	2.2	81	87	1016	1.26	0.00124	0.47	sludge layer	US
12/09/1997	38	1580	281	1219	153	3.2	2.4	82	87	1299	1.74	0.00134	0.60	sludge layer	US
13/09/1997	39	1787	178	1498	91	3.6	3.0	90	94	1609	1.79	0.00111	0.74	sludge layer	US
14/09/1997	40	1828	277	1756	194	3.7	3.5	85	89	1551		0.00000	0.71	sludge layer	US
15/09/1997	41	1754	274	1682	197	3.5	3.4	84	88	1480		0.00000	0.68	sludge layer	US
16/09/1997	42	2038	266	1393	156	4.1	2.8	87	89	1772	1.90	0.00107	0.82	sludge layer	US
17/09/1997	43	2089	344	1618	221	4.2	3.2	84	86	1745	1.90	0.00109	0.80	sludge layer	US
18/09/1997	44										2.00			sludge layer, no testing	US
19/09/1997	45										1.98			sludge layer, no testing	US
20/09/1997	46	2560	213	2314	106	5.1	4.6	92	95	2347	2.00	0.00085	1.08	sludge layer	US
21/09/1997	47	2140	192	2048	106	4.3	4.1	91	95	1948		0.00000	0.90	sludge layer	US
22/09/1997	48	2600	182	2520	125	5.2	5.0	93	95	2418		0.00000	1.11	sludge layer	US
23/09/1997	49	3360	328	2722	125	6.7	5.4	90	95	3032		0.00000	1.39	sludge layer	US
24/09/1997	50	3522	259	2975	223	7.0	6.0	93	93	3263		0.00000	1.50	sludge layer	US

Appendix A continue

		unfiltered		filtered		load		% COD removal		COD removed	gasproduction			status	*feed
date	day	COD in	COD out	COD in	COD out	unfiltered	filtered	unfiltered COD	filtered COD	unfiltered COD	ℓ gas/d	ℓ gas rate per	ℓ gas/d		
		mg/ℓ	mg/ℓ	mg/ℓ	mg/ℓ	kgCOD/m³ sludge vol./d				mg/ℓ		%COD removed			
25/09/1997	51										1.94			pump breakdown	US
26/09/1997	52										1.85			clean pipelines	US
27/09/1997	53										1.70			start feeding , no testing	US
28/09/1997	54	3410	166	2918	115	6.8	5.8	95	96	3244	1.21	0.00037	1.49	sludge layer	US
29/09/1997	55	3410	210	3461	115	6.8	6.9	94	97	3200	1.37	0.00043	1.47	sludge layer	US
30/09/1997	56	3133	221			6.3		93		2912	1.21	0.00042	1.34	sludge layer	US
01/10/1997	57	3727	233			7.5		94		3494	1.70	0.00049	1.61	sludge layer	US
02/10/1997	58	3667	156			7.3		96		3511	1.71	0.00049	1.62	sludge layer	US
03/10/1997	59	3686	217			7.4		94		3469		0.00000	1.60	sludge layer	US
04/10/1997	60	3819	213			7.6		94		3606		0.00000	1.66	sludge layer	US
05/10/1997	61	4223	204			8.4		95		4019	1.70	0.00042	1.85	sludge layer	US
06/10/1997	62	6508	286			13.0		96		6222	1.60	0.00026	2.86	sludge layer	US
07/10/1997	63	4366	396			8.7		91		3970	1.70	0.00043	1.83	sludge layer	US
08/10/1997	64	5000	313			10.0		94		4687	2.10	0.00045	2.16	sludge layer	US
09/10/1997	65	3922	293			7.8		93		3629	2.30	0.00063	1.67	sludge layer	US
10/10/1997	66	4308	228			8.6		95		4080	**1.77**	**0.00043**	1.88	sludge layer	US
11/10/1997	67	3983	256			8.0		94		3727			1.71	sludge layer	US
12/10/1997	68	3678	244			7.4		93		3434			1.58	sludge layer	US
13/10/1997	69	3658	260			7.3		93		3398		**average values**	1.56	sludge layer	US
14/10/1997	70	3942	252			7.9		94		3690			1.70	sludge layer	US
15/10/1997	71	3292	199			6.6		94		3093			1.42	sludge layer	US
16/10/1997	72	4064	236			8.1		94		3828			1.76	sludge layer	US
17/10/1997	73													sludge layer, no test	US
18/10/1997	74													sludge layer, no test	US
19/10/1997	75													sludge layer, no test	US
20/10/1997	76	3640	215			7.3		94		3425			1.58	sludge layer	US
21/10/1997	77	3640	232			7.3		94		3408			1.57	sludge layer	S
22/10/1997	78	4440	156			8.9		96		4284			1.97	sludge layer	S
23/10/1997	79	4276	185			8.6		96		4091			1.88	sludge layer	S
24/10/1997	80													sludge layer, no test	S
25/10/1997	81													sludge layer, no test	S
26/10/1997	82	3337	185			6.7		94		3152			1.45	sludge rinsed	S
27/10/1997	83	3790	2125			7.6		44		1665			0.77	sludge layer	S
28/10/1997	84	3420	2394			6.8		30		1026			0.47	sludge layer	S
29/10/1997	85	3901	3055			7.8		22		846			0.39	sludge layer	S
30/10/1997	86	3860	3137			7.7		19		723			0.33	sludge layer	S
31/10/1997	87	3880	2931			7.8		24		949			0.44	sludge layer	S
01/11/1997	88	3715	2663			7.4		28		1052			0.48	sludge layer	S
02/11/1997	89	3633	2806			7.3		23		827			0.38	sludge layer	S
03/11/1997	90	3922	2703			7.8		31		1219			0.56	sludge layer	S
04/11/1997	91	3502	2642			7.0		25		860			0.40	sludge layer	S
05/11/1997	92	3625	1782			7.3		51		1843			0.85	sludge layer	S
06/11/1997	93	3277	1290			6.6		61		1987			0.91	sludge layer	S
07/11/1997	94	4424	1434			8.8		68		2990			1.38	sludge layer	S
08/11/1997	95	4321	1311			8.6		70		3010			1.38	sludge layer	S
09/11/1997	96	4260	1270			8.5		70		2990			1.38	sludge layer	S
10/11/1997	97	4383	1234			8.8		72		3149			1.45	sludge layer	S
11/11/1997	98	4342	884			8.7		80		3458			1.59	sludge layer	S
12/11/1997	99	4153	637			8.3		85		3516			1.62	sludge layer	S
13/11/1997	100	3947	576			7.9		86		3371			1.55	sludge layer	S
14/11/1997	101	4030	781			8.1		81		3249			1.49	sludge layer	S
15/11/1997	102	4379	987			8.8		77		3392			1.56	sludge layer, shutdown	S

*** feed**
US = Feedstock type 1
S = Feedstock type 2

APPENDIX B

MAIN INVESTIGATION – DETAILED RESULTS

Note: -values that are omitted, no analysis were done.

UASB DETAILED RESULTS:- MAIN INVESTIGATION

Period1

		Reactor 1							Reactor 2						
date	day	COD in (mg/ℓ)	COD out (mg/ℓ)	effluent pH	flow (ℓ/d)	*load rate	% removal	feed/status	COD in (mg/ℓ)	COD out (mg/ℓ)	effluent pH	flow (ℓ/d)	*load rate	% removal	feed/status
10/03/1998	1							start-up: water							start-up: water
11/03/1998	2							water							water
12/03/1998	3							wine waste							wine waste
13/03/1998	4	°						wine waste							wine waste
14/03/1998	5							wine waste							wine waste
15/03/1998	6	1572			8	3		wine waste	1799			8	4		wine waste
16/03/1998	7	2088	1013	7	8	4	51	wine waste	1965	806	7	8	4	59	wine waste
17/03/1998	8	2709	724	7.5	8	5	73	wine waste	2937	889	7.4	9	7	70	wine waste
18/03/1998	9	3474	1282	7.44	10	9	63	wine waste	3433	1489	7.35	11	9	57	wine waste
19/03/1998	10	3332	858	7.52	10	8	74	wine waste	3311	1267	7.41	10	8	62	wine waste
20/03/1998	11	3337	1104	7.54	8	7	67	wine waste	3311	1288	7.42	10	8	61	wine waste
21/03/1998	12	3475	1042	7.6	9	8	70	wine waste	3720	1594	7.52	10	9	57	wine waste
22/03/1998	13	3475	940	7.57	10	9	73	wine waste	3475	1472	7.38	11	10	58	wine waste
23/03/1998	14	3332	1410	7.71	8	7	58	wine waste	3495	1594	7.35	10	9	54	wine waste
24/03/1998	15	3475	1063	7.81	9	8	69	wine waste	3740	1819	7.61	10	9	51	wine waste
25/03/1998	16	3659	1676	7.8	10	9	54	wine waste	3761	1513	7.45	11	10	60	wine waste
26/03/1998	17	3454	1600	7.5	10	9	54	wine waste	3454	1500	7.5	11	9	57	wine waste
27/03/1998	18	3454	1758	7.55	10	9	49	wine waste	3454	1758	7.22	11	9	49	wine waste
28/03/1998	19	3164	1344	7.42	9	7	58	wine waste	3391	1448	7.12	11	9	57	wine waste
29/03/1998	20	3619	1500	7.5	9	8	59	wine waste	3888	1500	7	11	11	61	wine waste
30/03/1998	21	3598	1572	7.47	9	8	56	wine waste	3598	1882	7.23	10	9	48	wine waste
31/03/1998	22	3598	1572	7.47	9	8	56	wine waste	3598	1882	7.23	10	9	48	wine waste
01/04/1998	23	4281	1365	7.51	10	11	68	wine waste	4281	1634	7.44	10	11	62	wine waste
02/04/1998	24	3846	1406	7.28	10	10	63	wine waste	3908	1406	7.69	10	10	64	wine waste
03/04/1998	25							wine waste							wine waste
04/04/1998	26	3805	1572	7.2	11	10	59	wine waste	3702	1510	7	12	11	59	wine waste
05/04/1998	27							wine waste							wine waste
06/04/1998	28	2544	1500	7.23	11	7	41	wine waste	2544	1500	7.14	12	8	41	wine waste
07/04/1998	29	4033	1737	7.42	10	10	57	wine waste	4033	1903	7.29	12	12	53	wine waste
08/04/1998	30							wine waste							wine waste
09/04/1998	31							wine waste							wine waste
10/04/1998	32							wine waste							wine waste
11/04/1998	33							wine waste							wine waste
12/04/1998	34							wine waste							wine waste
13/04/1998	35							wine waste							wine waste
14/04/1998	36	4023			7	7		wine waste	3698			12	11		wine waste
15/04/1998	37	3983	1380	7.82	7	7	65	wine waste	4064	2110	7.35	12	12	48	wine waste
16/04/1998	38	3983	1382	7.82	8	8	65	wine waste	4064	2113	7.35	12	12	48	wine waste
17/04/1998	39	3983	1382	7.94	8	8	65	wine waste	4044	2215	7.5	13	13	45	wine waste
18/04/1998	40	4064	1280	8.2	7	7	69	wine waste	4003	2255	7.45	12	12	44	wine waste

Period1 *continue*

		Reactor 1							Reactor 2						
date	**day**	**COD in**	**COD out**	**effluent pH**	**flow**	***load rate**	**% removal**	**feed/status**	**COD in**	**COD out**	**effluent pH**	**flow**	***load rate**	**% removal**	**feed/status**
		(mg/ℓ)	**(mg/ℓ)**		**(ℓ/d)**				**(mg/ℓ)**	**(mg/ℓ)**		**(ℓ/d)**			
19/04/1998	41	3818	1156	8.01	8	8	70	wine waste	3983	2270	7.47	14	14	43	wine waste
20/04/1998	42	4334	1073	8.1	7	8	75	wine waste	4231	2229	7.43	12	13	47	wine waste
21/04/1998	43	4541	846	8	7	8	81	wine waste	4479	2435	7	13	15	46	wine waste
22/04/1998	44	4561	1507	7.74	9	10	67	wine waste	4355	3013	6.73	13	14	31	wine waste
23/04/1998	45	4355	1568	7.7	7	8	64	wine waste	4954	3117	7.11	10	12	37	wine waste
24/04/1998	46	4355	1360	7.78	8	9	69	wine waste	4954	2740	7.2	13	16	45	wine waste
25/04/1998	47							wine waste							wine waste
26/04/1998	48							wine waste							wine waste
27/04/1998	49	4169	680	7.5	7	7	84	wine waste	4190	1420	7	10	10	66	wine waste
28/04/1998	50	4169	920	7.65	7	7	78	wine waste	4190	2140	7.43	10	10	49	wine waste
29/04/1998	51	4600	900	8.19	8	9	80	wine waste	4360	1680	7.6	11	12	61	wine waste
30/04/1998	52							wine waste							wine waste
01/05/1998	53							wine waste							wine waste
02/05/1998	54	4620	2120	7.93	8	9	54	wine waste	4780	2840	7.61	12	14	41	wine waste
03/05/1998	55	4460	1520	8.01	7	8	66	wine waste	4540	2540	7.52	11	12	44	wine waste
04/05/1998	56	4740	1500	7.99	8	9	68	wine waste	4680	1820	7.13	13	15	61	wine waste
05/05/1998	57	3140	1440	7.84	10	8	54	wine waste	3560	1500	7.31	15	13	58	wine waste
06/05/1998	58	4780	2300	7.87	8	10	52	wine waste	4920	3300	7.34	12	15	33	wine waste
07/05/1998	59	5007	2031	7.67	8	10	59	wine waste	4863	3570	7.1	13	16	27	wine waste
08/05/1998	60	3653	1313	7	9	8	64	wine waste	3755	3386	7	14	13	10	wine waste
09/05/1998	61							wine waste							wine waste
10/05/1998	62	3283	1313	8.14	9	7	60	wine waste	3550	3500	5.88	9	8	1	wine waste
11/05/1998	63	3755	1149	7.73	8	8	69	wine waste	3817	3304	6.44	13	12	13	wine waste
12/05/1998	64	4473	1765	7.74	9	10	61	wine waste	4391	4063	6.71	7	8	7	wine waste
13/05/1998	65	5130	2278	7.78	8	10	56	wine waste	5089	3119	7.15	5	6	39	wine waste
14/05/1998	66	4843	1683	8.97	8	10	65	wine waste	4802	2873	8.46	3	4	40	wine waste
15/05/1998	67	5192	1784	8.22	13	17	66	wine waste	4925	3468	8.24	16	20	30	wine waste
16/05/1998	68	4753	2489	8.13	12	14	48	wine waste	4978	3570	7.72	14	17	28	wine waste
17/05/1998	69	4835	2346	7.99	10	12	51	wine waste	4835	3692	7.63	13	16	24	wine waste
18/05/1998	70	4804	2305	7.87	11	13	52	wine waste	4692	3570	7.34	13	15	24	wine waste
19/05/1998	71	4814	1999	7.55	11	13	58	wine waste	4855	3468	7.18	13	16	29	wine waste
20/05/1998	72	4896	2570	7.12	11	13	48	wine waste	5059	4651	6.76	14	18	8	wine waste
21/05/1998	73	4794	2856	7.23	12	14	40	wine waste	3346	3264	7	13	11	2	wine waste
22/05/1998	74	4896	3080	7.14	12	15	37	wine waste	5182	2958	7.21	13	17	43	wine waste
23/05/1998	75	5182	3427	7.11	12	16	34	wine waste	4959	3876	6.83	13	16	22	wine waste
24/05/1998	76	5018	3427	7	12	15	32	wine waste	5059	3998	6.89	13	16	21	wine waste
25/05/1998	77	5182	3754	7.27	12	16	28	wine waste	5080	3917	7.22	14	18	23	wine waste
26/05/1998	78	5202	3468	7.25	12	16	33	wine waste	5345	3937	7.23	13	17	26	wine waste
27/05/1998	79	5100	3386	7.1	12	15	34	wine waste	4998	3774	7.08	13	16	24	wine waste
28/05/1998	80	4529	3346	7.09	12	14	26	wine waste	4692	3815	6.99	13	15	19	wine waste
29/05/1998	81							wine waste							wine waste
30/05/1998	82	4814	3386	8.08	12	14	30	wine waste	4855	4120	7.92	13	16	15	wine waste
31/05/1998	83	4937	3223	8.25	12	15	35	wine waste	5100	3917	8.39	14	18	23	wine waste
01/06/1998	84	4777	3117	8.34	12	14	35	wine waste	4777	4514	8.77	14	17	6	wine waste
02/06/1998	85							shutdown							shutdown
03/06/1998	86							for							for
04/06/1998	87							cleaning unit							cleaning unit

* load rate = kgCOD/m^3 sludge bed volume/d

Period 2		Reactor 1							Reactor 2						
date	day	COD in	COD out	effluent pH	flow	load rate	% removal	feed/status	COD in	COD out	effluent pH	flow	load rate	% removal	feed/status
		(mg/ℓ)	(mg/ℓ)		(ℓ/d)				(mg/ℓ)	(mg/ℓ)		(ℓ/d)			
05/06/1998	88	3441	1356		4	7	61	start-up: wine	3441	1983		4	6	42	start-up: wine
06/06/1998	89							new wine waste							new wine waste
07/06/1998	90	3704	1457	8.7	4	7	61	new wine waste	3704	2024	8.6	4	6	45	new wine waste
08/06/1998	91	3557	576	8.81	4	7	84	new wine waste	3516	1110	8.71	4	6	68	new wine waste
09/06/1998	92	3557	617	8.97	4	7	83	new wine waste	3516	1090	8.96	4	6	69	new wine waste
10/06/1998	93	3701	514	9.13	4	7	86	new wine waste	3906	1419	9.15	4	6	64	new wine waste
11/06/1998	94	3927	822	8.54	4	8	79	new wine waste	4318	411	8.43	4	7	90	new wine waste
12/06/1998	95	4030	206	8.49	4	8	95	new wine waste	4235	110	8.5	4	7	97	new wine waste
13/06/1998	96							new wine waste							new wine waste
14/06/1998	97	4017	296	8	4	8	93	new wine waste	3789	915	8	4	6	76	new wine waste
15/06/1998	98							new wine waste							new wine waste
16/06/1998	99	3968	349	8.52	4	8	91	new wine waste	3639	658	8.42	4	6	82	new wine waste
17/06/1998	100	5572	1110	8	4	11	80	new wine waste	5572	1337	8	4	9	76	new wine waste
18/06/1998	101	5572	592	8.52	4	11	89	new wine waste	5572	1265	8.25	4	9	77	new wine waste
19/06/1998	102							new wine waste							new wine waste
20/06/1998	103	4733	122	8.52	4	9	97	new wine waste	4733	510	8.3	4	8	89	new wine waste
21/06/1998	104	4978	347	8.56	3	7	93	new wine waste	4978	816	8.2	4	8	84	new wine waste
22/06/1998	105	4978	632	8.52	3	7	87	new wine waste	4978	1081	8.5	4	8	78	new wine waste
23/06/1998	106	4774	449	8.43	4	10	91	new wine waste	4488	979	8.32	5	9	78	new wine waste
24/06/1998	107							new wine waste							new wine waste
25/06/1998	108	5508	245	8.19	5	14	96	new wine waste	5569	1510	8.16	6	13	73	new wine waste
26/06/1998	109							new wine waste							new wine waste
27/06/1998	110	5564	403	8.34	5	14	93	new wine waste	5403	1774	8.1	6	13	67	new wine waste
28/06/1998	111	5040	282	8.41	5	13	94	new wine waste	5040	1633	8.37	5	10	68	new wine waste
29/06/1998	112	4516	363	8.39	5	11	92	new wine waste	5141	1290	8.31	6	12	75	new wine waste
30/06/1998	113							new wine waste							new wine waste
01/07/1998	114	5342	262	8.41	5	13	95	new wine waste	4738	202	8.2	5	9	96	new wine waste
02/07/1998	115	4778	222	8.42	5	12	95	new wine waste	4778	665	8.26	5	10	86	new wine waste
03/07/1998	116							new wine waste							new wine waste
04/07/1998	117							new wine waste							new wine waste
05/07/1998	118	4778	464	8.33	5	12	90	new wine waste	4778	746	8.15	5	10	84	new wine waste
06/07/1998	119	4641	539	8.54	5	12	88	new wine waste	5221	394	8.39	5	10	92	new wine waste
07/07/1998	120							new wine waste							new wine waste
08/07/1998	121	3108	456	8.53	5	8	85	new wine waste	2113	663	8.38	6	5	69	new wine waste
09/07/1998	122							new wine waste							new wine waste
10/07/1998	123	4310	249	8.29	5	11	94	new wine waste	3895	82.88	8.12	7	11	98	new wine waste
11/07/1998	124							new wine waste							new wine waste
12/07/1998	125	4600	456	8.2	5	12	90	new wine waste	4393	497	7.91	6	11	89	new wine waste
13/07/1998	126							new wine waste							new wine waste
14/07/1998	127	3917	204	8.28	6	12	95	new wine waste	4182	490	7.97	7	12	88	new wine waste
15/07/1998	128							new wine waste							new wine waste
16/07/1998	129	4570	571	7	6	14	88	new wine waste	4692	1265	7	7	13	73	new wine waste
17/07/1998	130							new wine waste							new wine waste
18/07/1998	131							new wine waste							new wine waste
19/07/1998	132	4651	755	8.19	7	16	84	new wine waste	5120	1999	7.92	8	16	61	new wine waste
20/07/1998	133	4651	673	8.34	7	16	86	new wine waste	5120	2407	8	8	16	53	new wine waste
21/07/1998	134							new wine waste							new wine waste
22/07/1998	135	4998	612	8.22	7	17	88	new wine waste	4998	1632	8.02	8	16	67	new wine waste
23/07/1998	136	5386	734	8.16	7	19	86	new wine waste	5039	1306	8.07	8	16	74	new wine waste
24/07/1998	137							new wine waste							new wine waste
25/07/1998	138	4876	469	8.18	7	17	90	new wine waste	5365	1000	8.1	8	17	81	new wine waste
26/07/1998	139	4827	264	8.29	7	17	95	new wine waste	5029	973	8.11	8	16	81	new wine waste
27/07/1998	140	4827	284	8.28	7	17	94	new wine waste	5029	973	8.07	8	16	81	new wine waste
28/07/1998	141	5050	486	8.35	7	18	91	new wine waste	5009	1196	8.03	8	16	76	new wine waste

Period 2 *continue*

		Reactor 1							Reactor 2						
date	day	COD in	COD out	effluent pH	flow	load rate	% removal	feed/status	COD in	COD out	effluent pH	flow	load rate	% removal	feed/status
		(mg/ℓ)	(mg/ℓ)		(ℓ/d)				(mg/ℓ)	(mg/ℓ)		(ℓ/d)			
29/07/1998	142							new wine waste							new wine waste
30/07/1998	143							new wine waste	5557	1298	8.03	8	18	77	new wine waste
31/07/1998	144	5070	466	8.29	7	18	91	new wine waste	5374	1318	8.02	8	17	75	new wine waste
01/08/1998	145	5313	466	8.2	7	19	91	new wine waste	5577	1217	8.11	8	18	78	new wine waste
02/08/1998	146	5273	385	8.26	7	18	93	new wine waste	5242	2641	7.29	8	17	50	new wine waste
03/08/1998	147	5020	343	7.28	7	18	93	new wine waste	5846	1351	7.25	9	21	77	new wine waste
04/08/1998	148	5544	544	7.26	7	19	90	new wine waste	5322	484	7.2	8	17	91	new wine waste
05/08/1998	149							new wine waste							new wine waste
06/08/1998	150							new wine waste							new wine waste
07/08/1998	151	4294	181	7.2	7	15	96	new wine waste	5322	484	7.36	8	17	91	new wine waste
08/08/1998	152							new wine waste							new wine waste
09/08/1998	153							new wine waste							new wine waste
10/08/1998	154							new wine waste							new wine waste
11/08/1998	155							new wine waste							new wine waste
12/08/1998	156	4778	302	7.3	7	17	94	new wine waste	4637	697	7.36	8	15	85	new wine waste
13/08/1998	157							new wine waste							new wine waste
14/08/1998	158	5362	665	7.26	7	19	88	new wine waste	4939	766	7.3	9	18	84	new wine waste
15/08/1998	159							new wine waste							new wine waste
16/08/1998	160	4453	182	7.29	7	16	96	new wine waste	4372	587	7.27	9	16	87	new wine waste
17/08/1998	161							new wine waste							new wine waste
18/08/1998	162	4453	567	7.29	7	16	87	new wine waste	4534	648	7.29	9	16	86	new wine waste
19/08/1998	163							new wine waste							new wine waste
20/08/1998	164	4898	283	7.31	7	17	94	new wine waste	4979	810	7.27	9	18	84	new wine waste
21/08/1998	165							new wine waste							new wine waste
22/08/1998	166	4817	405	7.3	7	17	92	new wine waste	5040	627	7.39	9	18	88	new wine waste
23/08/1998	167							new wine waste							new wine waste
24/08/1998	168	4798	302	7.26	7	17	94	new wine waste	5664	403	7.28	9	20	93	new wine waste
25/08/1998	169							new wine waste							new wine waste
26/08/1998	170							new wine waste							new wine waste
27/08/1998	171	5141	508	7.31	7	18	90	new wine waste	4978	508	7.2	9	18	90	new wine waste
28/08/1998	172							new wine waste							new wine waste
29/08/1998	173							new wine waste							new wine waste
30/08/1998	174	4836	325	7.23	7	17	93	new wine waste	5039	345	7.18	9	18	93	new wine waste
31/08/1998	175	5486	345	7.25	7	19	94	new wine waste	5588	488	7.24	9	20	91	new wine waste
01/09/1998	176							new wine waste							new wine waste

Period 2 *continue*

		Reactor 1							Reactor 2						
date	day	COD in	COD out	effluent pH	flow	*load rate	% removal	feed/status	COD in	COD out	effluent pH	flow	*load rate	% removal	feed/status
		(mg/ℓ)	(mg/ℓ)		(ℓ/d)				(mg/ℓ)	(mg/ℓ)		(ℓ/d)			
02/09/1998	177	5039	366	7.45	8	20	93	new wine waste	6096	427	7.31	9	22	93	new wine waste
03/09/1998	178	5039	325	7.36	7	18	94	unsettled grain+wine	5507	366	7.4	9	20	93	new wine waste
04/09/1998	179	4259	629	7.2	7	15	85	unsettled grain+wine	5500	608	7.3	9	20	89	new wine waste
05/09/1998	180							unsettled grain+wine							new wine waste
06/09/1998	181	* 4340	689	7.5	7	15	84	unsettled grain+wine	4015	446	7.54	9	14	89	new wine waste
07/09/1998	182							unsettled grain+wine							new wine waste
08/09/1998	183	4745	284	7.2	7	17	94	unsettled grain+wine	3873	426	7.45	9	14	89	new wine waste
09/09/1998	184							unsettled grain+wine							new wine waste
10/09/1998	185	4928	629	7.29	7	17	87	unsettled grain+wine	4664	446	7.26	8	15	90	new wine waste
11/09/1998	186	4340	487	7.25	8	17	89	unsettled grain+wine	4178	385	7.33	9	15	91	new wine waste
12/09/1998	187							unsettled grain+wine							new wine waste
13/09/1998	188	5374	547	7.24	7	19	90	unsettled grain+wine	4259	182	7.25	9	15	96	new wine waste
14/09/1998	189	4137	446	7.17	8	17	89	unsettled grain+wine	4218	284	7.25	9	15	93	new wine waste
15/09/1998	190							unsettled grain+wine							new wine waste
16/09/1998	191	4325	653	7.3	8	17	85	unsettled grain+wine	5126	530	7.44	9	18	90	new wine waste
17/09/1998	192	5260	245	7.29	8	21	95	unsettled grain+wine	5161	326	7.48	8	17	94	new wine waste
18/09/1998	193							unsettled grain+wine							new wine waste
19/09/1998	194							unsettled grain+wine							new wine waste
20/09/1998	195							unsettled grain+wine							new wine waste
21/09/1998	196	5141	245	7.2	8	21	95	unsettled grain+wine	5345	82	7.4	9	19	98	new wine waste
22/09/1998	197	4896	449	7.22	8	20	91	unsettled grain+wine	5345	408	7.33	9	19	92	new wine waste
23/09/1998	198							unsettled grain+wine							new wine waste
24/09/1998	199	5100	315		8	20	94	unsettled grain+wine							new wine waste
25/09/1998	200	4950	305		8	20	94	unsettled grain+wine							new wine waste
26/09/1998	201	5125	260		8	21	95	unsettled grain+wine							new wine waste
27/09/1998	202							unsettled grain+wine							new wine waste
28/09/1998	203	3978	551	7.1	7	14	86	settled grain +wine	5753	755	7.2	8	18	87	new wine waste
29/09/1998	204							settled grain +wine							new wine waste
30/09/1998	205	4039	551	7.1	8	16	86	only settled grain	5386	653	7.2	9	19	88	new wine waste
01/10/1998	206	4182	408	7.08	8	17	90	only settled grain	5516	1122	7.2	9	20	80	new wine waste
02/10/1998	207							only settled grain							new wine waste
03/10/1998	208							only settled grain							new wine waste
04/10/1998	209							only settled grain							new wine waste
05/10/1998	210	4590	490	7.1	8	18	89	only settled grain	4998	489	7.22	9	18	90	new wine waste
06/10/1998	211							only settled grain							new wine waste
07/10/1998	212							only settled grain							new wine waste
08/10/1998	213							only settled grain							new wine waste
09/10/1998	214	4284	388	7.1	8	17	91	only settled grain	6120	694	7.22	9	22	89	new wine waste
10/10/1998	215							only settled grain							new wine waste
11/10/1998	216	3672	469	7.1	8	15	87	only settled grain	5630	367	7.2	9	20	93	new wine waste
12/10/1998	217							only settled grain							new wine waste

Period 2 *continue*

		Reactor 1							Reactor 2						
date	day	COD in (mg/ℓ)	COD out (mg/ℓ)	effluent pH	flow (ℓ/d)	*load rate	% removal	feed/status	COD in (mg/ℓ)	COD out (mg/ℓ)	effluent pH	flow (ℓ/d)	*load rate	% removal	feed/status
13/10/1998	218	4243	571	7.26	8	17	87	only unsettled grain	5365	388	7.31	9	19	93	new wine waste
14/10/1998	219							only unsettled grain							new wine waste
15/10/1998	220							only unsettled grain							new wine waste
16/10/1998	221							only unsettled grain							new wine waste
17/10/1998	222							only unsettled grain							new wine waste
18/10/1998	223	3713	632	7.36	8	15	83	only unsettled grain	5202	551	7.3	9	19	89	new wine waste
19/10/1998	224							only unsettled grain							new wine waste
20/10/1998	225							only unsettled grain							new wine waste
21/10/1998	226	5500	1020	7.18	8	22	81	only unsettled grain	4488	367	7.36	9	16	92	new wine waste
22/10/1998	227							only unsettled grain							new wine waste
23/10/1998	228							only unsettled grain							new wine waste
24/10/1998	229							only unsettled grain							new wine waste
25/10/1998	230							only unsettled grain							new wine waste
26/10/1998	231	7058	959	7.1	8	28	86	only unsettled grain	5834	490	7.2	9	21	92	new wine waste
27/10/1998	232							only unsettled grain							new wine waste
28/10/1998	233	7507	653	7.1	8	30	91	only unsettled grain	5508	530	7.2	9	20	90	new wine waste
29/10/1998	234							only unsettled grain							new wine waste
30/10/1998	235	7000	1000		8	28	86	only unsettled grain							new wine waste
31/10/1998	236							only unsettled grain							new wine waste
01/11/1998	237	5374	635		8	21	88	only unsettled grain							new wine waste
02/11/1998	238							only unsettled grain							new wine waste
03/11/1998	239	5141	450		8	21	91	only unsettled grain							new wine waste
04/11/1998	240							only unsettled grain							new wine waste
05/11/1998	241	4950	600		8	20	88	only unsettled grain							new wine waste
06/11/1998	242							only unsettled grain							new wine waste
07/11/1998	243	5040	450		8	20	91	only unsettled grain							new wine waste
08/11/1998	244							only unsettled grain							new wine waste
09/11/1998	245	5010	510		8	20	90	only unsettled grain							new wine waste
10/11/1998	246							only unsettled grain							new wine waste
11/11/1998	247	5110	555		8	20	89	only unsettled grain							new wine waste
12/11/1998	248							shutdown							shutdown
14/01/1999	311							shutdown							shutdown

Period 3															
		Reactor 1							Reactor 2						
date	day	COD in	COD out	effluent pH	flow	*load rate	% removal	feed/status	COD in	COD out	effluent pH	flow	*load rate	% removal	feed/status
		(mg/ℓ)	(mg/ℓ)		(ℓ/d)				(mg/ℓ)	(mg/ℓ)		(ℓ/d)			
15/01/1999	312	1903	749	67.49	7	3	61	start-up: wine	2206	789	7.72	7	4	64	start-up: wine
16/01/1999	313							new wine waste							new wine waste
17/01/1999	314							new wine waste							new wine waste
18/01/1999	315	1903	810	7.65	7	3	57	new wine waste	1983	950	7.81	7	3	52	new wine waste
19/01/1999	316	2793	1194	7.57	7	5	57	new wine waste	2654	1214	7.71	7	5	57	new wine waste
20/01/1999	317	2753	992	7.59	7	5	64	new wine waste	2753	1275	7.69	7	5	54	new wine waste
21/01/1999	318							new wine waste							new wine waste
22/01/1999	319							new wine waste							new wine waste
23/01/1999	320							new wine waste							new wine waste
24/01/1999	321	2862	941	7.6	7	5	67	new wine waste	2724	902	7.91	7	5	67	new wine waste
25/01/1999	322	2753	686	7.63	7	5	75	new wine waste	2753	1039	8.03	7	5	62	new wine waste
26/01/1999	323	3842	980	7.59	7	7	74	new wine waste	3979	1215	7.8	7	7	69	new wine waste
27/01/1999	324	3842	980	7.59	7	7	74	new wine waste							
28/01/1999	325							new wine waste							new wine waste
29/01/1999	326							new wine waste	3441	1356		7	6	61	new wine waste
30/01/1999	327							new wine waste							new wine waste
31/01/1999	328							new wine waste	3704	1457		7	6	61	new wine waste
01/02/1999	329							new wine waste	3557	576		7	6	84	new wine waste
02/02/1999	330							new wine waste	3557	617		7	6	83	new wine waste
03/02/1999	331							new wine waste	3701	514		7	6	86	new wine waste
04/02/1999	332							new wine waste	3927	822		7	7	79	new wine waste
05/02/1999	333							new wine waste	4030	875		7	7	78	new wine waste
06/02/1999	334							new wine waste							new wine waste
07/02/1999	335	2724	294	7.7	7	5	89	new wine waste	2607	902	8.16	7	5	65	new wine waste
08/02/1999	336	3293	627	7.64	7	6	81	new wine waste	3312	725	7.6	7	6	78	new wine waste
09/02/1999	337	3685	412	7.56	7	6	89	new wine waste	3548	725	7.82	7	6	80	new wine waste
10/02/1999	338	4360	640	7.66	7	8	85	new wine waste	4320	780	7.99	7	8	82	new wine waste
11/02/1999	339							shutdown							shutdown
12/02/1999	340							for							for
13/02/1999	341							cleaning							cleaning
14/02/1999	342							of							of
15/02/1999	343							unit							unit

Period 3 *continue*

		Reactor 1							Reactor 2						
date	day	COD in (mg/ℓ)	COD out (mg/ℓ)	effluent pH	flow (ℓ/d)	*load rate	% removal	feed/status	COD in (mg/ℓ)	COD out (mg/ℓ)	effluent pH	flow (ℓ/d)	*load rate	% removal	feed/status
16/02/1999	344	4606	929	7.53	7	13	80	new wine waste	5010	727	7.67	7	14	85	new wine waste
17/02/1999	345							new wine waste							new wine waste
18/02/1999	346							new wine waste	4675	715		7	13	85	new wine waste
19/02/1999	347							new wine waste							new wine waste
20/02/1999	348							new wine waste	5150	695		7	14	87	new wine waste
21/02/1999	349							new wine waste							new wine waste
22/02/1999	350							new wine waste	3995	590		7	11	85	new wine waste
23/02/1999	351							new wine waste							new wine waste
24/02/1999	352							new wine waste	4590	610		7	13	87	new wine waste
25/02/1999	353							new wine waste							new wine waste
26/02/1999	354							new wine waste	5405	700		7	15	87	new wine waste
27/02/1999	355							new wine waste							new wine waste
28/02/1999	356							new wine waste	5100	655		7	14	87	new wine waste
01/03/1999	357							new wine waste							new wine waste
02/03/1999	358							new wine waste	5310	710		7	15	87	new wine waste
03/03/1999	359							new wine waste							new wine waste
04/03/1999	360							new wine waste							new wine waste
05/03/1999	361	5740	1960	7.5	7	16	66	new wine waste	5560	1040	7.75	7	16	81	new wine waste
06/03/1999	362							new wine waste							new wine waste
07/03/1999	363							new wine waste							new wine waste
08/03/1999	364							new wine waste							new wine waste
09/03/1999	365	5617	2141	7.5	7	16	62	new wine waste	5414	1353	7.74	7	15	75	new wine waste
10/03/1999	366							new wine waste							new wine waste
11/03/1999	367	4950	1503	7.5	7	14	70	new wine waste	6172	1002	7.6	7	17	84	new wine waste
12/03/1999	368							new wine waste							new wine waste
13/03/1999	369							new wine waste							new wine waste
14/03/1999	370	5170	1202	7.56	7	14	77	new wine waste	5170	1202	7.71	7	14	77	new wine waste
15/03/1999	371	5711	1483	7.32	7	16	74	new wine waste	5731	601	7.58	7	16	90	new wine waste
16/03/1999	372							new wine waste							new wine waste
17/03/1999	373	5611	2386		7	16	57	new wine waste	5451	681		7	15	88	new wine waste
18/03/1999	374							new wine waste							new wine waste
19/03/1999	375							new wine waste							new wine waste
20/03/1999	376							new wine waste							new wine waste
21/03/1999	377							new wine waste							new wine waste
22/03/1999	378							new wine waste							new wine waste
23/03/1999	379							new wine waste							new wine waste
24/03/1999	380							new wine waste							new wine waste
25/03/1999	381							new wine waste							new wine waste
26/03/1999	382							new wine waste							new wine waste
27/03/1999	383							new wine waste							new wine waste
28/03/1999	384	3407	461		7	10	86	new wine waste	4629	380		7	13	92	new wine waste
29/03/1999	385	4848	444		7	14	91	new wine waste	4848	384		7	14	92	new wine waste
30/03/1999	386	5292	1172		7	15	78	new wine waste	5434	510		7	15	91	new wine waste
31/03/1999	387							new wine waste							new wine waste
01/04/1999	388	5252	444		7	15	92	new wine waste	5131	545		7	14	89	new wine waste
02/04/1999	389							new wine waste							new wine waste
03/04/1999	390							new wine waste							new wine waste
04/04/1999	391							new wine waste							new wine waste
05/04/1999	392							new wine waste							new wine waste
06/04/1999	393	5737	606		7	16	89	new wine waste	5191	788		7	15	85	new wine waste
07/04/1999	394	4626	505		7	13	89	new wine waste	4202	586		7	12	86	new wine waste
08/04/1999	395	6686	444		7	19	93	new wine waste	5818	1151		7	16	80	new wine waste
09/04/1999	396							new wine waste							only settled grain
10/04/1999	397	5292	747		7	15	86	new wine waste	3979	444		7	11	89	only settled grain
11/04/1999	398	6525	869		7	18	87	new wine waste	3858	646		7	11	83	only settled grain
12/04/1999	399	6040	1111		7	17	82	new wine waste	4202	667		7	12	84	only settled grain
13/04/1999	400	7009	1091		7	20	84	new wine waste	4121	848		7	12	79	only settled grain
14/04/1999	401							new wine waste							only settled grain
15/04/1999	402							new wine waste							only settled grain
16/04/1999	403							new wine waste							only settled grain
17/04/1999	404							new wine waste							only settled grain
18/04/1999	405	6605	1232		7	18	81	new wine waste	5171	1010		7	14	80	only settled grain
19/04/1999	406							new wine waste							only settled grain
20/04/1999	407							new wine waste							only settled grain
21/04/1999	408	6181	1050		7	17	83	new wine waste	3939	162		7	11	96	only settled grain
22/04/1999	409							new wine waste							only settled grain
23/04/1999	410							new wine waste							only settled grain
24/04/1999	411							new wine waste							only settled grain
25/04/1999	412							new wine waste							only settled grain
26/04/1999	413							new wine waste							only settled grain
27/04/1999	414							new wine waste							only settled grain
28/04/1999	415							final shutdown							final shutdown

APPENDIX C

DETERMINATION OF THE STRUVITE SOLUBILITY PRODUCT

C.1 INTRODUCTION

This Appendix sets out details on the method used to calculate the struvite solubility product from the data derived from experiments in Chapter 6. The mineral struvite has the empirical formulation $MgNH_4PO_4 \cdot 6H_2O$ (Momberg, 1992). Accordingly, the true solubility product K_{sp} (i.e. at infinite dilution) is given by:

$$K_{sp} = (Mg^{2+})(NH_4^{+})(PO_4^{3-}) \qquad (C.1)$$

where

( ) = concentration on the activity scale.

Taking into account the Debye-Hückel ionic strength effects in the experimental solutions tested, this equation can be modified to give the apparent solubility product, K'_{sp}:

$$K'_{sp} = [Mg^{2+}][NH_4^{+}][PO_4^{3-}] \qquad (C.2)$$

where

[ ] = concentration on the molar scale.

The true and apparent solubility products are related trough the mono-, di- and tri-valent activity coefficients for NH_4^{+}, Mg^{2+} and PO_4^{3-} respectively as follows:

$$K_{sp} = K'_{sp}.f_t.\ f_d.\ f_m \qquad (C.3)$$

where

f_t, f_d, f_m = tri-, di- and mono-valent activity coefficients, for PO_4^{3-}, Mg^{2+} and NH_4^{+} respectively.

Thus, from Eqs (C.1), (C.2) and (C.3) above, if the molar concentrations of Mg^{2+}, NH_4^+ and PO_4^{3-} at equilibrium are available, then the apparent and true solubility products for struvite, K'_{sp} and K_{sp} respectively, can be determined. In the experiments in Chapter 6, $[Mg^{2+}]$ is available from direct measurements. However, for $[NH_4^+]$ and $[PO_4^{3-}]$ values available from measurement are FSA (i.e. $[NH_4^+] + [NH_3]$) and total orthophosphates (i.e. $[H_3PO_4] + [H_2PO_4^-] + [HPO_4^{2-}] + [PO_4^{3-}]$) respectively. For the FSA with pK=9.3, in the pH ranges of the experiments (6.5< pH <7, Tables 6.4 and 6.5) the concentration of NH_3 is very small compared to NH_4^+ and accordingly can be neglected. Therefore, the FSA measurement can be taken as equal to $[NH_4^+]$ as N. However, for the phosphorus, the concentrations of non- $[PO_4^{3-}]$ species are not negligible and need to be taken into account, i.e. the phosphate system needs to be speciated and $[PO_4^{3-}]$ determined. This can be done from equilibrium chemistry, as follows:

C.2 SPECIATION OF PHOSPHATE SYSTEM

The phosphate system can be speciated as follows (Loewenthal *et al.*, 1989):

For the phosphate system, the equilibrium equations are given by:

$$H_3PO_4 \leftrightharpoons H^+ + H_2PO_4^- \quad \text{(C.4a)}$$

$$H_2PO_4^- \leftrightharpoons H^+ + HPO_4^{2-} \quad \text{(C.4b)}$$

$$HPO_4^{2-} \leftrightharpoons H^+ + PO_4^{3-} \quad \text{(C.4c)}$$

From equilibrium chemistry (Loewenthal *et al.*, 1989):

$$P_T = [H_3PO_4] + [H_2PO_4^-] + [HPO_4^{2-}] + [PO_4^{3-}] \quad \text{(C.5)}$$

$$K_{p1} = [H^+][H_2PO_4^-]/[H_3PO_4] \quad \text{(C.6)}$$

$$K_{p2} = [H^+][HPO_4^{2-}]/[H_2PO_4^-] \quad \text{(C.7)}$$

$$K_{p3} = [H^+][PO_4^{3-}]/[HPO_4^{2-}] \quad \text{(C.8)}$$

where

$pK_{p1} = 2.148$ giving $K_{p1} = 7.11 \times 10^{-3}$

$pK_{p2} = 7.198$ giving $K_{p2} = 6.34 \times 10^{-8}$

$pK_{p3} = 12.023$ giving $K_{p3} = 9.48 \times 10^{-3}$

In Eq (C.5), for the pH ranges in the experiments the concentration of $[H_3PO_4]$ is very small compared to the other phosphate species and accordingly be neglected. Hence, substituting Eqs (C.7) and (C.8) into Eq (C.5):

$$P_T = [H^+]^2[PO_4^{3-}]/K_{p3}K_{p2} + [H^+][PO_4^{3-}]/K_{p3} + [PO_4^{3-}] \quad (C.9)$$

In the above equations, H^+ is available from pH measurement as an activity. Accordingly, $[H^+]$ need to be converted from molarity to activity. This can be done as follows:

$$(H^+)[H_2PO_4^-]/[H_3PO_4] = K_{p1}/f_m = K'_{p1} \quad (C.10)$$

$$(H^+)[HPO_4^{2-}]/[H^2PO_4^-] = K_{p2}f_m/f_d = K'_{p2} \quad (C.11)$$

$$(H^+)[PO_4^{3-}]/[HPO_4^{2-}] = K_{p3}f_d/f_t = K'_{p3} \quad (C.12)$$

where

(X) = activity of species X (mol ℓ^{-1})

[X] = molarity of species X (mol ℓ^{-1})

f = activity coefficient

K_p = thermodynamic equilibrium constant of species X

K'_p = thermodynamic equilibrium constant of species X, adjusted for Debye-Hückel effects

m = mono protic

d = di protic and

t = tri protic

These H^+ activity based K-values can now be substituted into Eqs (C.9) to give

$$P_T = (H^+)^2[PO_4^{3-}]/K'_{p3}K'_{p2} + (H^+)[PO_4^{3-}]/K'_{p3} + [PO_4^{3-}] \quad (C.13)$$

In Eq (C.13) above, a value for (H^+) is required. This is available from the pH measurement by noting that:

$$pH = -\log(H^+) \qquad (C.14)$$

Thus, Eq (C.13) can be solved to determine the value for $[PO_4^{3-}]$ from the measured total orthophosphate value P_T, as required in Eq (C.2).

C.3 ACTIVITY COEFFICIENTS

Eq (C.13) above requires values for K'_{p2} and K'_{p3}. Values for K_{p2} and K_{p3} are available from the literature, see above. These need to be converted to the required K'_{p2} and K'_{p3} by taking into account the Debye-Hückel ionic strength effects, i.e.

$$K_{p2} = K'_{p2} \cdot f_d \qquad (C.15a)$$

$$K_{p3} = K'_{p3} \cdot f_t \qquad (C.15b)$$

In Eq (C.15) above values are required for f_d and f_t and in Eq (C.3) additionally a value is required for f_m. For these, the ionic strength of the solution (μ) needs to be calculated, as follows:

$$\mu = \tfrac{1}{2} \Sigma C_i Z_i^2 \qquad (C.16)$$

where

μ = ionic strength
C_i = concentration of species i
Z_i = charge of species i

Once the ionic strength of the solution is known, using the Davies equation (Eq C.17), it is possible to calculate values for f_m, f_d and f_t. (Musvoto *et al.*, 1998, Appendix C). It is now possible to calculate the adjusted K values, K'_{p2} and K'_{p3} using Eq (C.15).

$$\log f_i = -AZ_i^2 \left(\frac{\sqrt{\mu}}{1 + \sqrt{\mu}} - 0.3\mu \right) \qquad (C.17)$$

C.4 CALCULATION OF SOLUBILITY PRODUCT

From the above, values for $[Mg^{2+}]$ and $[NH_4^+]$ are available from measurement, and $[PO_4^{3-}]$ can be calculated from the measured P_T using the procedures above. These values can be used to determine the apparent solubility product for struvite K'_{sp} using Eq (C.2), which can be used to determine the true solubility product K_{sp} with Eq (C.3).

C.5 CALCULATION EXAMPLE

C.5.1 Making up the experimental solution

If we wish to add 300 mg NH_4^+-N/ℓ

400 mg PO_4^{3-}-P/ℓ

300 mg Mg^{2+}/ℓ

We would first have to calculate how much of each chemical to weigh out. This can be done as follows:

First calculate the molecular weight of each chemical to be added:

Molecular Weight of NH_4Cl (MW) = 14,01 + 4(1,008) + 35,45
= 53,492 g/mol
= 53,492 mg/mmol

Molecular Weight of K_2HPO_4 = 2(39,1) + 1,008 + 30,97 + 4(16)
= 174,178 mg/mmol

Molecular Weight of $MgCl_2 \cdot 6H_2O$ = 24,31 + 2(35,45) + 12(1,008) + 6(16)
= 203,306 mg/mmol

Next work out an equivalent amount of chemical to be added:

NH_4Cl:	Original amount x MW/MW_N	= 300 x 53.492/14,01
		= 1145,44 mg NH_4Cl/ℓ
K_2HPO_4:	Original amount x MW/MW_P	= 400 x 174,178/30,97
		= 224,75 mg K_2HPO_4/ℓ
$Mg_2Cl_2 \cdot 6H_2O$:	Original amount x MW/MW_{Mg}	= 300 x 203,306/24,31
		= 2506,15 mg $MgCl_2.6H_2O/\ell$

C.5.2 Initial state

We are also able to calculate the initial concentrations of each chemical added as follows:

NH_4Cl:	Therefore no. of moles	= 300/24,31
		= 21,41 mmol/ℓ
K_2HPO_4:	Therefore no. of moles	= 400/30,97
		= 12,91 mmol/ℓ
$Mg_2Cl_2 \cdot 6H_2O$:	Therefore no. of moles	= 300/14,01
		= 12,34 mmol/ℓ

Once the initial concentrations are known, the test proceeds and concentrations are obtained from the experiment.

C.5.3 Final state

In our example we assume that the following final concentration data were obtained from our experiments:

Ammonia	= 228,62 mgN/ℓ
Orthophosphate	= 238,5 mgP/ℓ

Magnesium = 174,78 mgMg/ℓ

pH = 6,77

C.5.4 Concentrations precipitated

We can now work out the final molar concentrations and calculate the differences.

Ammonia: – (MW = 14,01)

Initial: 21,41 mmolN/ℓ

Final: 228,62 mg NH_4-N/ℓ (measured)

= 16,318 mmolN/ℓ

Difference: 21,41 – 16,318

= 5,092 mmolN/ℓ

Orthophosphate: – (MW = 30,97)

Initial: 12,91 mmolP/ℓ

Final: 238,5 mg P/ℓ (measured)

= 7,701 mmolP/ℓ

Difference: 12,91 – 7,701

= 5,209 mmolP/ℓ

Magnesium: – (MW = 24,31)

Initial: 12,34 mmolMg/ℓ

Final: 174,78 mg Mg/ℓ (measured)

= 7,190 mmolMg/ℓ

Difference: 12,34 – 7,19

= 5,150 mmolMg/ℓ

We can see that the differences obtained are closely equal, which is expected since struvite has a 1:1:1 molar ratio. We now need to convert the total phosphates into soluble phosphate species concentrations (PO_4^{3-} + HPO_4^{2-} + $H_2PO_4^-$ + H_3PO_4) for use in the formula.

$$K'_{sp} = [NH_4^+][Mg^{2+}][PO_4^{3-}]$$

C.5.5 Ionic strength and pK values

First calculate the ionic strength of the minerals present. This will allow us to find the activity coefficients to adjust the K-values.

We know that P_T $= 7{,}701$ mmolP/ℓ

$= 7{,}701 \times 10^{-3}$ molP/ℓ

For the purpose to calculating ionic strength, with little error it can be assumed that the concentrations of HPO_4^{2-} and $H_2PO_4^-$ are equal i.e.

$[HPO_4^{2-}] = [H_2PO_4^-]$ $= P_T/2$

$= 3{,}85 \times 10^{-3}$ molP/ℓ

$N_T = NH_4^+$ $= 16{,}32 \times 10^{-3}$ molN/ℓ

Mg^{2+} $= 7{,}19 \times 10^{-3}$ molMg/ℓ

Cl^- $= 30{,}7 \times 10^{-3}$ molCl/ℓ

K^+ $= 7{,}701 \times 10^{-3}$ molK/ℓ

Now find the ionic strength

$$\mu\ (IS) = \tfrac{1}{2} \Sigma\ C_i\ Z_i^2$$

where

C = final concentration (mol/ℓ)

Z = charge

$= ½ (3,8505 \times 10^{-3} + 16,318 \times 10^{-3} + 30,698 \times 10^{-3} + 7,701 \times 10^{-3}) \times (1)^2$

$+ ½ (3,8505 \times 10^{-3} + 7,190 \times 10^{-3}) \times (2)^2$

$= 0,0403$ mol/ℓ

Using the Davies equation (Section C.3) gives activity coefficients of:

$f_m = 0,83$

$f_d = 0,48$

$f_t = 0,185$

This is used to give new K_{p2} and K_{p3} values, K'_{p2} and K'_{p3} respectively:

$$K'_{p2} = f_m K_{p2}/f_d = 1,096 \times 10^{-7}$$

$$K'_{p3} = f_d K_{p3}/f_t = 2,460 \times 10^{-12}$$

C.5.6 Calculate PO_4^{3-}

Using the calculated K'_p values, known pH and known P_T, it is possible to solve for a PO_4^{3-} concentration using the adjusted formula below;

$$P_T = (H^+)^2[PO_4^{3-}]/K'_{p3}\,K'_{p2} + (H^+)[PO_4^{3-}]/K'_{p3} + [PO_4^{3-}]$$

where

pH = 6,77 which gives (H^+) $= 1,698 \times 10^{-7}$

P_T $= 7,701 \times 10^{-21}$ molP/ℓ

This gives a PO_4^{3-} concentration $= 4,376 \times 10^{-8}$ molPO_4^{3-}P/ℓ

C.5.7 Calculate solubility product

Substituting this into K'_{sp} $= [Mg^{2+}][NH_4^+][PO_4^{3-}]$

$= (7{,}19 \times 10^{-3})\ (16{,}32 \times 10^{-3})\ (4{,}376 \times 10^{-8})$

$= 5{,}13 \times 10^{-12}$

We can now use this value to find K_{sp} using the equation below;

$K_{sp} = K'_{sp} \cdot f_m \cdot f_d \cdot f_t$

$= (5{,}13 \times 10^{-12})\ (0{,}83)\ (0{,}48)\ (0{,}185)$

$= 3{,}78 \times 10^{-13}$

therefore

$pK_{sp} = -\log K_{sp}$

$= 12{,}42$

This is the final value that we are looking for.

APPENDIX D

DETAILED RESULTS

Table D.1 Detailed results for batch aeration of anaerobic digester liquor from UASB reactor at SFW Wellington Distillery; Batch Test 1.

Time (min)	pH	SC mS/m	FSA (mgN/ℓ)	P_T (mgP/ℓ)	Mg (mgMg/ℓ)	Ca (mgCa/ℓ)	Fe (mgFe/ℓ)	SCFA (mg/ℓ as HAc)	H_2CO_3*Alkalinity (mg/ℓ as CaCO3)	C_T (mg/ℓ as $CaCO_3$)
0	6.80	116	150	93.7	98	48	0.22	0	2444	3366
2	7.37	479	155	87.8	98	48	0.20	63	2464	2712
4	7.65	430	160	74.7	94	42	0.20	48	2604	2737
6	7.88	470	160	65.2	88	38	0.21	54	2632	2706
8	8.05	420	160	54.6	80	35	0.20	144	2542	2583
10	8.18	450	155	64.0	80	30	0.22	61	2542	2565
12	8.30	470	155	85.4	74	28	0.22	33	2387	2395
15	8.44	440	155	51.0	70	27	0.22	16	2443	2435
20	8.62	475	155	32.0	52	26	0.24	37	2524	2494
30	8.81	480	157	36.8	60	25	0.22	16	2444	2388
60	9.10	470	130	17.8	36	24	0.35	7	2265	2158
90	9.32	470	145	13.0	34	24	0.42	42	2525	2335

Table D.2 Detailed results for batch aeration of anaerobic digester liquor from UASB reactor at SFW Wellington Distillery; Batch Test 2.

Time (min)	pH	SC mS/m	FSA (mgN/ℓ)	P_T (mgP/ℓ)	Mg (mgMg/ℓ)	Ca (mgCa/ℓ)	Fe (mgFe/ℓ)	SCFA (mg/ℓ as HAc)	H_2CO_3*Alkalinity (mg/ℓ as CaCO3)	C_T (mg/ℓ as $CaCO_3$)
0	6.80	390	150	75.9	96	53	0.21			
4	7.55	380	152	61.7	84	42	0.23	0	2097	2213
8	7.90	410	152	49.8	70	33	0.18	71	2287	2335
12	8.14	470	148	38.0	60	28	0.18	40.3	2583	2601
15	8.27	430	132	79.5	56	26	0.23	52.1	2249	2250
20	8.41	400	148	75.9	48	25	0.23			
25	8.46	400	116	21.3	46	24	0.30	53	2160	2141
30	8.50	400	140	15.4	46	24	0.27	29	2253	2228
35	8.54	400	146	13.0	40	24	0.36	49	2163	2135
40	8.58	400	142	13.0	38	23	0.33	17.5	2293	2258
50	8.66	400	108	9.5	34	23	0.43			
60	8.75	400	90	7.1	32	23	0.45	70.8	2147	2091
90	8.97	400	120	3.6	28	22	0.64	40.8	2201	2071
120	9.09	400	84	2.4	28	22	0.67			

LIST OF REFERENCES

Abbona, F., L ndager Madsen, H.E. & Boistelle, R. (1982). Crystallisation of two magnesium phosphates, struvite and newberyite: effect of pH and concentration. *J. Cryst. Growth.*, **57**(1), 6-14.

Britz, T.J. (Personal communication).

Britz, T.J., Trnovec, W., van Schalkwyk, C. and Roos, P. (1999). Enhanced granulation in upflow anaerobic sludge-bed digesters (UASB) by process induction and microbial stimulation. *WRC Report No 667/1/99*, Water Research Commission, PO Box 824, Pretoria 0001, South Africa.

Baresi, L., Mah, R.A., Ward, D.M. and Kaplan, I.R. (1978). Methanogenesis from acetate. Enrichment studies. *Appl. Environ. Microbiol.*, **36**(1), 186-197.

Butler, J.N (1964). Ionic equilibrium – a mathematical approach. Addison-Wesley Publishing Co. Inc., Reading, Massachusetts.

Cohen, A., van Gemert, J.M., Zoetemeyer, R.J. and Breure, A.M. (1984). Main characteristics and stoichiometric aspects of acidogenesis of soluble carbohydrate containing waste waters. *Process Biochemistry*, pp 228-232.

Dolfing, J., Griffwen, A., van Neerven, A.R.W. and Zevenhuizen, L.P.T.M. (1985).Chemical and bacteriological composition of granular methanogenic sludge. *Can. J. Microbiol.*, **31**, 744-750.

Driessen, W.J.B.M., Tielbaard, M.H. and Vereijken, T.L.F.M. (1994). Experience on anaerobic treatment of distillery effluent with the UASB process. *Wat. Sci. Tech.*, **30**(12), 193-201.

Ferguson, T.J. and Mah, R.A. (1983). Effects of H_2CO_3 on methanogenesis from acetate or methanol in *Methanosarcina* spp. *Appl. Environ. Microbiol.*, **46**(2), 348-355.

Fourie, J.M. (1974). A guide to the treatment of winery effluent. *The Council for Scientific and Industrial Research (CSIR Guide K18)*, 1-16.

Goodwin, J.A.S. and Stuart, J.B. (1994). Anaerobic digestion of malt whisky distillery pot ale using upflow anaerobic sludge blanket reactors. *Bioresource Technology*, **49**, 75-81

Harada, H., Uemura, S., Chen, A. and Jayadevan, J. (1996) Anaerobic treatment of recalcitrant distillery wastewater by thermophillic UASB reactor. *Bioresource Technology*, **55**, 215-221.

Jones, d.T. and Woods, D.R. (1986). Acetone-Butanol fermentation revisited. *Microb. Rev.*, **50**(4), 484-524.

Kida, K., Tanemura, K., Sonoda, Y. and Hikami, S. (1994). Anaerobic treatment of distillery wastewater from Barley-*Shochu* Making by UASB. *Journal of Fermentation and Bioengineering*, 77 (1), 99-93.

Lehninger, A.L. (1972). Biochemistry. Worth Publishers Inc., 70 Fifth Avenue, New York, N Y 10011.

Lin, K. & Yang, Z. (1991). Technical review on the UASB process. *International Journal of Environmental Studies*, **39**, 203-222.

Lettinga, G. and Hulshoff Pol, L.W. (1991). UASB-process design for various types of wastewaters. *Wat. Sci. Tech.*, **28**(8), 87-107.

Lettinga, G., van Velsen, A.F.M., Hobma, S.W., and De Zeeuw, W. (1979). *The application of anaerobic treatment to industrial pollution treatment. Proc. 1st Int.Symp. on Anaerobic digestion,* Cardiff.

Lettinga, G., van Velsen, A.F.M., Hobma, S.W., De Zeeuw, W. and Klapwijk, A. (1980). Use of the upflow sludge blanket (USB) reactor concept for biological wastewater treatment, especially for anaerobic treatment. *Biotechnology Bioengineering*, **22**, 699-734

Loewenthal, R.E. (1997). Application of chemical equilibrium to the control of struvite and calcite precipitation in waste water treatment. *WRC Report No K5/602.*

Loewenthal, R.E., Ekama, G.A. and Marais, G.v.R. (1989). Mixed weak acid/base systems, Part I – Mixture characterisation. *Water SA*, **15**(1), 3-24.

Loewenthal, R.E., Kornmüller, U.R.C. and van Heerden, E.P. (1994). Modelling struvite precipitation in anaerobic treatment systems. *Wat. Sci. Tech.*, **30**(12), 107-116.

Loewenthal, R.E.and Marais, G.v.R. (1976). *Carbonate chemistry of aquatic systems: Theory and application*. Ann Arbor Science Publishers, P.O. Box 1425, Ann Arbor, Michigan 48106.

Loewenthal, R.E.and Marais, G.v.R. (1984). *Carbonate Chemistry of Aquatic System,* Vol II, *High Salinity Waters*, Butterworths, Massachusetts.

Loewenthal, R.E. and Morrison, I. (1997). Struvite 3.1 – A calculator for struvite precipitation/dissolution. Dept. of Civil Eng., Univ. of Cape Town, Rondebosch 7701, Cape Town, South Africa.

Loewenthal, R.E. and Morrison, I. (1998). Control of pH and fouling due to struvite and calcium carbonate in anaerobic digestion. *Biennial Conference and Exhibition of the WISA,* (Papers: Volume 3, paper 3B-7), Cape Town, South Africa.

Loewenthal, R.E., Wentzel, M.C., Ekama, G.A. and Marais, G.v.R. (1991). Mixed weak acid/base systems, Part II: Dosing estimation, aqueous phase. *Water SA*, 17, 107-122.

Loewenthal, R.E., Wiechers, H.N.S. and Marais G.v.R. (1986). *Softening and Stabilisation of Municipal Waters*. Published by the Water Research Commission, PO Box 824, Pretoria 0001, South Africa.

Mamais, D., Pitt, P.A., Cheng, Y.W., Loiacono, J. and Jenkins, D. (1994). Determination of ferric chloride dose to control struvite precipitation in anaerobic sludge digester. *Water Environ. Research* **66**(7), 912-918.

McInerney, M.J., Bryant, M.P. and Stafford, D.A. (1979). In: *Anaerobic Digestion.* Eds. D.A. Stafford, B.I. Wheatly and D.E. Hughes. Applied Science Publishers Ltd., Ripple Road, Barking, Essex, England.

Momberg, G. (1992). Phosphate fixation in waste water by means of controlled struvite formation. *WRC Project No 250,* Water Research Commission, South Africa.

Moosbrugger, R.E., Loewenthal, R.E. and Marais, G.v.R. (1990). Pelletization in a UASB system with protein (casein) as substrate. *Water SA*, **16**(3), 171-178.

Moosbrugger, R.E., Wentzel, M.C., Ekama, G.A. and Marais, G.v.R. (1992). Simple titration procedures to determine H_2CO_3* alkalinity and short chain fatty acid concentrations in aqueous solutions containing known concentrations of ammonium, phosphate and sulphide weak acid/bases. *Research Report W74*, Water Research Commission, PO Box 824, Pretoria 0001, South Africa.

Moosbrugger, R.E., Wentzel, M.C., Ekama, G.A. and Marais, G.v.R. (1993a). Lauter tun (brewery) waste in UASB systems – Feasibility, alkalinity requirements and pH control. *Water SA*, **19**(1), 41-52.

Moosbrugger, R.E., Wentzel, M.C., Ekama, G.A. and Marais, G.v.R. (1993b). Grape wine distillery waste in UASB systems – Feasibility, alkalinity requirements and pH control. *Water SA*, **19**(1), 53-68.

Musvoto, E.V., Ekama, G.A., Wentzel, M.C. and Loewenthal, R.E. (2000). Extension and application of the three phase weak acid/base kinetic model to the aeration treatment of anaerobic digester liquors. *Water SA*, **26**(4), 417-438.

Musvoto, E.V., Wentzel, M.C., Ekama, G.A., and Loewenthal, R.E. (1998). Mathematical modelling of integrated chemical, physical and biological treatment of wastewaters. *Research Report W97*, Univ. of Cape Town, Dept. of Civil Eng. Rondebosch 7701, Cape Town.

Musvoto, E.V., Wentzel, M.C., Loewenthal, R.E. and Ekama, G.A. (1997). Kinetic based model for mixed weak acid/based systems. *Water SA*, **23**(4), 311-322.

Murray, K. and May, P.M. (1996). *Joint Expert Speciation System (JESS). An international computer system for determining chemical speciation in aqueous and non-aqueous environments*. Murdoch University, Murdoch 6150, WA, Australia and the Division of Water Technology, CSIR, PO Box 395, Pretoria, 0001, South Africa.

Pitman, A.R. (1995). Practical experiences with biological nutrient removal on full-scale plants in South Africa. Presented at Internationale Konferenz Zur Vermehrten Biologischen Phosphorelimination, Hanover, Germany.

Randall, G. (1998). Determination of struvite solubility product in distilled water at 37°C. *Final year undergraduate thesis*, Dept. of Civil Eng., University of Cape Town, Rondebosch 7701, Cape Town, South Africa.

Reichert, P. (1994). *Concepts underlying a Computer Program for the Identification and Stimulation of Aquatic Systems*. Swiss Federal Institute for Environmental Science and Technology (EAWAG). CH-8600 Dübendorf, Switzerland.

Ross, W.R. (1989). Anaerobic treatment of industrial effluents in South Africa. *Water SA*, **15**(4), 231-245.

Sam-Soon, P.A.L.N.S., Loewenthal, R.E., Dold, P.L. and Marais, G.v.R. (1987). Hypothesis for pelletization in the upflow anaerobic sludge bed reactor. *Water SA*, **13**(2), 69-80.

Sam-Soon, P.A.L.N.S., Loewenthal, R.E., Wentzel, M.C. and Marais, G.v.R. (1989). Pelletization in the upflow anaerobic sludge bed (UASB) reactor. *Research Report W72,* Dept. Civil Eng., Univ. of Cape Town, Rondebosch 7701, South Africa.

Sam-Soon, P.A.L.N.S., Loewenthal, R.E., Wentzel, M.C. and Marais, G.v.R. (1990). Growth of biopellets on glucose in upflow anaerobic sludge bed (UASB) systems. *Water SA*, **16**(3), 151-164.

Scott, W.D., Wrigley, T.J. and Webb, K.M. (1991). A computer model for struvite solution chemistry. *Talanta,* **38**(8), 889-895.

Smith, P.H. and Mah, R.A. (1978). Growth and methanogenesis by Methanosarcina Strain 227 on acetate and Methanol. *Appl. Environ. Microbiol.,* **36**(6) 870-879

Souza, M.E., Fuzaro, G. and Polegato, A.R. (1992). Thermophilic anaerobic digestion of vinasse in pilot plant UASB reactor. *Wat. Sci. Technol.*, **25**(7), 213-222.

Standard Methods (1985). *Standard Methods for the Examination of Water and Wastewater*. 16th Edn. APHA, AWWA & WPCF, New York.

Steffen Robertson and Kirsten (1993). Water and Waste-water management in the Wine industry. *WRC Report No TT 51/90*, Water Research Commission, PO Box 824, Pretoria 0001, South Africa.

Stumm, W. and Morgan, J.J. (1981). *Aquatic Chemistry: An introduction emphasizing Chemical Equilibria in Natural Waters*. Wiley - Interscience, New York.

Taylor, A.W., Frazier, A.W. and Gurney, E.L. (1963). *Trans. Faraday Soc.* **59**, 1580.

Thauer, R.K., Jungermann, K. and Decker, K. (1977). Energy conservation in chemotrophic anaerobic bacteria. *Bact. Rev.*, **41**, 100-180.

Ohlinger, K., Young, T. and Schroeder, E. (1998). Predicting struvite formation in digestion. *Wat. Res.*, **32**(12), 3607-3614.

Wentzel, M.C., Moosbrugger, R.E., Sam-Soon, P.A.L.N.S., Ekama, G.A. and Marais, G.v.R. (1994). Tentative guidelines for waste selection, process design, operation and control of upflow anaerobic sludge bed reactors. *Wat. Sci. Tech.*, **30**(12), 31-42.

Wolin, M.J. (1974). Metabolic interaction among intestinal microorganisms. *Am. J. Clin. Nutr.*, **27**, 1320-1328.

Wood, H.G. (1982). Of oxygen, fuels and living matter, Part 2. G. Semenza (Ed). John Wiley and Sons, New York.

Wolmarans, B*. and Driessen, W.** (1996). Full scale BIOPAQ® UASB installation treating distillery effluent in Wellington, RSA. *Biwater (Pty) Ltd., PO Box 2216, Honeydew 2040, South Africa. ** Paques BV., PO Box 52, 8560 AB Balk, The Nederlands.

Zehnder, A.J.B. and Wuhrman, K. (1977). Physiology of a *Methanobacterium* Strain AZ. *Arch. Microbiol.*, **111**, 199-205.